1965

Surface temperature distribution of thermocouple alloys by infrared photography

Albert Eugene Bolon
Iowa State University

SURFACE TEMPERATURE DISTRIBUTION OF THERMOCOUPLE ALLOYS BY INFRARED PHOTOGRAPHY

by

Albert Eugene Bolon

A Dissertation Submitted to the
Graduate Faculty in Partial Fulfillment of
The Requirements for the Degree of
DOCTOR OF PHILOSOPHY

Major Subject: Nuclear Engineering

Approved:

Signature was redacted for privacy.
In Charge of Major Work

Signature was redacted for privacy.
Head of Major Department

Signature was redacted for privacy.
Dean of Graduate College

Iowa State University
Of Science and Technology
Ames, Iowa

1965

TABLE OF CONTENTS

		Page
I.	INTRODUCTION	1
II.	LITERATURE REVIEW	4
III.	DISCUSSION OF THE PROBLEM	16
	A. Fundamentals of Thermoelectricity	16
	B. Thermal Conductivity of Thermocouple Alloys	24
IV.	EXPERIMENTAL PROCEDURE	38
	A. Methods of Measuring Surface Temperature	38
	B. Thermocouple Techniques	40
	C. Infrared Photography of Hot Bodies	41
V.	RESULTS	48
VI.	DISCUSSION OF RESULTS	102
VII.	CONCLUSIONS	106
VIII.	BIBLIOGRAPHY	108
IX.	ACKNOWLEDGMENTS	113
X.	APPENDIX A. PROPERTIES OF THERMOCOUPLE ALLOYS	114
XI.	APPENDIX B. DETERMINATION OF ELECTRON AND PHONON CONTRIBUTIONS TO THERMAL CONDUCTIVITY	123
XII.	APPENDIX C. SAMPLE CALCULATIONS OF MATHEMATICAL CONSIDERATIONS	125
XIII.	APPENDIX D. TRAVELING MICROMETER DISTANCE MEASUREMENTS AND THERMOCOUPLE THERMAL EMF MEASUREMENTS	128
XIV.	APPENDIX E. LIST OF SYMBOLS	150

I. INTRODUCTION

Several of the recent United States space systems have contained an auxillary power device which is based on the thermoelectric generator concept. Although the exact description of these devices is not available, certain information has been inferred.

The basic principle on which these thermoelectric devices depend was discovered by Dr. Gunnar A. F. Winckler and Dr. Richard C. Evans and was announced (1) in May 1961 at the Fifteenth Annual Power Sources Conference. They reported a means by which the efficiency of a thermoelectric generator incorporating thermocouple alloy strips as the generator elements could be substantially improved.

Results reported by Winckler and Evans indicate that there is an "isthmus effect" which brings about a pronounced increase in temperature drop. However, their data are not clearly described nor conclusive. They have reported no further research on the problem because they have been engaged in manufacturing generators incorporating the "isthmus effect" for United States satellites.

Several advantages of thermoelectric devices over the more conventional power systems for general usage are as follows:

1. long lifetime, because of no moving parts
2. virtually maintenance free
3. noiseless
4. high temperature operation (as high as 1600°C at the source and 600°C at the sink)
5. size-independent efficiency

6. self contained

7. self sustained (so long as there is a temperature gradient).

The main disadvantage of thermoelectric generators is that they are expensive. Secondly most of the heat supplied to the hot end flows directly and wastefully, by conduction, to the cold end. The ratio between the useful electrical output and the heat input in a thermoelectric generator is thus lowered.

It is in the areas of military and space requirements that thermoelectric devices can be practically applied. However, with the development of specific devices, material problems and limitations in generator performance have become apparent. The major problems with semiconductor thermoelectric materials have been concerned with their poor mechanical integrity and high impurity-poisoning susceptibility.

Two space systems that have been developed are SNAP (Systems for Nuclear Auxillary Power)-3 which produces approximately three watts of electrical power, and SNAP-9A which generates approximately 25 watts (2). Both systems employ lead telluride material and operate between 950°F and 220°F at between five and six percent efficiencies. The SNAP-3 incorporates the radioisotope Polonium 210 as its heat source and the SNAP-9A uses Plutonium 238.

Nuclear reactors in which the heat of the fission reaction is directly converted to electricity by thermoelectric devices have also been designed and developed. Such systems could be used in space but would be suited for application in a number of other remote, unattended environments, such as the Arctic or on (or under) the oceans.

The objective of the research reported in this dissertation was to investigate experimentally the surface temperature distributions of thermocouple alloys (specifically Advance, Chromel-P, and Nichrome V) as strips of various prescribed configurations. It was undertaken to ascertain whether or not the introduction of transverse slits across strips in which a thermal gradient exists would cause a pronounced increase in the temperature drop. Such an increased temperature drop would lead to an increased Carnot efficiency and, thus, an increased overall efficiency.

II. LITERATURE REVIEW

This investigation was stimulated by an article published in the Proceedings of the Fifteenth Annual Power Sources Conference, 9-11 May 1961. The article, Isthmus effect -- a new thermoelectric phenomena (1), was written by Gunnar A. F. Winckler and Richard C. Evans of the Olin Mathieson Chemical Corporation, New Haven, Connecticut. The article was brief and because of its importance to this investigation it is presented in its entirety at this point.

"All things considered, the greatest drawback to the use of metal couples in thermoelectric generators is probably not their low Seebeck voltage but rather their high thermal conductivity. Automatic fabrication machinery can be designed which can weld in series hundreds of metallic couples with less difficulty than that involved in making a single semiconductor thermoelement, so the voltage generated by each individual unit is relatively unimportant. The increase in internal resistance brought about by series connection can, of course, be minimized by using material of appropriately large cross-sectional area. When, however, large numbers of metal couples having appreciable cross sections are used, it is difficult to maintain a temperature difference between hot and cold junctions and therefore the usefulness of the metallic thermoelement in power generation will depend upon finding a solution to the heat transfer problem -- a solution that does not increase the electrical resistance proportionately.

"When the Wiedemann-Franz ratio is carefully stated, it relates the flow of electricity to only the electrical portion of the flow of

heat and not to the total flow which would include the vibrational portion as well. It is therefore no contradiction to that principle to decrease the thermal conductivity of a material to a greater degree than the electrical by structural means, when such a procedure mainly affects the vibrational component. While such a structure may offer some difficulty in its theoretical analysis, it is simple enough to prepare and incorporate into practical devices. One of the most effective may be constructed from strips of thermoelectric alloy slit transversely until nearly, but not quite, severed (Figure 1). Easier than slitting is spot welding and then folding back the metal so that only the spot or several spots serve to connect the segments of the thermocouple leg. Intuitively, the impedance to heat flow by these 'thermal barriers' would be admitted. It is, after all, somewhat analogous to the conditions present in a transformer core which is saturated by overloading. What is surprising is that electrical resistance is affected to a lesser extent.

"While experimental evidence for this is not extensive, a series of efficiency measurements have been made; these seemed to be more pertinent than mere measurements of thermal conductivity and electrical resistance. The simplest experiment consists of a single couple, embodying a thermal barrier of the type just described, with its hot junction inserted into a slot cut into the copper of an electric soldering iron. The cold junctions hang free, cooled by convection and radiation. The electrical resistance and equilibrium temperature difference between hot and cold junction are compared with these same

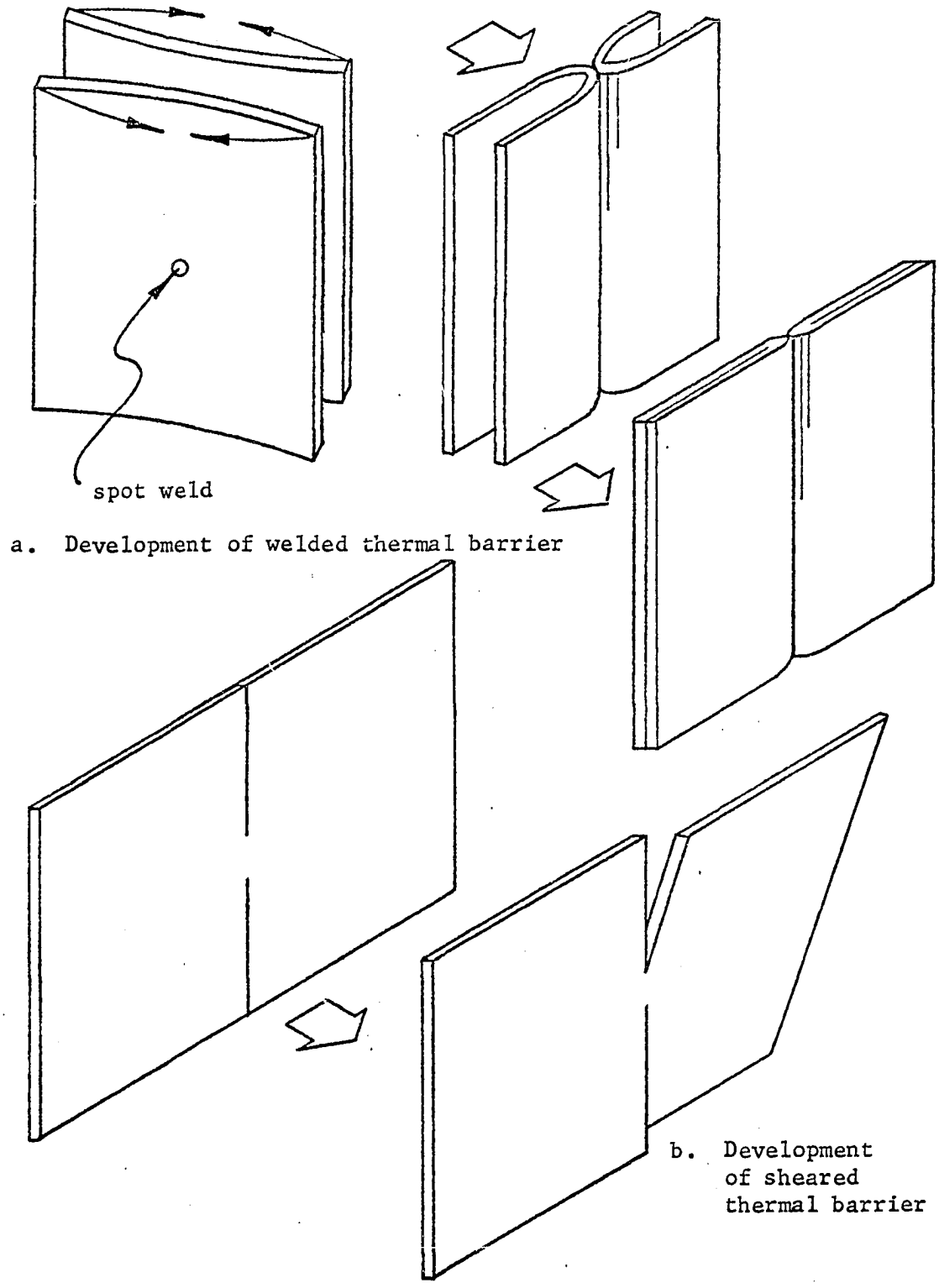

Figure 1. Means of forming the thermal barriers

measurements made upon a control couple having no thermal barriers in an otherwise identical experiment.

"The electrical resistance has been increased 35% while the temperature difference was increased 230% for an approximately constant heat source. In a second experiment the apparatus consisted of six couples made from thin strips of chromel and constantan, welded in series (Figure 2). These couples embodied two thermal barriers in the control. They were mounted in a transite board so that the hot junctions just protuded while the cold junction was immersed in a calorimeter up to the first barrier. The flame from a blast lamp was played on the hot junctions and the heat which passed through the couples into the water of the calorimeter was measured. The electrical energy produced was divided by the heat picked up by the water to obtain the efficiency. It must be emphasized that this efficiency is that of conversion of the heat which passed through the couple; it is not concerned with total fuel used nor with flue losses nor radiation losses. These exploratory experiments yielded the following results:

control: no barrier	0.2% efficiency
single barrier per leg	0.6% efficiency
two barriers per leg	1.1% efficiency

	hot junction temperature	cold junction temperature	temperature difference	electrical resistance
Without barrier	565°F	445°F	120F°	0.045 ohms
With barrier	565°F	169°F	396F°	0.061 ohms

This strategem has by no means been exhausted. It is presented here as a means of utilizing metal alloys for constructing useful generators

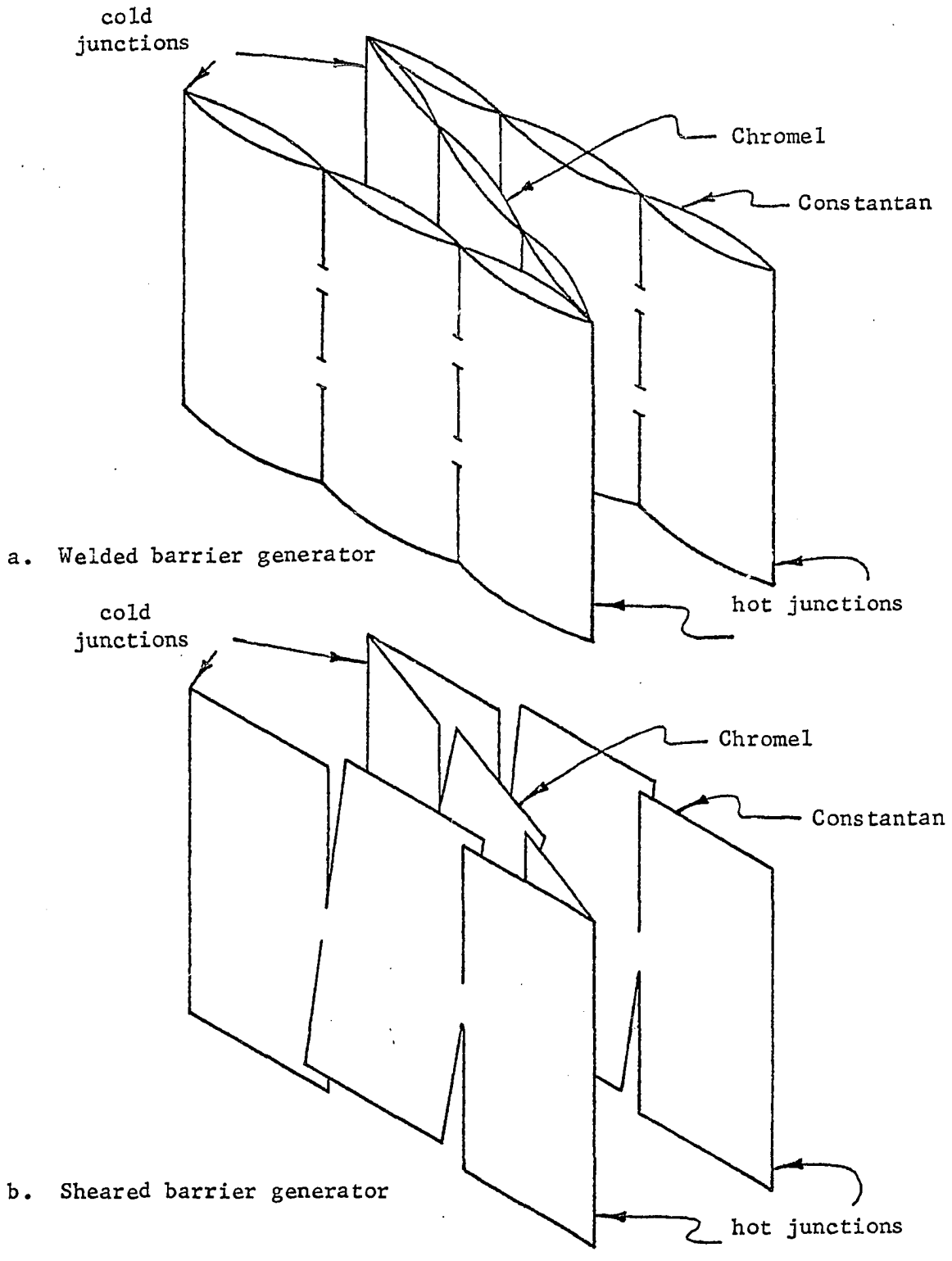

Figure 2. Means of fabricating thermoelectric generator elements

where the fragility, instability or cost of semiconductors precludes their use. In contrast to semiconductors, metal thermoelements show negligible interfacial deterioration and allow use of the art of welding. The advantage over soldering or hot pressing contact junctions is obvious. Our own test on a one-barrier type couple has been producing ½ ampere continuously for 10 months without any measurable change in output and with no atmospheric protection whatever. Metal alloys may be selected which enable the units to operate at higher temperatures and therefore higher Carnot efficiencies. To demonstrate the practicality of the idea, a one-watt generator has been assembled having sixty chromel-constantan couples arranged in a ring around the burner of a propane camp stove (Figure 3). Such couples have shown no deterioration after thousands of hours of service.

"While attention has been directed largely toward the metal alloys, it is probable that the impedance of heat flow by structural means in semiconductors could also be effective subject to differences in the relative importance of electronic and vibrational modes of thermal conductivity and to the difficulty of making constrictions in brittle material."

It is to be noted that little scientific data were reported in this paper. The specific materials for which the data were given were not identified, nor were any dimensions of the specimens given. Also the "efficiency" was defined as the electrical energy produced divided by the amount of heat conducted down the strip and transferred to the water. This is quite different from the Carnot efficiency (which they did mention). The Carnot efficiency is defined in the usual thermo-

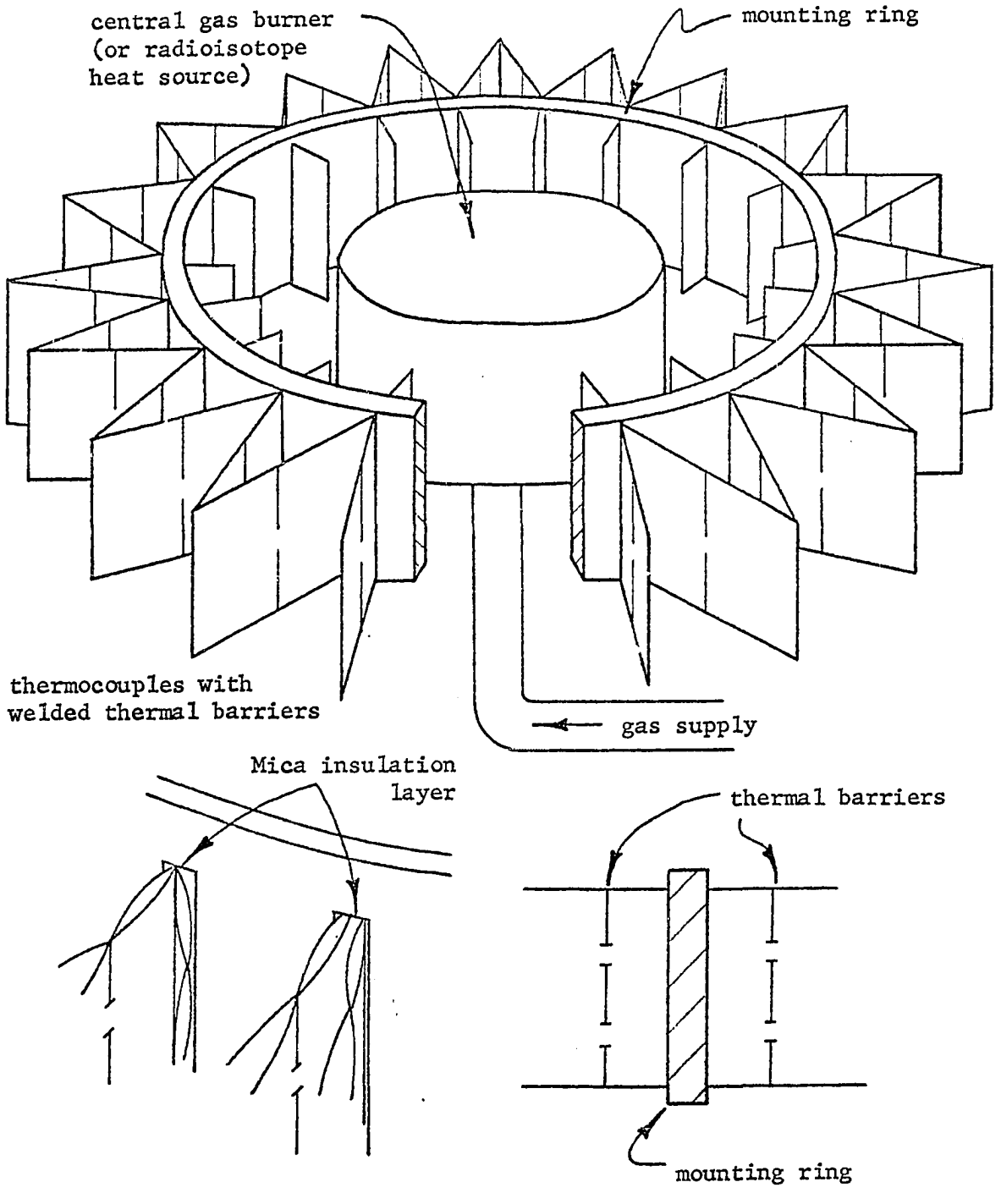

Figure 3. Thermoelectric generator incorporating the "isthmus effect"

dynamic sense as the amount of work produced divided by the heat input to a heat engine.

The possibility of studying this reported "isthmus effect", or the effect of configuration on the efficiency of thermoelectric materials -- especially the semiconductors, did seem worthwhile. Several reasons why the introduction of these "thermal barriers", or "isthmuses", might bring about a significant temperature drop in either thermocouple alloys or in semiconductors were deduced. These reasons were concerned with the anomalous increase of thermal conductivity with increasing temperature of the alloys, and the believed significant contribution of the lattice, or phonons, to the thermal conductivity of alloys and semiconductors.

Although no papers have been written directly pertaining to Winckler and Evans' results, it was discovered that they have a United States Patent, No. 3,048,643, for a thermoelectric generator unit (3) incorporating the "isthmus effect" in semiconductors.

In their patent Winckler and Evans state, "An ideal thermoelectric unit is one that sets up a thermal barrier in the junction of the dissimilar thermoelectric elements while not affecting electrical resistivity.

"The significant point to note with respect to conformation of the metal strip ... (cut and twisted 90^{o}) as against ... (plain rectangular strip) is that its total electrical resistance is not greatly affected by the marked degree to which the metal strip has been severed while the thermal conductivity of the sheet has been greatly changed."

Even in the patent Winckler and Evans state their belief that the property, thermal conductivity, changes due to the introduction of the thermal barrier.

The patent has three claims, one of which is stated as follows:

1. "A thermoelectric generator unit consisting of a first thermoelectric element, a cooling means spaced from said first element, a second thermoelectric element disposed in the space between the first element and the cooling means, said second element being in physical contact with said first element and with said cooling means and said second element being formed in at least two main sections connected by at least one neck portion."

The second claim is a slight modification of the first, and the third patents the method of fabrication.

Jaumot stated in his article, Thermoelectric effects (4, p. 52), "Given a material with a high figure of merit, the possibility of increasing its usefulness by reducing its thermal conductivity by mechanical means should be investigated."

Sherman, Heikes, and Ure (5) in their paper, Calculation of efficiency of thermoelectric devices, report that the arms of the thermoelectric generator are assumed to have uniform cross-sectional area along their length. This restriction was made due to the work by Gelhoff, Justi, and Kohler (6) showing that the performance of a thermoelectric device is not improved by making the elements in a non-cylindrical shape.

Boerdijk (7, p. 1080) summarized, "The maximal values of the efficiencies obtained by variation of the shape of the bars are independent

of the shape."

However, Boerdijk considered only the overall dimensions of the elements such as truncated cones, truncated wedges, circular cylinders, and prisms. Thus, his theoretical results were as would be intuitively expected, and were not directly related to pronounced discontinuities in the geometry.

On 13 February 1964 Dr. Richard C. Evans was contacted by telephone. He and Dr. Winckler were both employed at the Johns Hopkins University Applied Physics Laboratory, Silver Spring, Maryland.

They had been trying for three years to take advantage of an "isthmus effect" in semiconductors, but had discontinued the effort for the following distinct reasons:

1. The semiconductor materials are very, very brittle.

2. There are temperature gradients of the order $100F^{o}/0.01$ inch at the thermal barrier and semiconductors cannot withstand such high thermal stresses.

3. The materials are highly susceptible to aging and poisoning from impurities in the environment, especially at the contacts. Because of their susceptibility to oxidation most thermoelectric materials must be hermetically sealed if they are to be operated above 500^{o} or $600^{o}F$.

Evans disclosed that other persons had expressed interest in the "isthmus effect", but experimental attempts to reproduce their results had failed. Failure, according to Dr. Evans, was probably because sufficiently thin material had not been used. Winckler and Evans' strips had been 5 mil (0.005 inch) thick and an inch wide. No length

was given. Chromel-P with spot-welded fabrication gave the best results. Advance, which has opposite thermal emf polarity, also gave satisfactory results. Theoretical descriptions of the phenomenon had failed, Evans believed, because for best results the neck length must approach zero, and such a system could not be properly described mathematically. Evans stated that he felt the "isthmus effect" was contained within a quarter of an inch circle about the neck, thus, the difficulty in investigating it experimentally.

On 28 February 1964, Evans was telephoned again. During that conversation it was mentioned that this author had considered attempting to measure the surface temperature distributions by infrared photography plus thermocouples.

A letter dated 2 March 1964 was received from Evans. In it he wrote, "There are certain pitfalls in the field that we should like to discuss that might lead to worthwhile study. The first is the indiscriminate use of the electrical resistivity and thermal conductivity of a material without realizing that the definition specifies the shape (a centimeter cube, or something readily calculated from a centimeter cube). ... The second pitfall concerns thermal gradient. We have found in several experiments that the effectiveness of the thermal barrier is roughly proportional to the thermal gradient across it and would recommend that you do everything possible to maximize the gradient, such as keeping the cross section of the isthmus small and the length of the isthmus as close to zero as you can."

The materials they had studied were commercial polycrystalline strips, annealed dead soft. The cross section of the spot welds were

"perhaps 1/32 inch, determined by the welder tips".

At the present time the state-of-the-art of the reported "isthmus effect" appears to be completely based upon the experimental work and opinions of Winckler and Evans.

III. DISCUSSION OF THE PROBLEM

A. Fundamentals of Thermoelectricity

Thermoelectric effects is a generic name for three basic phenomena, which may be simply described as

1. the Seebeck effect -- the generation of a voltage in a circuit made up of two dissimilar conductors, A and B, the junctions of which are at different temperatures (Figure 4). The voltage drop, e_{AB}, measured for a given combination of materials increases with increasing difference of temperature, $dT = T_h - T_c$. In general the Seebeck coefficient is temperature dependent so

$$e_{AB} = \alpha_{AB}\,(T)\,dT \qquad (1)$$

where α is called the Seebeck coefficient, or the thermoelectric power. This coefficient is, physically, an entropy per unit charge. The sign convention on this and the other thermoelectric coefficients are assigned arbitrarily. Thermoelectric generators, which directly convert heat to electricity, apply the Seebeck effect (Figure 5).

2. the Peltier effect -- the generation or absorption of heat at the junction of two dissimilar conductors during the passage of electrical current. The rate of heat transferred, dq, is proportional to the amount of current, di, that flows.

$$dq = \pi_{AB}\,(T)\,di \qquad (2)$$

where π is the Peltier coefficient. This coefficient is a latent heat per unit charge.

3. the Thomson effect -- the generation or absorption of heat

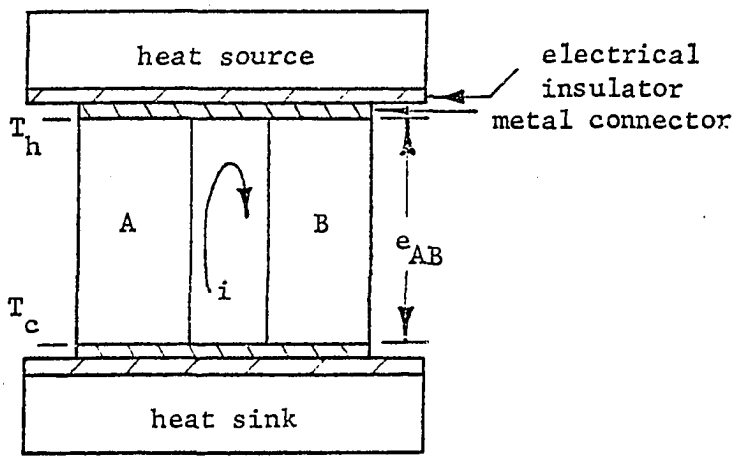

Figure 4. Seebeck effect

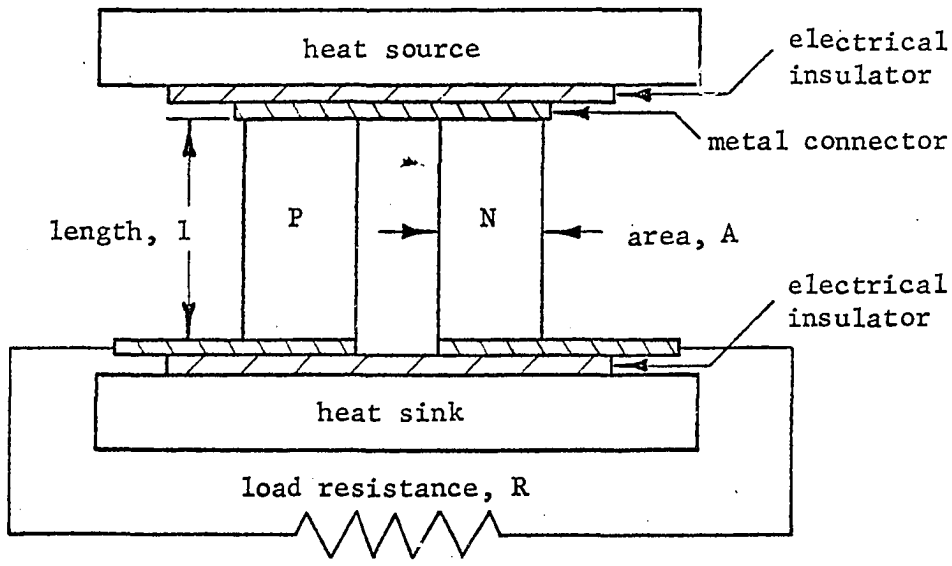

Figure 5. Thermoelectric generator

within a single conductor across which there is a thermal gradient during the passage of electrical current. If within an increment of length dx of a material A, there is a temperature gradient $\delta T/\delta x$, with a current flow i, the rate at which Thomson heat dq will be transferred is

$$dq = \tau_A(T)\ i\ \frac{\delta T}{\delta x}\ dx \tag{3}$$

where τ is the Thomson coefficient, which is a specific heat per unit charge.

The coefficients characterizing all three effects are interlinked by two relations. These relations have been derived, both classically and rigorously by irreversible thermodynamics, in Cadoff and Miller, (8, p. 5), Kaye and Welsh, (9, p. 14), Ioffe, (10, p. 8), and Chang (11, p. 69).

The following assumption was made in deriving the relations: thermoelectric effects are reversible and occur independently of the irreversible effects which arise simultaneously within the conductor. These irreversible effects are Joule heating and Fourier thermal conduction.

The entropy changes due to the three thermoelectric effects can be examined independently. Specifically, the requirement is that the sums of all of the changes of entropy within the system be zero. If such conditions are applied then

$$\alpha_{AB} = \frac{\pi AB}{T} \tag{4}$$

and

$$\alpha_{AB} = \alpha_B - \alpha_A = \int_0^T \frac{\tau_B}{T}\, dT - \int_0^T \frac{\tau_A}{T}\, dT \tag{5}$$

These are known as the Kelvin relations. They together with the equation

$$e_{AB}(T_1,T_2) = \int_{T_2}^{T_1} \alpha_{AB}(T)\, dT \qquad (6)$$

are the basic equations of thermoelectricity. For all practical purposes, since all three fundamental thermoelectric effects are interrelated, the Seebeck coefficient is the important quantity and is the only one appearing in the equations pertinent to device design.

The previously given assumption in the development of the Kelvin relations could not be deduced from thermodynamics and criticism is usually directed at that point. Boltzmann (12) was the most outspoken of the critics. However, all experimental work tend to corroborate Kelvin's relations within the limits of accuracy of measurement.

Onsager (13) developed a general method for building theories with reciprocal relationships of irreversible stationary effects. Domenicali (14, 15) and Domenicali and Otter (16) seem to be the strongest proponents for this irreversible thermodynamics of thermoelectricity. However, Jaumot (17, p. 221) points out "The fact is that any attempt to develop a maximum limit (of efficiency) short of the Carnot limit by thermodynamic means indicates a lack of understanding of either thermodynamics or thermoelectricity. Actually, it is felt safe to make the general statement that no entirely convincing argument has ever been advanced for applying thermodynamics to transport phenomena." Although these approaches provide a more solid foundation, the new thermodynamics left Kelvin's relations unaffected.

The derivation of the Kelvin relations seems to mark the limit of usefulness of the thermodynamic theory of thermoelectric effects. Generally the expressions derived for the thermoelectric force in metals are correct for semiconductors also, as long as it is remembered that in semiconductors -- as distinct from metals -- the electron gas is non-degenerate and classical statistics holds. A non-degenerate system is one in which each allowed state has a fixed value of energy and the same wave function.

In order to determine which factors are involved in the efficiency of a thermoelectric device (Figure 5), one must write down the expression for the efficiency from first principles. Then, after a series of optimizations with respect to internal versus external, or load, resistances and the geometrical factors involved, one may conclude that efficiency is expressed only in terms of the temperatures at the cold and hot junctions and a factor containing all of the relevant parameters of the materials. This factor is called the figure of merit, Z, and it determines the merit of a material for practical applications -- apart from mechanical properties, melting point, and volatility. The figure of merit for a single material is

$$Z = \frac{\alpha^2}{k\rho} \tag{7}$$

where k is the thermal conductivity (watt/cm^{o}K) and ρ the electrical resistivity (ohm-cm). The term Z enters the expression for the efficiency of the material, ξ_m,

$$\xi_m = \frac{\sqrt{\bar{Z}\bar{T} + 1} - 1}{\sqrt{\bar{Z}\bar{T} + 1} + \frac{T_c}{T_h}} \tag{8}$$

where $\bar{T}$ is the mean temperature between T_h and T_c.

The overall thermoelectric generator efficiency, η, is a product of the Carnot efficiency and the efficiency of the material

$$\eta = \frac{T_h - T_c}{T_h} \frac{\sqrt{\bar{Z}\bar{T} + 1} - 1}{\sqrt{\bar{Z}\bar{T} + 1} + \frac{T_c}{T_h}} \tag{9}$$

The figure of merit for a thermoelectric device made up of two elements with opposite Seebeck coefficients (Figure 5) may be written as

$$Z_{couple} = \frac{(\alpha_1 - \alpha_2)^2}{(\sqrt{k_1\rho_1} + \sqrt{k_2\rho_2})^2} \tag{10}$$

The assumptions involved in deriving the efficiency equation are as follows:

1. Resistance of contacts between the thermoelectric materials and the heat reservoirs is negligible.

2. There is perfect thermal insulation; so no heat is lost from the hot reservoir except through the thermoelements.

3. The arms have constant cross-sectional area A along their length l.

4. The properties α, ρ, and k are independent of temperature.

Then the ratio of the area of the thermoelements divided by their length, if they are made of semiconductor N and P materials, and the load resistance are related to the value which maximizes the efficiency.

The ratio is

$$\frac{A_N \, l_N}{A_P \, l_P} = \sqrt{\frac{k_P \, \rho_N}{k_N \, \rho_P}} \tag{11}$$

Note, if the maximum power output per unit weight were desired, then α^2/ρ would be maximized, not Z.

The Equation 7 for figure of merit for a single material may also be written

$$Z = \frac{\alpha^2}{(k_e + k_p)} \tag{12}$$

where the thermal conductivity k is made up of k_e, the electron contribution, and k_p, the phonon or lattice contribution. This equation is deceptively simple and by analyzing it the following may be observed:

If the free charge carrier concentration in a material is increased, the factor α decreases logarithmically, the electrical conductivity σ (reciprocal of electrical resistivity, ρ) increases directly and k_e increases directly, according to Redemske (18).

The free electron contribution, k_e, is believed to follow the Wiedemann-Franz relation

$$k_e = L\sigma T = 2.45 \times 10^{-8} \, \sigma T \tag{13}$$

where L, the Lorentz number, is $\frac{\pi^2}{3} (K/e)^2$ for a degenerate material, where K is the Boltzmann's constant, e the electron charge, and π the ratio of circumference to diameter of a circle. The Lorentz number may be derived from statistical mechanics.

After a thorough analytical consideration Jaumot (17, p. 212) reports, "... the thermal conductivity ... it is this parameter which holds the most promise for improvement of presently available materials

since, of all the variables involved, it exhibits the least interdependence with the others. Also, it may be the least understood.

"... All in all, the best possibility for increasing Z is to decrease the lattice thermal conductivity. Perhaps the best way to achieve this is by introducing into the lattice another substance, either element or compound, which crystallizes in a similar lattice and has approximately the same lattice constant. Such a system should exhibit fairly extensive solid solubility. (Note this is essentially what the thermocouple alloy systems do.) The distortion of the basic lattice by the added impurity is then relatively small and is limited to crystal regions in direct contact with impurity atoms. Such distortions are reasonably effective in scattering thermal oscillations, whose wave lengths at normal temperatures are of the order of the lattice constant. As a result, lattice thermal conductivity may be reduced appreciably, but the current carrier mobility is not affected significantly because lattice periodicity is not greatly affected and, thus, the electron waves with their longer wave lengths are not effectively scattered."

Semiconductor materials have brought about the fruition of thermoelectric devices in which the useful effects are at least comparable to the wasteful effects of i^2R loss and conduction of heat. In order to understand semiconductor charge-carrier mechanisms it would be necessary to know something of the detailed band structure of such material.

Thermoelectric generators usually employ N-type and P-type semiconductor materials. The N-type materials have concentrations of electrons; P-type materials have concentrations of "holes", or locations devoid of electrons. In a thermoelectric generator, the temperature

gradient causes electrons in the N-type materials and holes in the P-type material to move toward the cold ends, thus creating a potential difference.

The existence of thermoelectric effects is not limited to semiconductors, as they exist in metals and alloys as well. However, in metals and alloys these effects are less pronounced and the reason for their existence is more obscure and subtle.

There is reason to believe that the Seebeck emf is generated by a difference in the density of free electrons in one metal compared to a second metal in the circuit with the first. When the two different metals or alloys are connected to form a junction, electrons may diffuse from one to the other. The Thomson effect could be attributed to a temperature dependence of the density of free electrons in a single material.

B. Thermal Conductivity of Thermocouple Alloys

In the previous section, Fundamentals of Thermoelectricity, the importance of thermal conductivity was emphasized. The thermal conductivity and other properties of the material were studied in order ascertain how each affected the efficiency of thermoelectric generators. It was seen that due to the complex nature of the thermal conductivity, it perhaps could be decreased by structural means and thus bring about an increase in generator efficiency.

There is considerable lack of agreement among values of thermal conductivity given in the literature. One of the reasons for this is that, for most types of materials, there is no universally accepted

or standard method of measuring thermal conductivity. Similar methods might be employed to measure the thermal conductivity of like materials, but widely different methods are used to measure the conductivity of different types of materials.

The thermal conductivity is a difficult property to measure (much more so than, say, electrical resistivity or even specific heat). It is essential that various geometries be used for materials which have conductivities in different ranges. Descriptions of the difficulties involved in measuring thermal conductivities and the many techniques involved are given by Ginnings (19, 20), Bauerle, Sutter, and Ure (21), Campbell (22), and Drabble and Goldsmid (23).

Another reason that the data are inconsistent is that thermal conductivity varies greatly with the physical texture for many materials. Slight differences of chemical composition are also important. In most published data, description of the properties of the materials studied has been inadequate. However this has recently become recognized as an important factor and a description is usually included when the data are published.

In general for solids it is observed that the heat flux at a point is directly proportional to the temperature gradient at the point. In isotropic media

$$q_T = - k \quad \delta T/\delta x \tag{14}$$

The negative sign implies that the heat flux q_T is down the temperature gradient. The dimensions of q_T are (energy/length^2 - time); therefore, the dimensions of k are (energy/length-time-temperature). Any mathematical indication of a temperature dependence of k has been neglected.

The previous equation presents a macroscopic description of heat flow, but gives no information about k as a function of materials. For such a description a microscopic picture is necessary.

Basically, thermal conduction on a microscopic scale is a diffusion process. The entities which diffuse are capable of absorbing and releasing heat energy. The principal heat transporting entities are the following:

1. free electrons and/or holes
2. phonons (quantized lattice vibrations)
3. electron-hole pairs
4. excitons (bound electron-hole pairs)
5. photons (internal radiation)

The diffusion characteristic implies that these entities do not travel through the solid unlimited distances, rather are scattered by various mechanisms. If it were not for these scattering mechanisms, the thermal conductivity would be infinite. Klemens (24) and Keyes and Bauerle (25) have reviewed the studies of these mechanisms.

Although the processes leading to thermal resistance are understood in a qualitative manner, it seems that there is no reliable quantitative theory. Some important experimental and theoretical contributions have been made and surveys of these include that of Williams (26), Keyes and Bauerle (25), and Krumhansl and Williams (27).

Ewing, Walker, Spann, Steinkuller, and Miller (28, p. 252) state, "... an exciton transfer by electron-hole pairs ... can be considered insignificant for temperatures up to 2000°C (3632°F)."

Cusack (29, p. 187) explains, "Lattice scattering may therefore be referred to as the interaction of a system of electrons with a system of phonons. Whereas in Drude and Lorentz's theory electrons were imagined to collide with ions, in contemporary resistivity theory electron waves are scattered by phonons."

For a long time a close numerical connection between thermal conductivity and electrical conductivity has been observed. In fact, as long ago as 1853 Wiedemann and Franz (30), stated on the basis of experimental evidence the rule that the ratio of the electrical and thermal conductivities is, at any given temperature, approximately the same for all metals.

There have been theoretical derivations based on statistical mechanics which give a relationship between the two conductivities. The basic assumptions involved are as follows:

1. The mean free path of the electrons is the same regardless of the fact that the disturbing influence on the electron gas is an electric field or a temperature gradient. The mean free path is defined as that distance required for the intensity of the electron wave to be attenuated to 1/e of its original value.

2. The electron gas is degenerate.

Ioffe (10, p. 45) points out that, "very high concentrations of free electrons (more than 2.5×10^{19}/cc)," are required before a material can be considered as degenerate. Metals and alloys would be in this class.

The original derivation of the relationship between thermal and electrical conductivities is not definitely attributed to any one

person; however, Drude and also Lorentz, incorporating a Maxwellian distribution of electron velocities, have been mentioned. Mott and Jones (31, p. 305) present a thorough derivation. They arrive at

$$k_e/\sigma = L\,T = \frac{\pi^2}{3}\left(\frac{K}{e}\right)^2 T \qquad (15)$$

where K is the Boltzmann constant (1.38×10^{-16} erg/C^o), e the charge on an electron (1.602×10^{-19} coul), and L the Lorentz number (2.45×10^{-8} (volts/C^o)^2).

Mott and Jones (31, p. 307) state, "The derivation ... does not depend on any assumption about the form of the energy surfaces, and is therefore valid for all metals and not merely the monovalent metals. It is valid whether the resistance is mainly due to impurities, or to disorder in alloys, or to the thermal agitation of the atoms. In the latter case, however, it is only valid if $T>\theta_D$. (Where θ_D is the Debye temperature, which is a characteristic temperature that corresponds to the maximum frequency in the frequency spectrum used by Debye in his theoretical explanation of specific heat.) It is, moreover, only correct to the first order in $K\,T/\zeta$ (where ζ is the parameter known as the Fermi energy, which is defined as that energy at which one-half the electron states are filled), and therefore, for metals for which ζ is small (such as the transition metals, or bismuth), deviations may be expected at high temperatures. It neglects, further, the contribution made by the lattice vibrations to the thermal conductivity, and will therefore give in general too low a value for the (total) thermal conductivity, expecially for poor conductors (e.g. bismuth or alloys with high resistance)."

For non-degenerate materials, including semiconductors, the Wiedemann-Franz relation becomes

$$k_e/\sigma = 2\left(\frac{K}{e}\right)^2 T \qquad (16)$$

Actually, the numerical proportionality constant (which is 2 in the completely non-degenerate case) is sensitive to the scattering mechanism. The calculation of this factor for an arbitrary degree of degeneracy can be carried out, according to Ioffe (10, p. 45). The principal assumption is that the electron scattering can be described by an electron mean free path which is proportional to the r power of the kinetic energy of the electron. In the general case the proportionality factor is (r + 2) which for atomic lattices with r = 0 reduces to 2.

Calculations of the electronic component of thermal conductivity of thermocouple alloys used in the study and several metals are included in Table 18., Appendix B.

Debye (32) in 1914 presented his theory that elastic waves interacted and brought about anharmonicities which could provide the coupling necessary for equilibrium. He expressed the vibrational thermal conductivity as

$$k_p \simeq C\, v\, \lambda \qquad (17)$$

where C is the heat capacity per unit volume, v velocity of sound, and λ the mean free path (the distance in which the phonon wave is attenuated to 1/e of its original intensity). At temperatures sufficiently great that the specific heat becomes constant (that is, above the Debye temperature), the velocity of sound is essentially constant, the mean

free path varies as 1/T, so the thermal conductivity also varies as 1/T.

Some rules have been developed by Joffe (33) which allow the estimation of the value of the thermal conductivity and the influence of the temperature on the conductivity. His rules are primarily for semiconductors, but they carry over for thermoelectric alloys in some cases. It is realized that care should be taken when the knowledge of the properties of semiconductors is carried over into the domain of alloys. This is because of the differences in bonding, crystal structures, valencies, number of components, and types of defects. Joffe stated that

1. The actual value of k_p cannot be derived from theoretical considerations.

2. The thermal resistivity beyond the Debye temperature would be proportional to the absolute temperature.

3. The total heat conductivity would be composed of the electronic and phonon components.

The rules he deduced were

1. For substances with similar structures k_p decreases as the mean atomic weight of the elements composing the material increases.

2. The k_p decreases with increase of the portion of the ionic part of the chemical bond.

The phonon thermal conductivity is a vital factor to consider in the light of chemical bonding and crystal structure. To a first approximation, Jaumot (4, p. 60) writes

$$k_p = \frac{1}{3} C v \lambda_p \simeq \frac{\lambda p}{W^{1/2}} \qquad (18)$$

where C is the specific heat per unit volume, v the velocity of sound in the material, λ_p the phonon mean free path, and W the mean atomic weight.

The relation for the figure of merit, Equation 7, may now be approximated by proper substitution, according to Redemske (18).

$$Z \simeq \frac{\lambda e}{\lambda_p} \frac{W^{1/2}}{m} \text{ for covalent bonding} \qquad (19)$$

$$Z \simeq \frac{\lambda e}{\lambda_p} W^{1/2} \text{ for ionic bonding} \qquad (20)$$

where λ_e is the electron mean free path and m the effective mass of the charge carrier. The fact that a large mean atomic weight is desirable is evident.

However, a small λ_p is desired and this is as a rule, obtained as a result of a high degree of anharmonicity in the lattice, which is usually found in conjunction with a large, anisotropic thermal expansion and anomalously low Debye temperature. Thus the crystal structure will be of low crystal symmetry or a defect structure of a simple lattice.

Peierls (34) then in 1929 quantized the elastic waves in solids as phonons in a manner similar to the quantization of electromagnetic waves. This is still the basis of the theory of lattice thermal conductivity, although refinements have been added. Peierls' theory indicated that the lattice component decreased exponentially with increasing temperature at low temperatures, but at high temperatures had the 1/T dependence. He introduced three phonon processes which do not conserve momentum (unless the whole lattice is considered). These he called "Umklapp" processes, and they are still regarded as the main scattering

mechanisms in a pure dielectric at ordinary temperatures.

Keyes and Bauerle (25, p. 96) describe phonon-phonon scattering as "... usually the most important phonon scattering at high temperatures. It arises from the fact that the normal modes of the lattice are weakly coupled to one another by the anharmonic part of the lattice potential. Thus the anharmonic terms can cause transitions between phonon modes.

"In the phonon-phonon scatterings, vibrational energy is conserved and wave vector is conserved to within a reciprocal lattice vector. That is, if, for example phonons 1 and 2 interact to form phonon 3, then

$$\hbar\omega_1 + \hbar\omega_2 = \hbar\omega_3 \tag{21}$$

and

$$\bar{q}_1 + \bar{q}_2 = \bar{q}_3 + \bar{Q} \tag{22}$$

where $\hbar$ is Planck's constant divided by 2π, ω is the angular frequency, $\bar{q}$ is the wave vector, and $\bar{Q}$ is a reciprocal lattice vector. To the extent that dispersion is neglected (v, the phonon velocity, is assumed to be independent of $\bar{q}$) the phonon energy is $\hbar\omega = h\,v\,q$, and the contribution of a phonon to the energy current is $h\,v^2\,q$. Thus, in this approximation, Equation 22 with $\bar{Q} = 0$ implies conservation of the energy current. It is only those collisions for which $\bar{Q} \neq 0$, called by Peierls 'Umklapp' collisions, which produce thermal resistance. This conclusion is not essentially modified by the inclusion of dispersion in the theory."

Keyes and Bauerle (25, p. 102) discuss alloy scattering. The scattering of phonons by the randomness introduced into a crystal by alloying is of major importance. Some alloys have properties which are sub-

stantially more favorable for thermoelectric application than either of the pure components. No theory of the alloy scattering based on fundamental principles is available.

In metals, in which the electron concentration is about one per atom, scattering of the phonons by electrons may be important. At low temperatures electron scattering is believed to predominate.

Phonons also interact with lattice imperfections, more so than do electrons.

Generally the thermal conductivities of metals have been experimentally investigated in the low temperature region (less than, say, the freezing point of nitrogen, -345.8^{o}F), because certain interferring mechanisms are then eliminated. The review by Krumhansl and Williams (27) places more attention on the high temperature effects. The high temperature region is the one of primary importance in thermoelectric generator design.

Metals are known to be good electrical and thermal conductors, and the electronic thermal conductivity predominates. Either by alloying, or cold working, the thermal conductivity may possibly be reduced by an order of magnitude at room temperature and even more in the low temperature range.

At very low temperatures the effect of imperfections may be of importance; however, in the range of concern in this investigation (i.e. room temperature to 1000^{o}F) there are essentially only two mechanisms of heat transfer -- electronic and phonon.

Experimentally the thermal conductivity of metals and alloys (specifically the thermocouple alloys, Chromel-P, Nichrome V, Advance,

and Alumel) has been investigated in the high temperature range.

Shelton and Swanger (35) in 1933 measured thermal conductivities of zinc, nickel, a few nickel alloys (including Chromel-P, Alumel, and Nichrome V) and twenty irons and steels. A comparative method was chosen because it did not involve absolute determination of quantities of heat.

The results of Shelton and Swanger's research (35, p. 1070) showed, "For the pure metals, the irons and low alloy steels, the thermal conductivities decreased with increase in temperature. The conductivities of the high alloy steels and of the nickel alloys increased with increase in temperature." (The chemical analyses of the materials Alumel, Chromel-P, and Chromel-A (also known as Nichrome V) are given in Table 13., Appendix A., the thermal conductivities in Table 17., and plotted on Figure 45.) "In general, the thermal conductivities of all the materials tested were linear functions of the temperature within the range of the temperature in which measurements were made. A notable exception is nickel: the change from a negative to a positive temperature coefficient of thermal conductivity undoubtedly coincided with the magnetic transformation of the nickel which occurred between 350° and 365°C (660° and 690°F).

"A small and somewhat indefinite change in the temperature coefficient of thermal conductivity was also found in the nickel alloy Alumel. ... This change also probably was coincident with the magnetic transformation of the alloy, although it occurred at a lower temperature than for pure nickel.

"... The results obtained on the nickel base alloys Alumel and Chromel, indicated that the thermal conductivity of nickel decreased fairly regularly as the total amount of alloying elements added to nickel was increased."

Silverman (36) in 1953 investigated the thermal conductivities of metals and alloys used in the electron tube industry, which included Nichrome V and Advance. The method used was a modified comparative technique similar to that used by Shelton and Swanger.

The chemical analyses of the materials which are pertinent to this work that Silverman investigated are in Table 13., Appendix A., the thermal conductivities in Table 17. and plotted on Figure 45. Silverman noted that the metals iron and titanium show a decrease in conductivity with increasing temperature while most of the alloys show an increase. No explanation was set forth.

There is a definite discrepancy between the values of thermal conductivity for Nichrome V as found by Silverman and Chromel-A found by Shelton and Swanger. (See Table 17., Appendix A.) The values of Silverman are used in the manufacturer's catalogs (37) and are 20 years more recent; therefore will be used in this work.

Powell (38) in 1954 reported some more thermal conductivity data for high temperatures, as well as gave a review of some of the more recent investigations and the methods applied in each. He, too, noted the increase of thermal conductivity of many alloys with increasing temperature, but offered no explanation. His most important conclusion was that he observed a tendency for the thermal conductivities of certain groups of materials (iron and steels, particularly) to converge

towards a common value at high temperatures near 1000°C (1832°F).

The reason for the "anomalous" rise in the thermal conductivities of certain ceramics, semiconductors, and alloys with increasing temperature which is also characteristic of thermocouple alloys, has not been explained in the literature. Values of k_e (as computed from the Wiedemann-Franz relation) are compared to the total k in Tables 18. and 19., Appendix B. for the thermocouple alloys.

It can be seen that the electronic component increases, while the electrical resistivity also rises with temperature. Pure metals also have positive temperature coefficients of resistance. For instance, copper has a coefficient of 0.00393 ohms/ohm-C°, while Nichrome V has 0.00011 ohms/ohm-C°, and Advance has a resistivity which is independent of temperature, in the range of room temperature to 500°C (932°F), according to the manufacturer (37). However, the value of resistivity for copper at room temperature is 1.72×10^{-6} ohm-cm, for Nichrome V is 108×10^{-6} ohm-cm, and for Advance is 48.8×10^{-6} ohm-cm, according to the same source.

Considering the Wiedemann-Franz rule, Equation 15, in which the electronic thermal conductivity is directly proportional to the absolute temperature and inversely proportional to the electrical resistivity; one may conclude that for alloys the increase of temperature is more influential than the slight increase in resistivity, and the thermal conductivity thus increases.

The increase could be due to an annealing out of the imperfections. Rhodes and Cram (39, p. 441) report, "For Chromel-P annealing of strains occurs at temperatures near 600°K (572°F)." With a reduction in scat-

tering centers the thermal conductivity should rise. The reproducibility of the thermal conductivity data has not been mentioned in the original presentations, nor was any indication of the effect of history given.

IV. EXPERIMENTAL PROCEDURE

A. Methods of Measuring Surface Temperature

The experimental portion of this investigation was concerned with measuring surface temperature distributions of thermocouple alloy strips. The problem was somewhat simplified since steady-state conditions were to be studied.

The use of thermocouple probes was considered, but the problem of making reproducible contact and the difficulty of accurately determining the position precluded such a suggestion.

Permanent thermocouples attached in a grid pattern were considered. However, the introduction of a number of thermocouples on the surface perhaps would alter the temperature distribution on the surface due to the heat conducted away by the thermocouple wires. The fabrication problems of such a system would also be a discouraging factor.

The possibility of utilizing thermistors (thermal-sensitive resistors) was investigated. A thermistor is made of a semiconducting material that exhibits a high negative temperature-coefficient of resistance. These devices permit much more precise measurement of minute spans of temperature than do resistance thermometers or thermocouples. The uncertainty of making a reproducible contact, and the difficulty of determining position would be problems.

According to Atkins (40), the upper temperature limit for thermistors is the order of 500^{o}F and above that thermocouples are more favorable. The hot junction temperature of the specimens in this study were to be near 1000^{o}F. If operating conditions were going to be dupli-

cated, thermistors could not be used.

A technique called thermography (for thermal photography) was investigated as a possible means of measuring the surface temperatures. Urbach (41) describes the process in which temperature-sensitive phosphors are coated on to the body of which the temperature distribution is desired. Ultra-violet light from the hotter portions of the surface activates the phosphor and causes it to radiate in the visible region. This is then photographed with ordinary panchromatic film. This approach was not believed to be able to provide the definition about the small area adjacent to the isthmus which was desired.

Likewise some of the standard temperature measuring devices such as optical pyrometers and total radiation pyrometers were disregarded because of their inability to take into account the dimensions of the hot bodies and their inability to achieve the accurate resolution, or definition, required.

The Tempil temperature indicators were considered. A description of them is included in Kehl (42, p. 382). These are constant melting point compounds available as pellets, crayons, or paints. These indicators cover a wide range of temperatures (from 125° to 1600°F) and are particularly useful for determining within close limits ($\pm$ 1.0%) the surface temperature. The paint Tempilaq did seem to have potential application, but besides being time consuming and of questionable reproducibility, it would be expensive to acquire a complete set of the paints which are graduated for every 50°F from 350° to 1600°F.

Simply photographing light in the visible region emitted from the high temperature surfaces was considered, but Siviter and Strass (43)

claim that the lower limit of applicability is 1400°F using conventional cameras and emulsions.

The application of infrared photography with thermocouples spot welded to the surfaces so that they could be used both as temperature and position references was decided upon as the most feasible method of measuring the surface temperature distributions, especially near the isthmuses. Gluing the thermocouples to the surface with wax or adhesives is not generally accurate or reproducible, according to Green (44, p. 6-3).

B. Thermocouple Techniques

There have been several articles published on the use of spot-welded thermocouples for surface-temperature measurement. Moen (45) after a literature search and consultation with many engineers reported that two forms are most often used, these are the Type X and Type P. The Type X has a crossed-wire junction and Type P has parallel wires which do not necessarily touch each other, but are attached to a common conducting surface. In the Type X thermocouple the junction is approximately a wire diameter above the surface of the body being measured; because of this the parallel-wire type is recommended.

White (46) agrees with the conclusion that the parallel, separated junction is better than the X-junction or the conventional bead junction when the couples are to be welded to a surface. Parallel junctions do not require heat transfer to a second body, and they have much better mechanical strength. Steady-state results are reported to be accurate within one percent.

A review of the literature was made in order to ascertain which materials were best suited for the temperature range from room temperature to 1000°F. Most industrial applications utilize iron and Constantan, or Chromel-P and Alumel. There are standard guarantees on both types. Based on a 32°F reference temperature, the guarantee is ± 4°F from 0° to 530°F and 3/4% of the Fahrenheit temperature from 530°F up to the high temperature limit for the thermocouple wire. These standards are stated in ISA Bulletin R.P. 1.3 (47). On the basis of these wire guarantees, the maximum error of a thermocouple with ice-bath reference temperature, is 7½°F to 1000°F.

C. Infrared Photography of Hot Bodies

Numerous articles have been written on the possibility of applying infrared photography techniques to determine relative temperature distributions on the surfaces of hot bodies. However, no simple, accurate method of determining quantitative values of temperature by infrared photography have been reported.

Clark (48) devoted a section of his book, Photography by infrared, to the photography of hot objects, in which he writes the following:

"If an object reflecting or emitting light is photographed on a panchromatic film, the negative gives a record of the distribution of brightness over the surface. If suitable precautions are taken, the actual brightness at different points can be determined quantitatively. Similarly, if the infrared radiation emitted by a hot object is recorded on an infrared-sensitive film, some idea of the distribution of infrared emissivity, which is related to the temperature of the surface, may be

obtained. In this way, we have the subject of photographic thermometry, analogous to photographic photometry.

"... Infrared photography can be used for studying the distribution of temperature of surfaces from about 250°C (482°F) to approaching 500°C (932°F). For temperatures below 250°C the exposure times are far too long, whereas above 450 to 500°C visible radiation is emitted and panchromatic films can be used.

"... The temperature range which can be covered properly by one exposure on one sheet of film does not exceed about 150°C (270F°). Its limits are determined by the latitude of the film. The actual position of the temperature range of the total temperature scale will naturally determine the exposure required. It will be longer, the lower the temperature.

"In order to be able to interpret infrared exposures of hot objects quantitatively, it is necessary to employ the precautions which are used in photographic photometry. The most important of these is to include on the negative a series of exposures of a standard hot body operated at known temperatures. The densities in the negative of the hot object can then be compared with those of the calibrating exposures and the temperature ascertained. A convenient way of applying the standard exposure series suggested by E. W. H. Selwyn (in a private communication to Clark) consists in photographing a triangular piece of metal foil through which an electric current is passed. Such a foil will vary in temperature according to its width and is calibrated with a pyrometer or thermocouple. Alternatively, a group of electrically heated objects of known temperatures may be photographed, or a metal

bar, heated at one end as the well-known bars for determining melting points, and having a temperature gradient throughout its length. These must naturally be calibrated for temperature by a thermocouple or other means."

An exposure curve may be drawn relating temperature to the exposure required to produce a particular density at a particular aperature. There would be a fairly wide range on such a curve where the relationship between temperature and log relative exposure would be practically linear.

Some research has been done on the development of heat-sensitive papers which could measure surface temperatures over a lower range than that which can be recorded photographically. The aspect of obtaining quantitative information has not been solved, however.

"The intensity of infrared radiation can be measured by physical detectors which are sensitive to it; for instance, the bolometer and the thermopile, and by a photographic method. ... With proper technique and intelligent interpretation of the results and a proper knowledge of the characteristics of photographic materials, photographic photometry is capable of a high degree of precision. Particular attention must be paid to wave length sensitivity, intermittency effect, reciprocity failure, gamma-wave length relationship, errors of development, and nonuniformity of effective sensitivity," according to Clark (48, p. 345).

The conditions which must be fulfilled in order that two samples of radiant energy may be stated to be of equal intensity have been defined clearly by Jones (49). They are as follows: "The exposure

to the two sources should be made of small areas of the plate which are immediately juxtaposed; in no circumstances should exposures on one plate be compared with those on another even if they are from the same box; the exposures should be made nonintermittently and simultaneously, and the times should be equal; the wave lengths should be equal; the densities must be equal; (and the temperatures must be equal)."

The Eastman Kodak Company has an advanced data book (50) which describes the characteristics of their infrared films, use of correct filters, suggestions on the practice of infrared photography, and the art of photographing hot objects.

On the use of the proper filters they point out that photography of hot objects should be done in a completely darkened room; otherwise, the photograph would be obtained by reflected, not emitted, infrared and visible light. However, a Kodak Wratten Filter No. 25 or 87 would eliminate the blue component, if stray light is unavoidable or long exposures are necessary.

In, or near, 1956 several companies developed systems with which temperatures could be measured by photography. One of the concerns which developed an apparatus was Barnes Engineering Company. Their instrument is called the Barnes Far Infrared Camera and can measure surface temperatures between -170° and 300°C (51). Another similar device has been developed by Baird Associates and is called EVA the Evapograph. It is reported (52) to be accurate to $\pm 4^{\circ}$ at 1800°F. These two systems incorporate thermistors, servo-mechanisms, curved mirrors, wave length convertors, and polaroid cameras; thus their

costs eliminates them for consideration for use in this research.

The adaptation of military sniperscopes, which were designed to be attached to rifles, or snooperscopes, which are telescopes that convert infrared to visible light, were considered. The main concern was whether sufficient resolution would be possible and how information could be permanently recorded.

Although it was realized that quantitative results could not be validly obtained by photographing samples incorporating isthmuses by themselves; qualitative results could be obtained. The film has a different response, or sensitivity, at different wave lengths, and different rolls (as well as different segments of the same roll) have variations in their chemical composition. Also there could possibly be significant deviations due to differences in the developing of the film, not necessarily due to poor technique, but due to deterioration of developing solutions.

It was decided that the solution to these problems would be to place two specimens of like material side-by-side, one with a thermal barrier, the other one plain. Both samples could have thermocouples attached to establish calibration of temperature and references for position determinations (Figures 6 and 7). Then accurate temperatures could be determined for given film densities on each individual frame.

Several heater systems were investigated and it was decided that a 250-watt soldering iron regulated by a variable transformer which had a maximum voltage output of 140 volts would be satisfactory.

Kodak Infrared Film (IR 135) in roll form was determined to be the most applicable for use in this research. Directions for its use

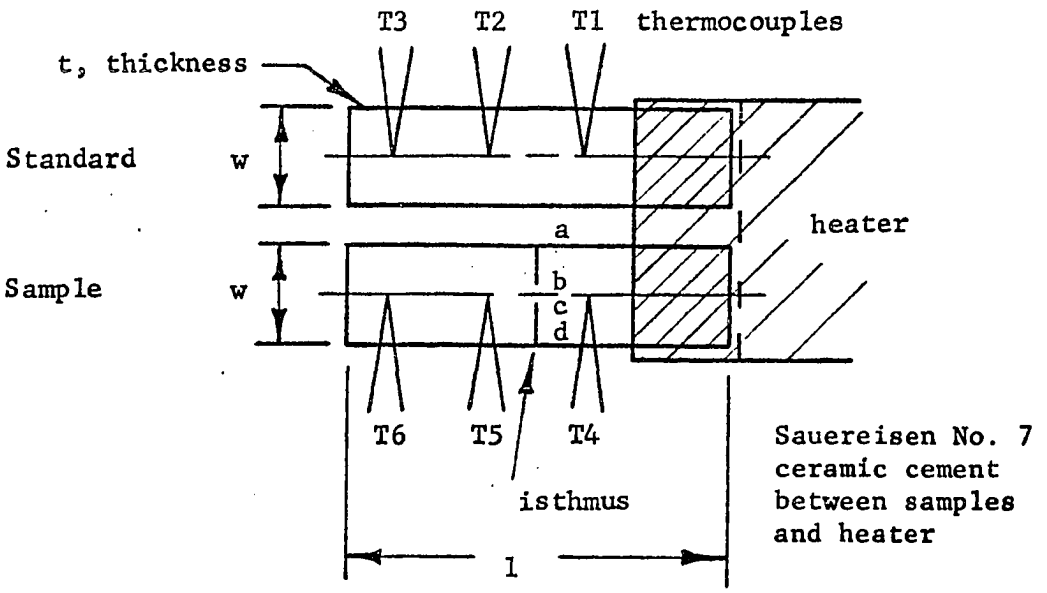

Figure 6. Drawing of juxtaposed standard and sample (2X)

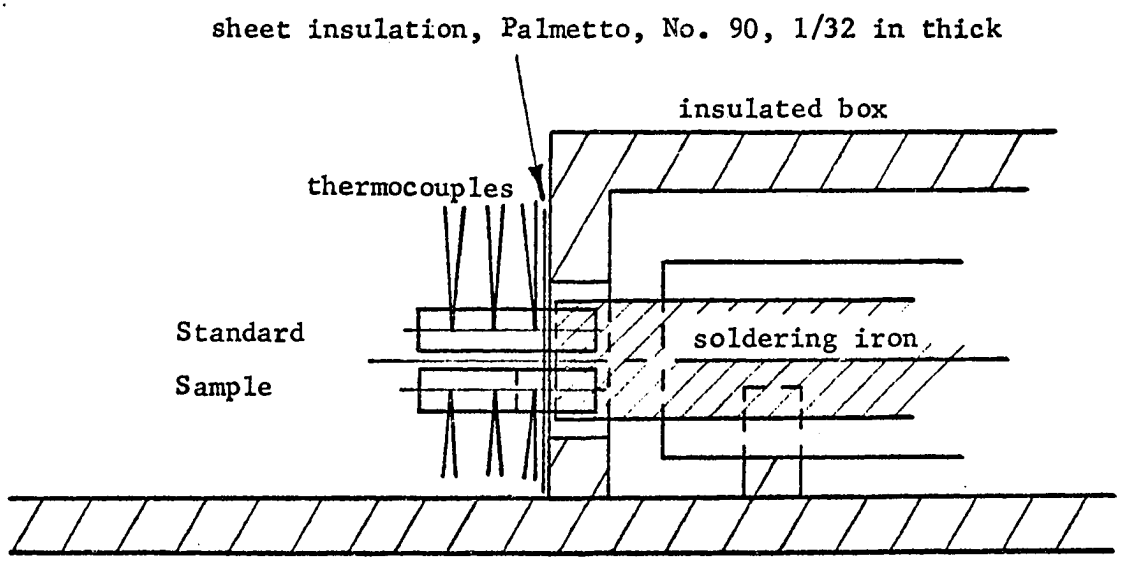

Figure 7. Drawing of experimental arrangement

may be found in the manual, Infrared and ultraviolet photography (50, p. 28).

The most favorable frames on the 35 mm. film were enlarged to 8 inch by 10 inch transparencies. The regions of equal film density were then determined by the photographic densitometer at the Photographic Laboratory and recorded on a tracing paper overlay. The photoconducting detector on the densitometer is approximately an eighth of an inch in diameter. With length scales between the specimen and transparencies of approximately 12, this would correspond to only 0.01 inch on the specimen. Smaller detectors could have been used, but the graininess of the film would have become more influential. The detector employed, in effect, integrated the film density over a larger area.

Lines of a given film density on the overlay corresponding to the standard were correlated to the temperature at the same point along the centerline which had been determined by drawing continuous curves through the thermocouple data. This same temperature was then assigned to the same film density contour on the overlay corresponding to the sample, and the curves of temperature distribution according to the infrared photography technique were recorded on the same plot as the thermocouple data.

V. RESULTS

The results of this experimental investigation are presented in the form of tables of centerline temperatures and distances, curves of the same data, infrared photographs indicating the two-dimensional surface temperature distributions, and figures in which the contour lines describe lines of equal temperature.

The effect of the environment surrounding the specimens on the temperature difference was one of the first problems investigated. Run 1 was performed with the sample and the heater surrounded by two inches of diatomaceous earth contained within an insulated box. Run 3 was performed with the sample exposed to the air and the heater enclosed in an insulated box (Figure 7). The deviation of temperature difference at a heater voltage of 46.7 volts was only 4% (Figure 12); thus, it was decided that the sample could be exposed and the infrared photography technique attempted. The reason that the heater voltage for Run 1 was not raised was because there was a concern that the system might burn.

The proper voltage required to maintain the samples at the hot junction temperature in order that infrared photography might be used (about $1000^{o}F$) was studied in Run A. Line voltage (110v) was found not to be sufficient. However, by including a variable transformer in the circuit, a sufficient voltage of 140v was obtained. The resistance of the heaters was approximately 67 ohms at the maximum temperature. The power at the heater was thus 293 watts.

Most of the samples were oriented in a vertical position with the heater to the side (Figure 6). A series of experiments, Run 7, was made in order to ascertain the influence of orientation of the samples on the centerline temperature distribution. The samples were rotated about the centerline of the heater. The results of this series of experiments are shown in Figures 33 and 34.

When several of the experiments indicated that the steady-state temperatures on both the standard and the sample with the isthmus were approximately the same, it was decided that the transient temperatures during heating should be investigated. This was done in Run 5. It was seen that the temperatures on both the standard and the sample approached the steady-state values in the same length of time (Figure 35).

The mean temperatures with standard deviations have been included for the three materials of concern (Advance, Chromel-P, and Nichrome V) and the temperature differences were calculated. The designation of temperatures is given as ^{o}F, whereas the designation of temperature differences is F^{o}.

The hot thermocouple temperature was taken as the reference temperature on each specimen. A definite temperature at the hot thermocouple could not be established; because of the variation in the line voltage, the necessity of using several different heaters (due to their deterioration and subsequent failure), and the impossibility of obtaining a reproducible contact between specimens and the heater.

Carnot efficiencies were calculated for each sample between the hot and cold junctions. These are not the efficiencies of the generator elements, but rather the ultimate limits since they do not take into account the efficiency of the materials. Temperature gradients were determined between each thermocouple.

In order to take into account the slight variations in length between the hot and cold thermocouples on the specimens, the Carnot efficiencies were divided by the distance between the thermocouples. These values definitely do not imply that by doubling the length of an element the Carnot efficiency could also be doubled.

The infrared photographs and corresponding contour diagrams indicate the two-dimensional surface temperature distributions.

Thermoelectric generator elements which had been fabricated by Winckler and Evans (Figures 8 and 10) were heated and photographed separately. Standards of the same materials with similar geometries (Figures 9 and 11) were investigated and the results of the thermocouple data were compared.

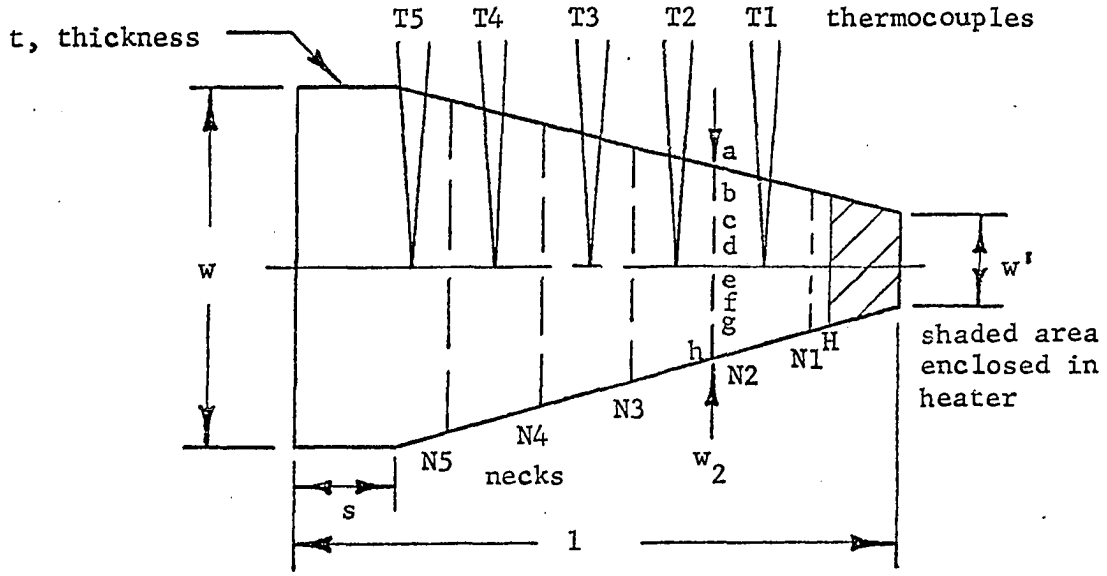

Figure 8. Drawing of wedge shaped thermoelectric generator element (2X)

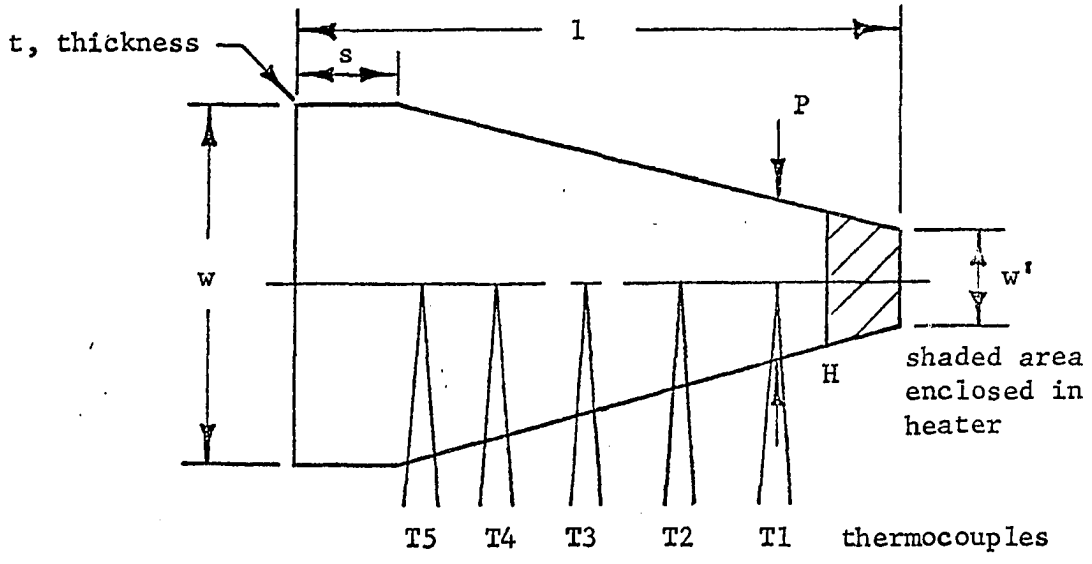

Figure 9. Drawing of standard similar to wedge shaped thermoelectric generator element (2X)

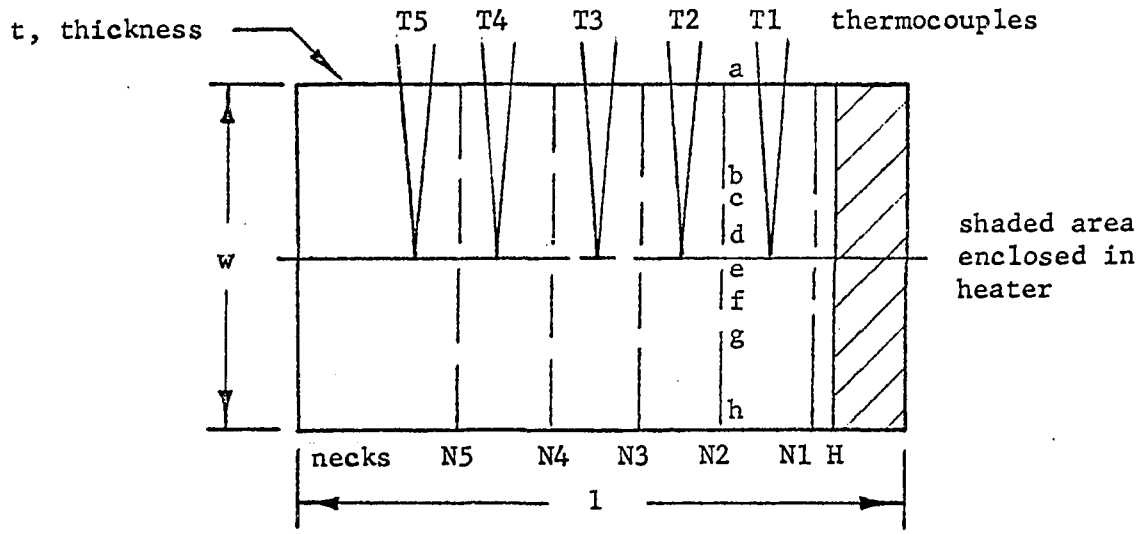

Figure 10. Drawing of rectangular thermoelectric generator element (2X)

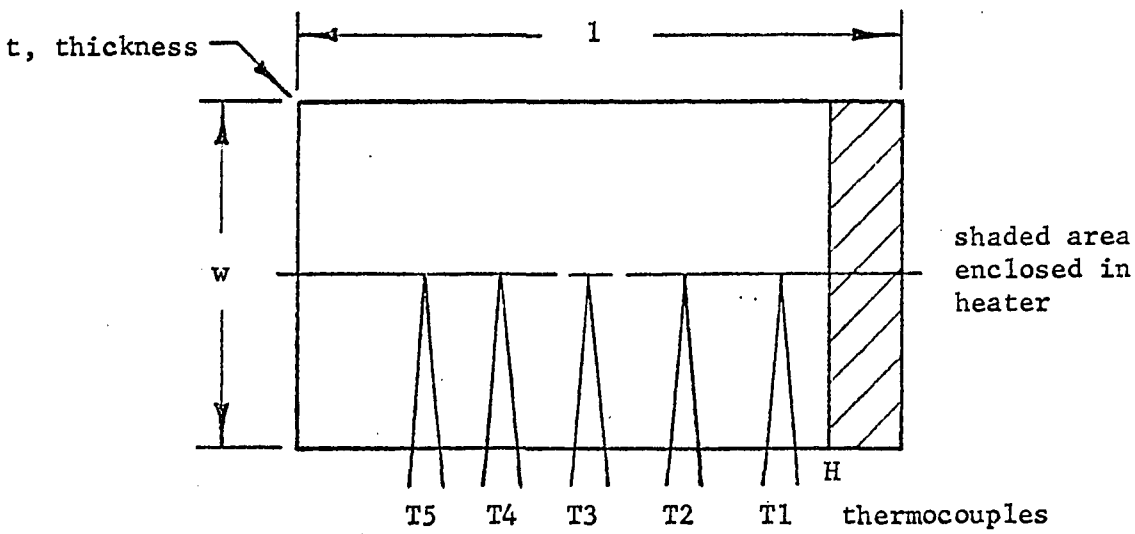

Figure 11. Drawing of standard similar to rectangular thermoelectric generator element (2X)

Table 1. Effect of environment on temperature difference Chromel-P. Runs 1 and 3. (Spot-welded sample. Heat flow parallel to rolling direction. (Figure 6 without standard)

Dimensions, isthmus position, and centerline distances

dimension	length (in)
1	0.97
w	0.66
t	0.0100
isthmus position	
a	0
b	0.318
c	0.341
d	0.663
centerline distance	
T4	0
I	0.24
T5	0.49

Mean temperatures (^{o}F) for different heater voltages, and different surroundings.

Run 1. Sample and heater surrounded by two inches of diatomaceous earth within an insulated box

heater voltage (v)	16.8	22.0	27.1	32.0	46.7
position					
T4	189.5	247.5	316.5	378.5	621.5
T5	151.0	188.5	235.5	275.5	441.0
T4-T5	38.5	59.0	81.0	103.0	180.0

Table 1. (Continued)

Run 3. Sample exposed to air, heater enclosed within an insulated box						
heater voltage (v)	16.8	22.0	27.1	32.0	46.7	56.2
position						
T4	135.5	165.5	195.0	225.5	340.0	422.0
T5	98.0	110.5	119.5	130.5	167.0	193.5
T4-T5	37.5	55.0	75.5	96.0	173.0	228.5

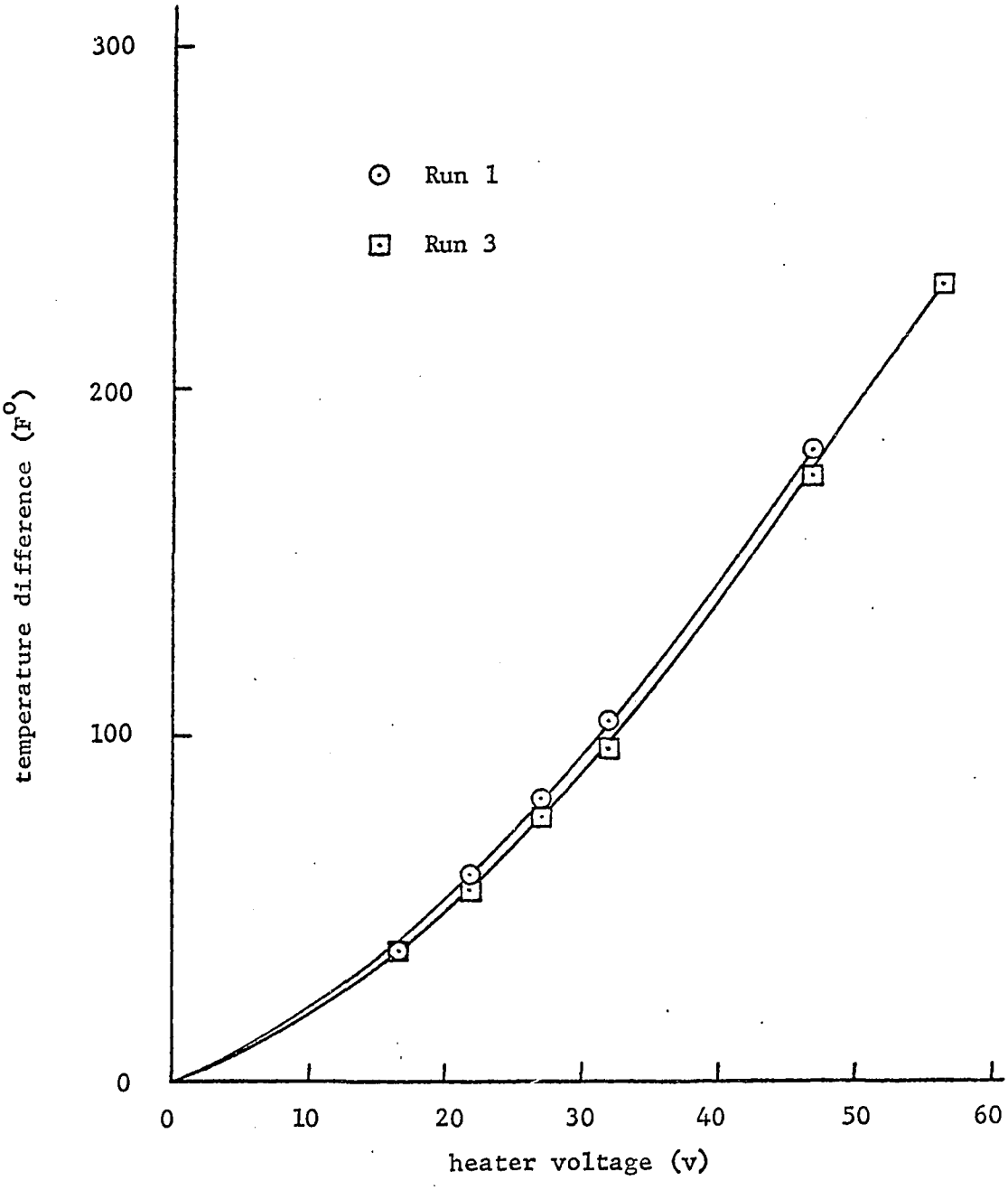

Figure 12. Effect of environment on temperature difference Chromel-P. Run 1 in diatomaceous earth and Run 3 in air.

Table 2. Temperature distributions Advance. Run A. (Wedge shaped generator element. Heat flow parallel to rolling direction. (Figure 8))

Dimensions, isthmus position, and centerline distances

dimension	length (in)
l	1.58
w	0.92
t	0.0100
s_1	0.25
w_1	0.25
w_2	0.475
position of isthmuses	
a	0
b	0.064
c	0.089
d	0.198
e	0.221
f	0.320
g	0.344
h	0.475
centerline distances	
T1	0.000
N2	0.114
T2	0.223
N3	0.348
T3	0.460
N4	0.578
T4	0.708
N5	0.810
T5	0.926

Mean temperatures (^{o}F) and standard deviations (^{o}F) for different heater voltages

heater voltage (v)	85	104	122	140
position				
T1	595.0±2.0	769.5±1.5	916.5±2.5	1077.5±7.5

Table 2. (Continued)

T2	398.5±4.5	517.0±1.0	618.5±2.5	726.0±11.5
T3	268.5±2.5	336.0±0.0	397.0±2.0	475.0±10.5
T4	186.5±2.0	228.0±1.0	264.0±1.0	315.0±8.0
T5	154.5±1.5	184.5±2.5	208.5±0.5	247.0±7.0

Temperature differences, carnot efficiencies, temperature gradients, and Carnot efficiencies divided by distance between T_h and T_c for heater voltage of 140v

T	T_h (^oR)	diff. (F^o)	Carnot eff.	grad. (F^o/in)	Carnot eff./in
1	1537.5				
2		351.5±14.0	0.229	1580	1.03
3		251.0±16.0		1060	
4		160.0±13.5		645	
5		68.0±10.5		312	
1-5		839.5	0.540	897	0.583

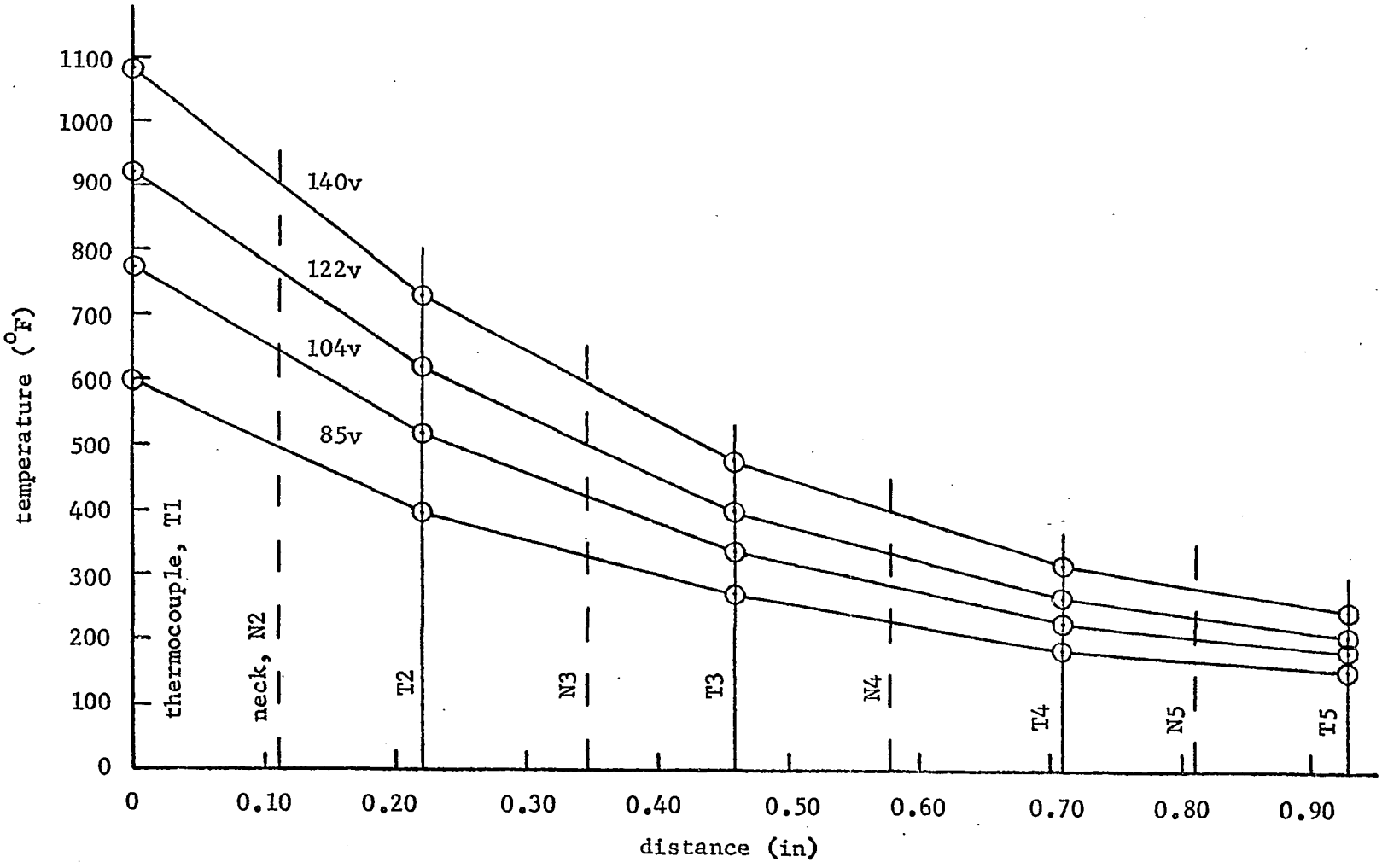

Figure 13. Temperature distributions Advance. Run A.

Figure 14. Infrared photograph Advance. Run A. (Exposure: 64 min, stop: f/5.6, filter: 87, film: Kodak IR 135-20) (9.1X)

Figure 15. Diagram of film density (temperature) contours Advance. Run A. (9.1X)

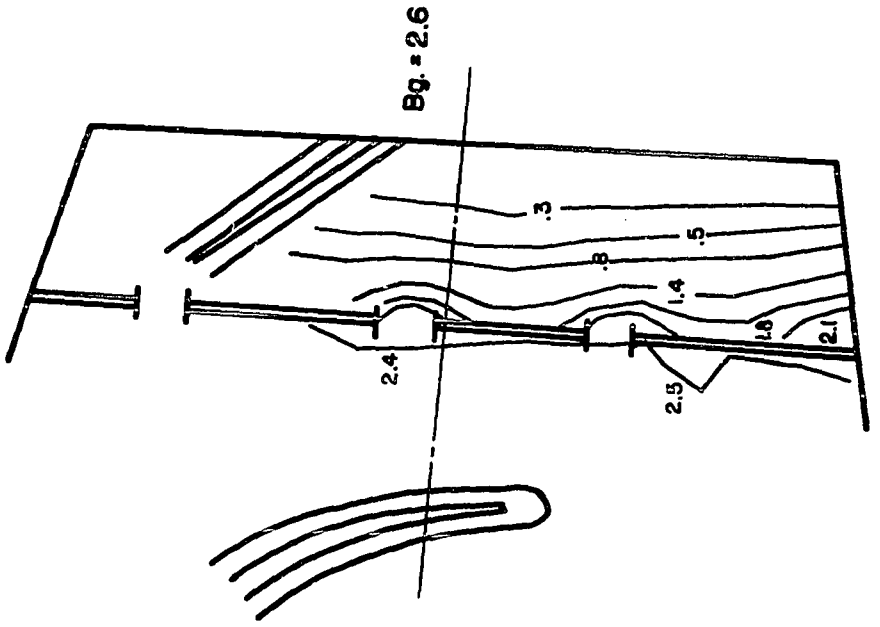
Bg. = 2.6
.3
.5
.8
1.4
1.8
2.1
2.4
2.5

Figure 16. Infrared photograph Advance. Run A. (Exposure: 9 hr 10 min, stop: f/4.0, filter: 87, film: Kodak IR 135-20) (8.7X)

Figure 17. Diagram of film density (temperature) contours Advance. Run A. (8.7X)

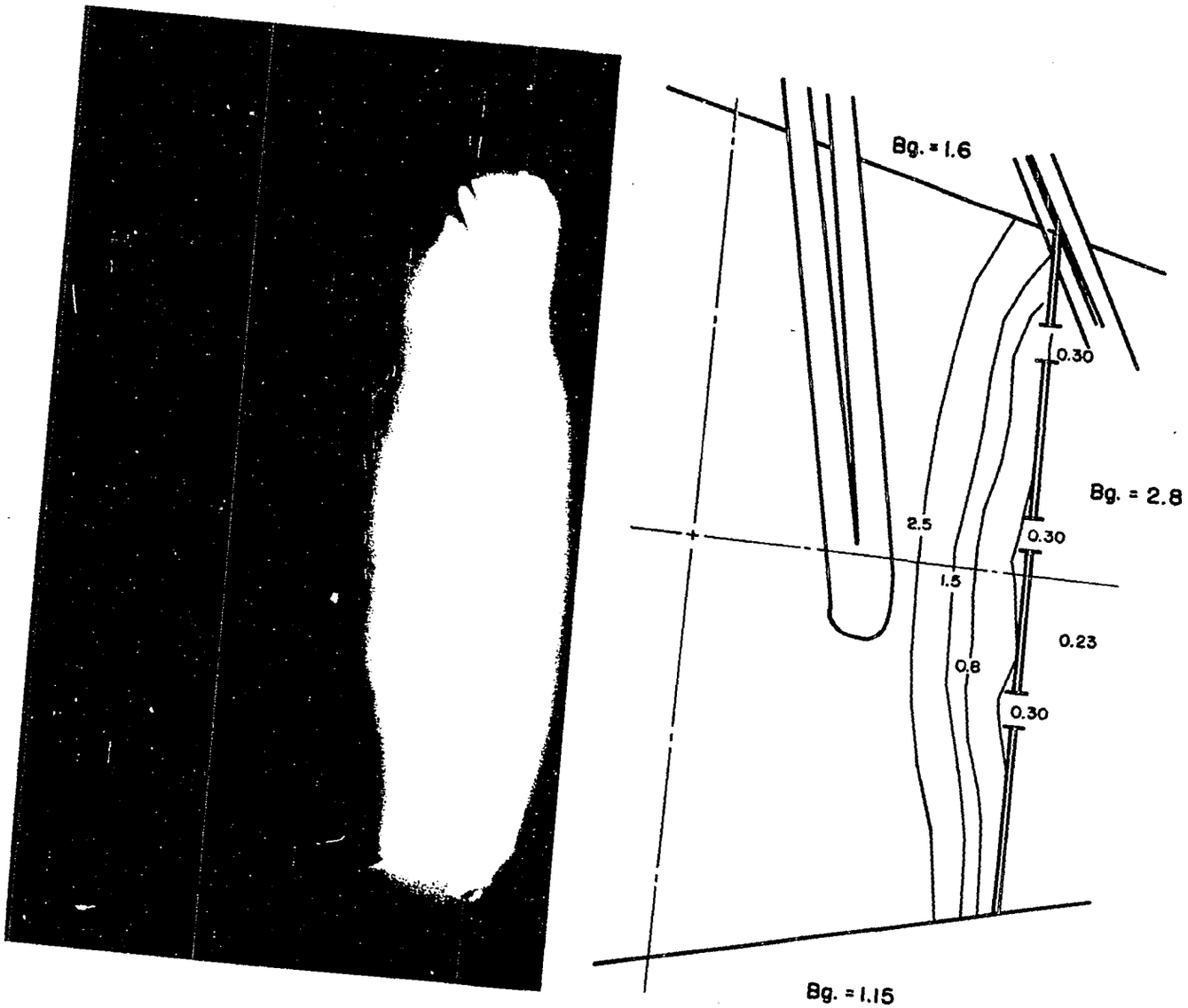
Bg. = 1.6
0.30
Bg. = 2.8
2.5
0.30
1.5
0.23
0.8
0.30
Bg. = 1.15

Table 3. Temperature distributions Advance. Run 11. (Wedge shaped standard. Heat flow parallel to rolling direction. (Figure 9))

Dimensions

dimension	length (in)
l	1.578
w	0.999
t	0.0050
s_1	0.267
w	0.246
p	0.456

Centerline distances, mean temperatures and standard deviations for heater voltage of 140 volts (before and after infrared photography)

position	distance (in)	temp. (^oF) before	after
T1	0.000	867.0±5.0	844.0±2.5
T2	0.224	557.0±1.5	546.0±1.0
T3	0.448	347.5±0.0	341.0±1.0
T4	0.712	234.0±1.5	231.0±0.0
T5	0.924	183.5±0.5	183.5±0.5
End	1.221		

Temperature differences, Carnot efficiencies, temperature gradients and Carnot efficiencies divided by distance between T_h and T_e (before infrared photography)

T	T_h (^oR)	diff. (F^o)	Carnot eff.	grad. (F^o/in)	Carnot eff./in
1	1327				
2		310.0±5.0	0.234	1380	1.04
3		209.5±1.5		935	
4		113.5±1.5		430	
5		50.5±1.5		238	
1-5		683.5	0.515	740	0.558

Table 3. (Continued)

Temperature differences, Carnot efficiencies, temperature gradients, and Carnot efficiencies divided by distance between T_h and T_c (after infrared photography)

T	T_h (^oR)	diff. (F^o)	Carnot eff.	grad. (F^o/in)	Carnot eff./in
1	1304				
2		298.0±2.5	0.228	1330	1.02
3		205.0±1.0		915	
4		110.0±1.0		417	
5		47.5±0.5		224	
1-5		660.5	0.506	715	0.548

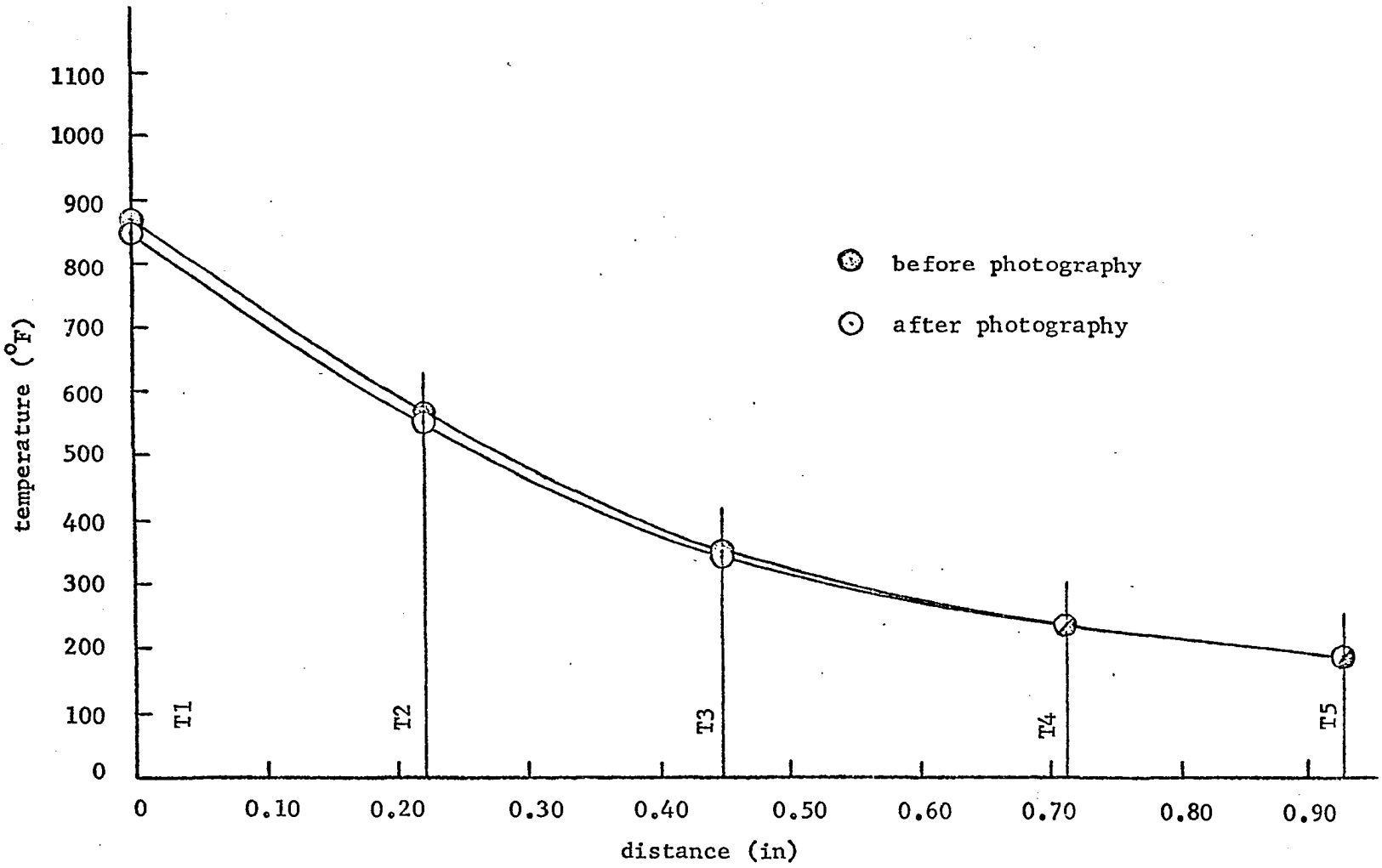

Figure 18. Temperature distributions Advance. Run 11.

Table 4. Temperature distribution Advance. Run 8. (Juxtaposed standard and spot-welded sample. Heat flow parallel to rolling direction (Figure 6))

Dimension and isthmus position

dimension	Length (in) standard	sample
l	1.00	1.00
w	0.243	0.256
t	0.0050	0.0100
isthmus position		
a		0
b		0.131
c		0.149
d		0.256

Centerline distances, mean temperatures and standard diviations for heater voltage of 140 volts

position	distance (in)	temp. (^{o}F)	T_h (^{o}R)	diff. (F^{o})	Carnot eff.	grad. (F^{o}/in)	Carnot eff./in
T1	0	913.0±0.5	1373				
T2	0.240	615.0±4.5		298.0±4.5	0.217	1240	0.903
T3	0.489	457.5±4.5		157.5±6.0		632	
End	0.615						
T4	0	931.0±1.5	1391				
I	0.110						
T5	0.246	620.0±2.0		311.0±2.5	0.224	1260	0.906
End	0.616						

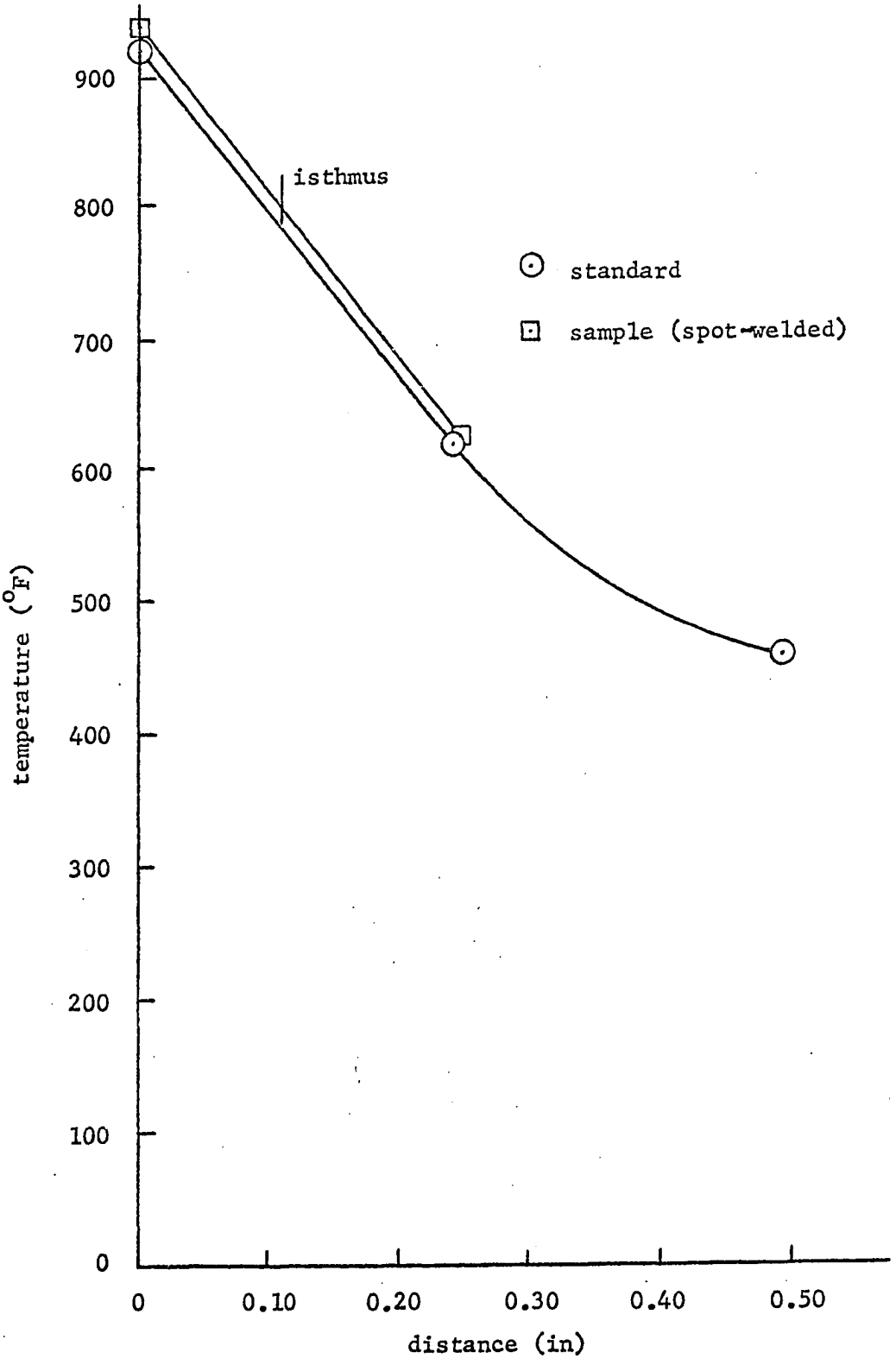

Figure 19. Temperature distribution Advance. Run 8.

Table 5. Temperature distribution Advance. Run 6. (Juxtaposed standard and spot-welded sample. Heat flow perpendicular to rolling direction. (Figure 6))

Dimensions and isthmus position

dimension	length (in) standard	sample
l	1.00	1.00
w	0.251	0.257
t	0.0050	0.0100
isthmus position		
a		0
b		0.128
c		0.142
d		0.257

Centerline distances, mean temperatures and standard deviations for heater voltage of 140 volts (before infrared photography)

position	distance (in)	temp. (^{o}F)	T_h (^{o}R)	diff. (F^{o})	Carnot eff.	grad. (F^{o}/in)	Carnot eff./in
T1	0	928.0±3.5	1388	1388			
T2	0.255	624.0±3.5		304.0±4.5	0.219	1190	0.857
T3	0.493	455.0±3.0		169.0±4.5		710	
T4	0	937.5±1.0	1397.5				
I	0.133						
T5	0.267	613.0±1.5		324.5±1.5	0.232	1220	0.873
(after infrared photography)							
T1		930.0±0.0	1390				
T2		620.0±1.0		310.0±1.0	0.223	1220	0.878
T3		455.0±0.5		165.0±1.0		693	
T4		934.5±0.5	1394.5				
I							
T5		607.0±1.5		327.5±1.5	0.235	1230	0.882

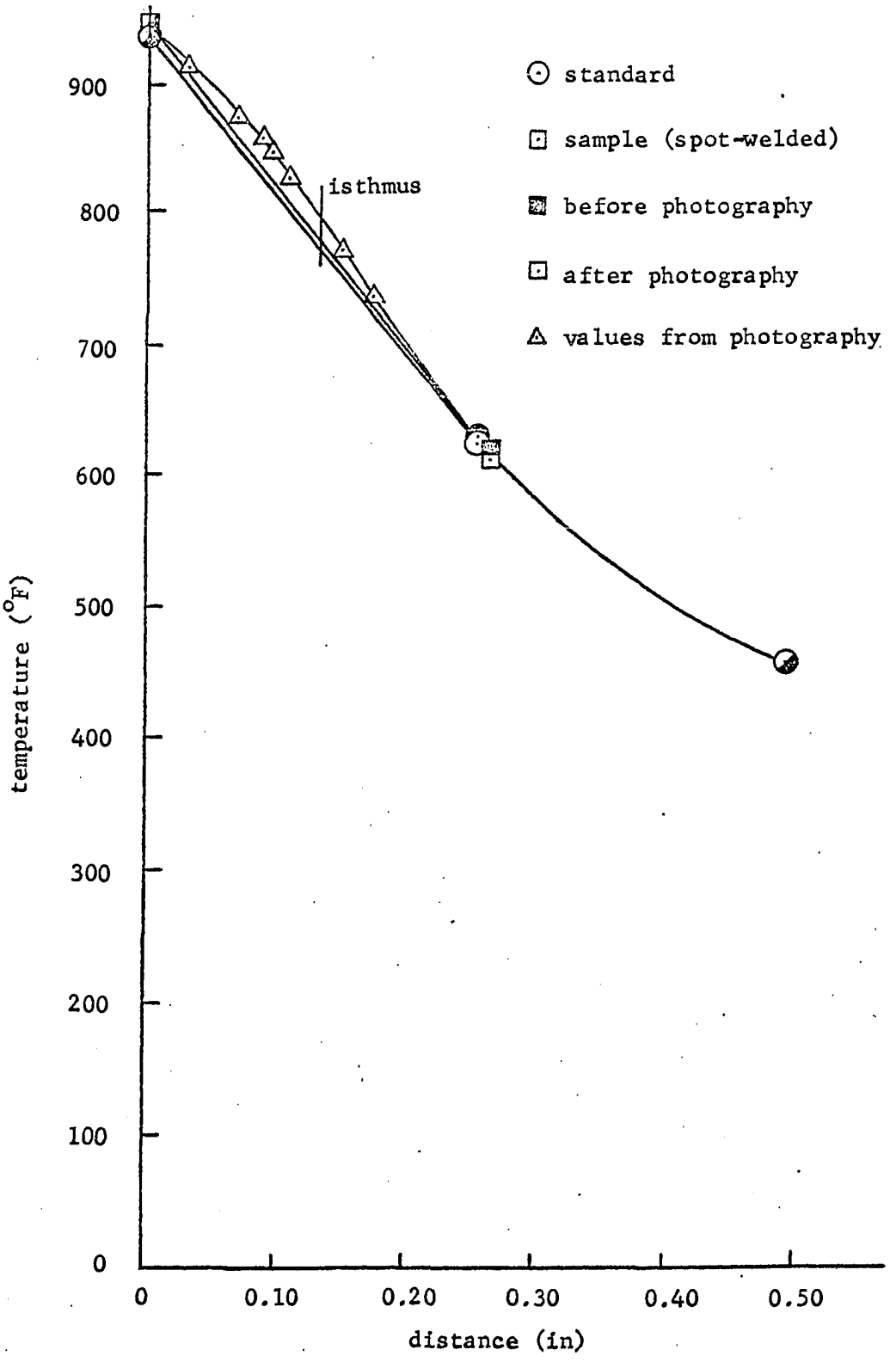

Figure 20. Temperature distribution Advance. Run 6.

Figure 21. Infrared photograph Advance. Run 6. (Exposure: 16 hr 15 min, stop: f/4.0, filter: 87, film: Kodak IR 135-20) (11X)

Figure 22. Diagram of film density (temperature) contours Advance. Run 6. (11X)

film density	temp. (°F)
0.25	905
0.5	867
1.0	850
1.5	840
2.0	820
2.6	765
2.7	730

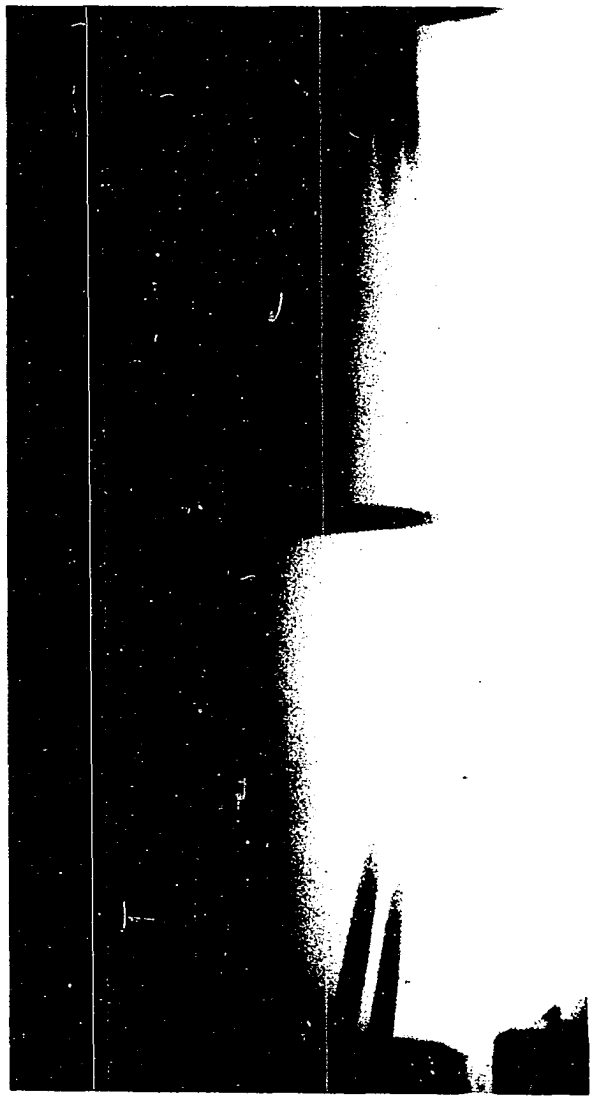

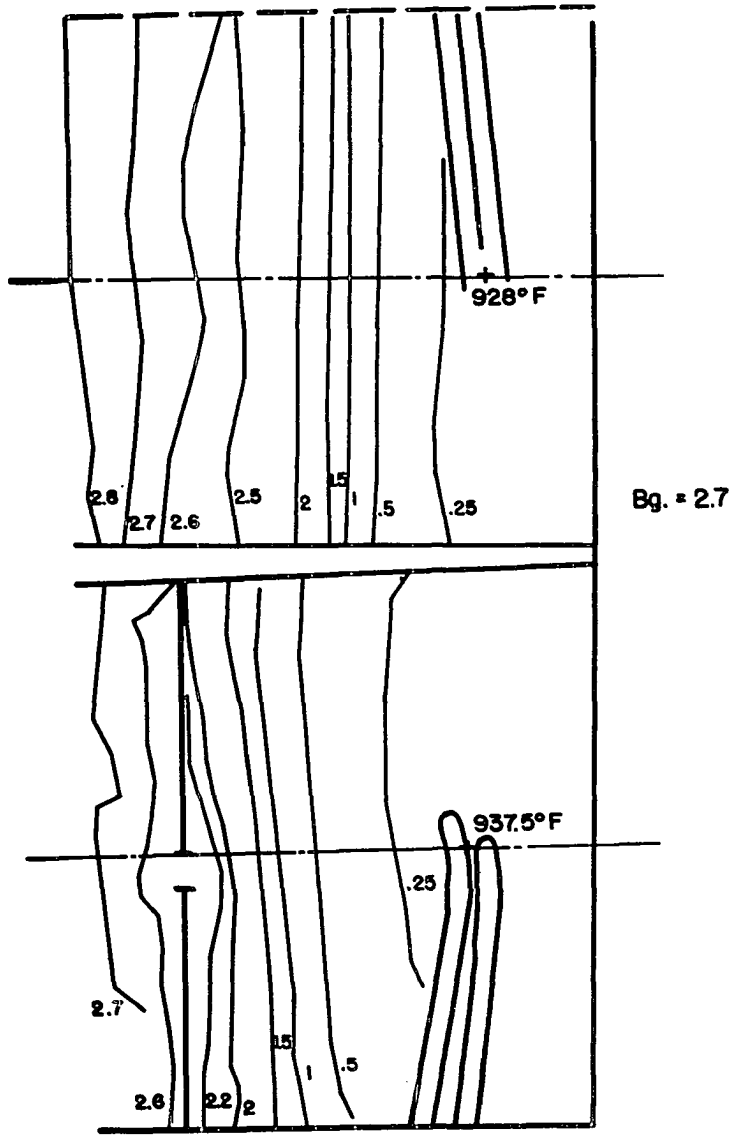

Bg. = 2.7

Table 6. Temperature distribution Advance. Run 13. (Juxtaposed standard and shears-cut sample. Heat flow perpendicular to rolling direction. (Figure 6))

Dimensions and isthmus position

dimension	length (in) standard	sample
l	1.00	1.00
w	0.257	0.255
t	0.0050	0.0050
isthmus position		
a		0
b		0.104
c		0.143
d		0.255

Centerline distances, mean temperatures and Standard deviations for heater voltage of 140 volts

position (standard)	distance (in)	temp. (^{o}F)	T_h (^{o}R)	diff. (F^{o})	Carnot eff.	grad. (F^{o}/in)	Carnot eff./in
T1	0	865.0±1.0	1325				
T2	0.268	529.5±0.5		355.5±1.0	0.253	1250	0.943
T3	0.508	375.0±0.0		154.5±0.5		644	
End	0.636						
(sample)							
T4	0	868.0±0.0	1328				
I	0.117						
T5	0.239	404.0±1.0		464.0±1.0	0.349	1940	1.46
T6	0.492	289.0±0.5		115.0±1.0		454	
End	0.606						
(sample--2nd segment twisted 90^{o})							
T4	0	876.5±0.0	1336.5				
T5	0.239	364.0±0.5		512.5±0.5	0.383	2140	1.60
T6	0.492	267.0±2.0		97.0±2.0		384	
(sample--2nd segment broken off)							
T4	0	910.0±0.0					

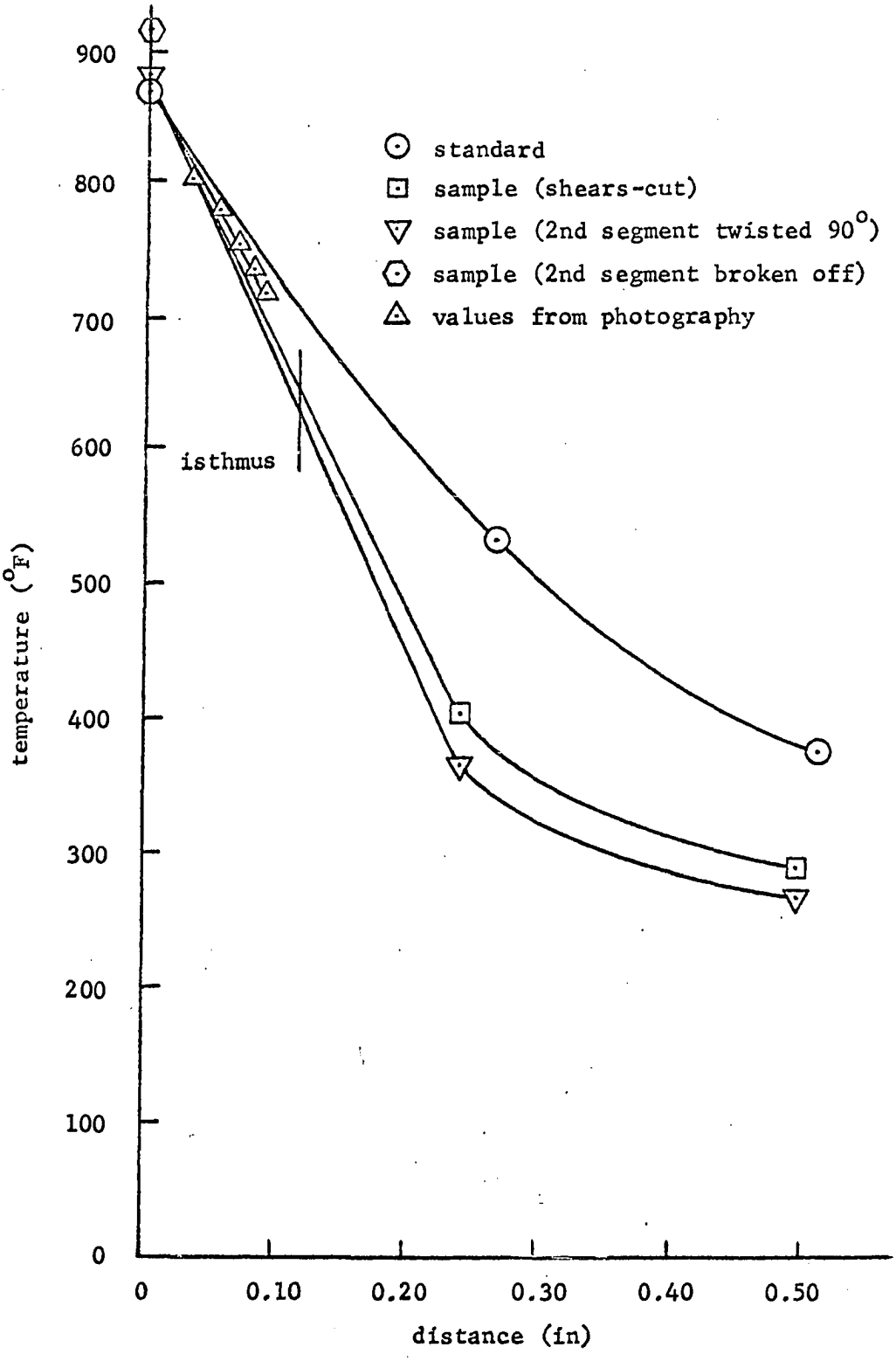

Figure 23. Temperature distribution Advance. Run 13.

Figure 24. Infrared photograph Advance. Run 13. (Exposure: 16 hr, stop: f/4.0, filter: 87, film: Kodak IR 135-20) (6.3X)

Figure 25. Diagram of film density (temperature) contours Advance. Run 13. (6.3X)

film density	temp. (^{o}F)
0.5	825
1.0	800
2.0	775
2.4	750
2.7	730
2.8	715

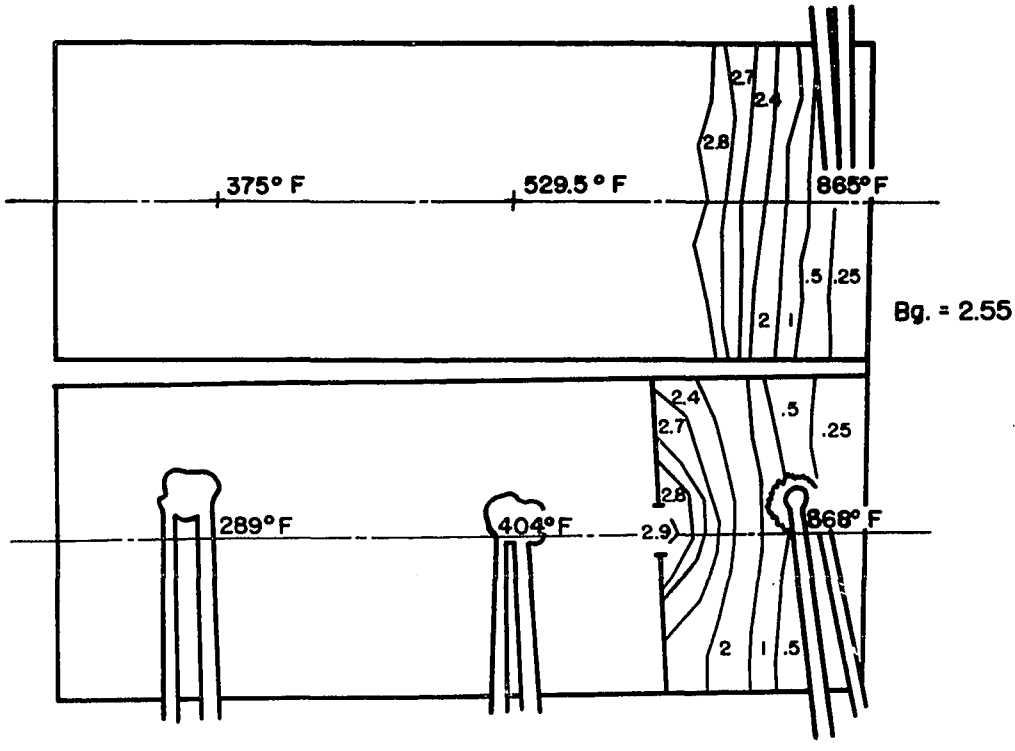
375° F
529.5° F
865° F
2.7
2.4
2.8
.5
.25
2
1
Bg. = 2.55
2.4
2.7
.5
.25
2.8
289° F
404° F
2.9
868° F
2
1
.5

Table 7. Temperature distribution Chromel-P. Run 9. (Rectangular generator element. Heat flow parallel to rolling direction. (Figure 10))

Dimensions, position of isthmuses, and centerline distances

dimension	length (in)
l	1.57
w	1.00
t	0.010
position of isthmuses	
a	0
b	0.395
c	0.423
d	0.509
e	0.537
f	0.647
g	0.675
h	1.000
centerline distances	
T1	0
N2	0.120
T2	0.223
N3	0.347
T3	0.450
N4	0.574
T4	0.685
N5	0.804
T5	0.929

Mean temperatures and standard deviations for different voltages

(For heater voltage 140v)

position	temp. (^{o}F)	T_h (^{o}R)	diff. (F^{o})	Carnot eff.	grad. (F^{o}/in)	Carnot eff./in
T1	924.5±0.5	1384.5				
T2	614.0±0.0		310.5±0.5	0.224	1390	1.00
T3	418.0±1.0		196.0±1.0		863	

Table 7. (Continued)

position	temp. (^{o}F)	T_h (^{o}R)	diff. (F^{o})	Carnot eff.	grad. (F^{o}/in)	Carnot eff./in
T4	301.0±0.0		117.0±1.0		498	
T5	233.0±1.0		68.0±1.0		279	
T1-T5			691.5	0.499	744	0.537
(For heater voltage 158v)						
T1	1036.5±0.5					
T2	681.0±0.5		355.5±1.0		1590	
T3	459.0±1.5		222.0±1.5		978	
T4	331.5±1.5		127.5±2.0		542	
T5	246.0±1.0		85.5±2.0		350	

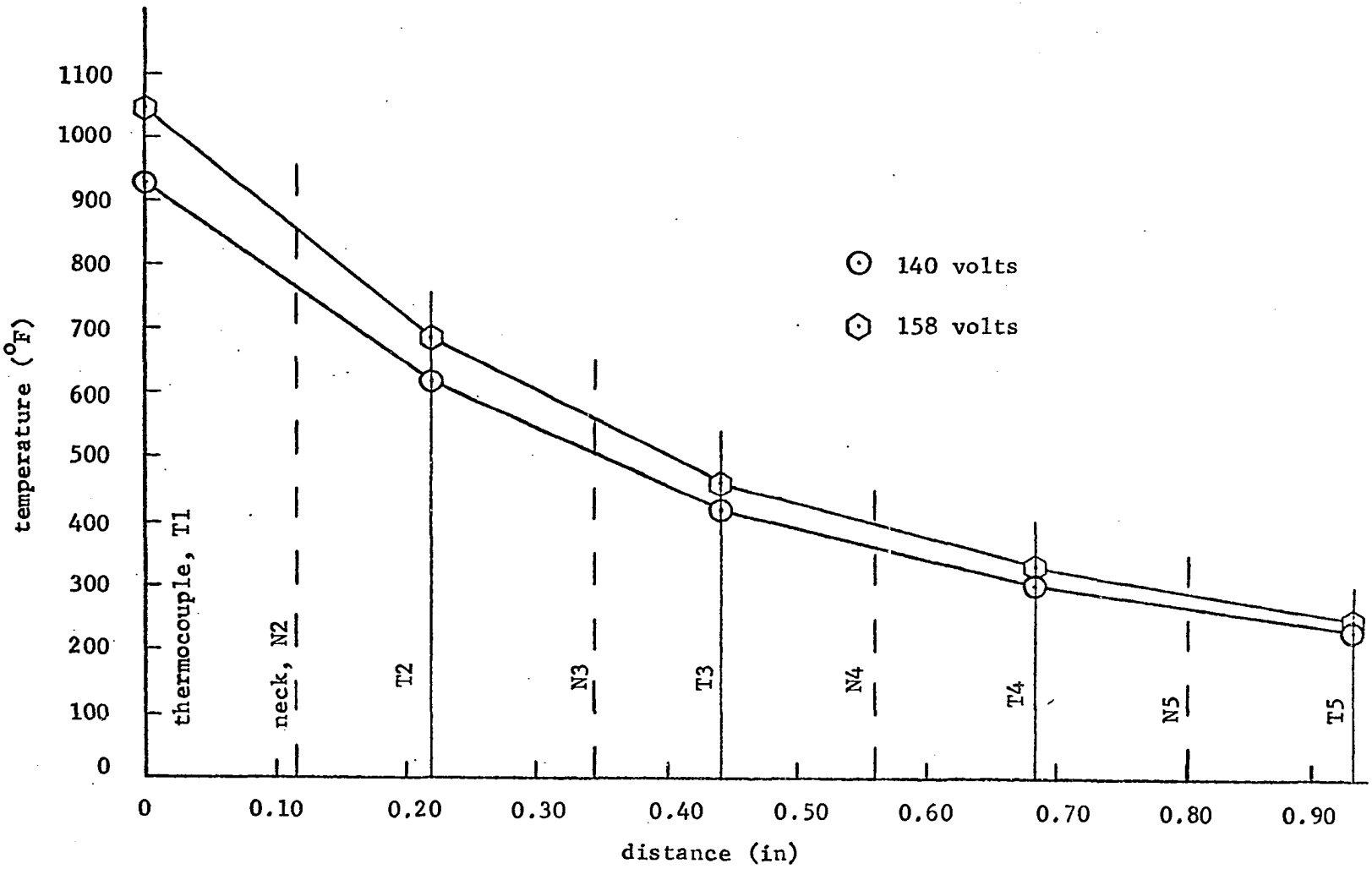

Figure 26. Temperature distributions Chromel-P. Run 9.

Figure 27. Infrared photograph Chromel-P. Run 9. (Exposure:) 16 hr, stop: f/4.0, filter: 87, film: Kodak IR 135-20, T_h=924.5°F) (11X)

Figure 28. Diagram of film density (temperature) contours Chromel-P. Run 9. (11X)

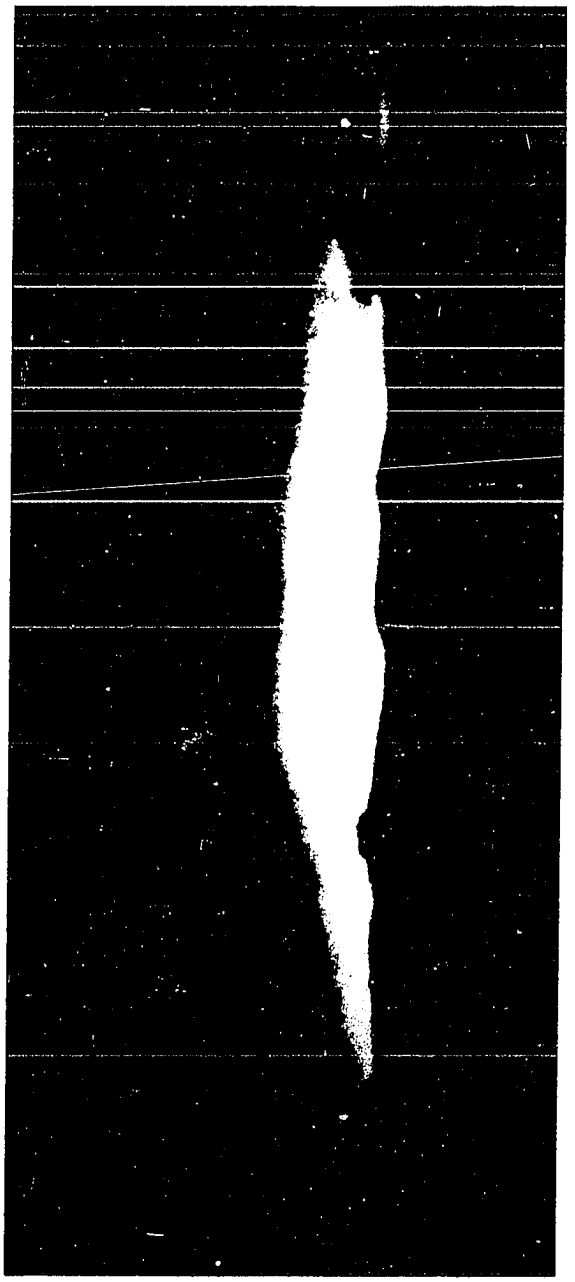

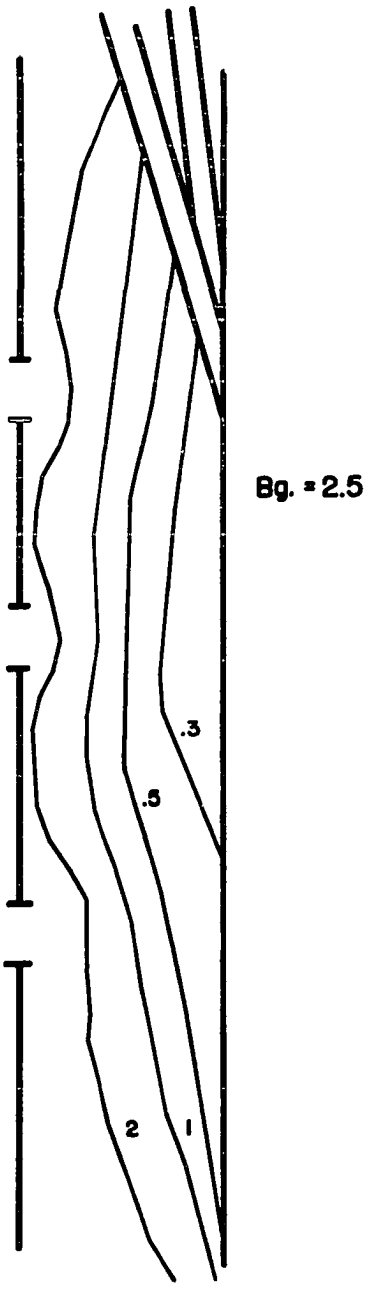
Bg. = 2.5
.3
.5
2
1

Figure 29. Infrared photograph Chromel-P. Run 9. (Exposure: 3 hr, stop: f/4.0, filter: 87, film: Kodak IR 135-20, T_h= 1036.5°F) (9.7X)

Figure 30. Diagram of film density (temperature) contours Chromel-P. Run 9. (9.7X)

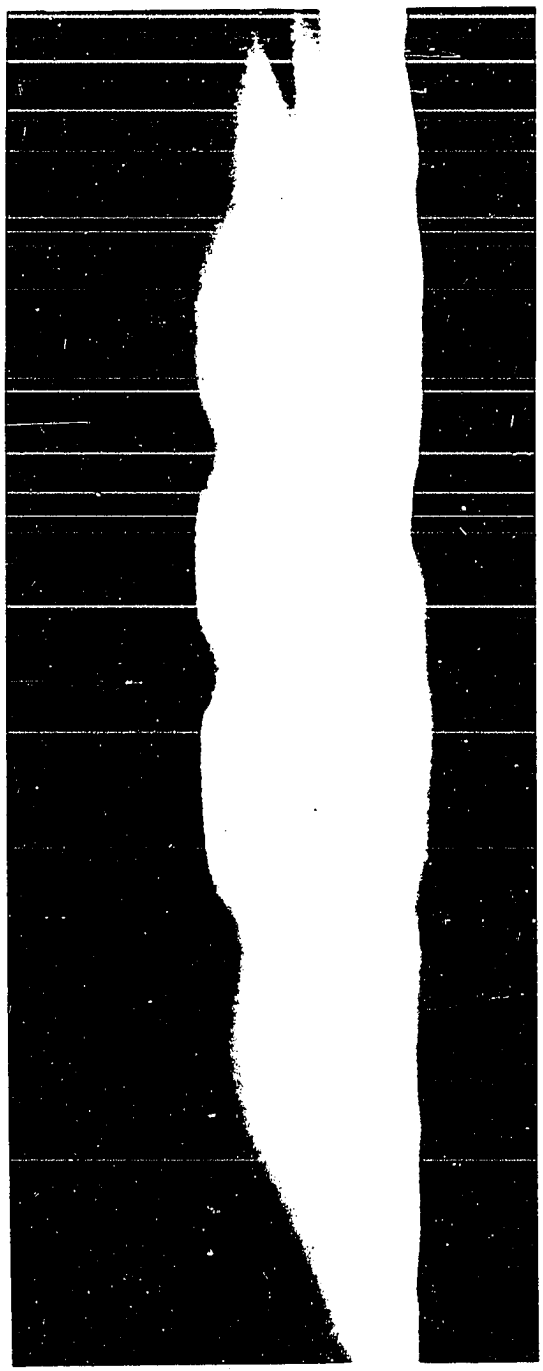

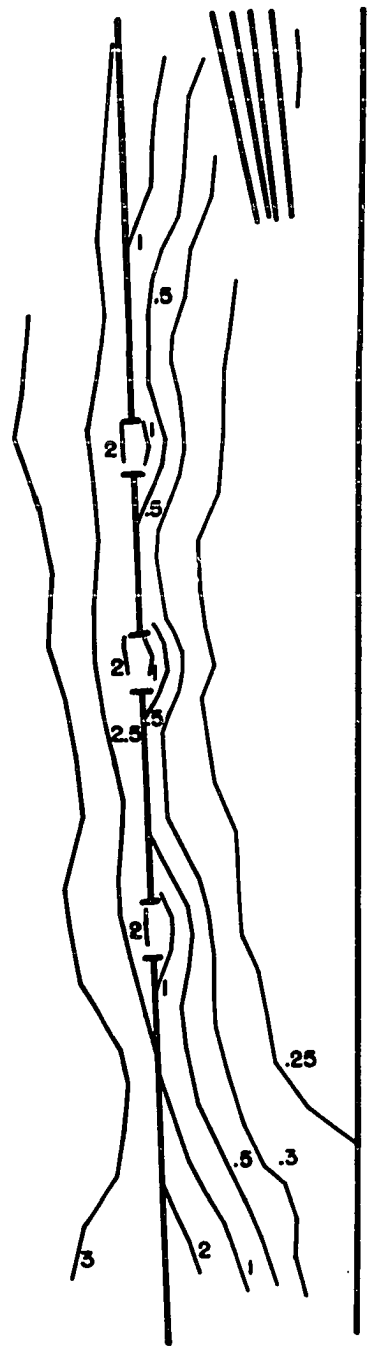

Bg. = 2.8

Table 8. Temperature distributions Chromel-P. Run 10. (Rectangular standard. Heat flow parallel to rolling direction. (Figure 11))

Dimensions and centerline distances

dimension	length (in)
l	0.426
w	0.999
t	0.0050
centerline distances	
T1	0
T2	0.223
T3	0.464
T4	0.703
T5	0.917
End	1.181

Mean temperatures and standard deviations for heater voltage of 140 volts (Thermocouples on rear side of sample)

position	temp. (^{o}F)	T_h (^{o}R)	diff. (F^{o})	Carnot eff.	grad. (F^{o}/in)	Carnot eff./in
T1	895.0±2.0	1355				
T2	566.5±1.0		328.5±2.5	0.242	1470	1.08
T3	370.5±0.5		196.0±1.0		813	
T4	245.5±1.5		116.0±1.5		485	
T5	199.0±1.0		55.5±2.0		259	
End						
T1-T5			696.0	0.514	759	0.560
(Thermocouples on front side)						
T1	860.0±1.0	1320				
T2	535.5±1.5		324.5±2.0	0.246	1460	1.11
T3	340.5±1.5		195.0±2.5		809	
T4	235.5±0.0		105.0±1.5		439	
T5	177.5±1.5		58.0±1.5		271	
T1-T5			682.5	0.517	754	0.564

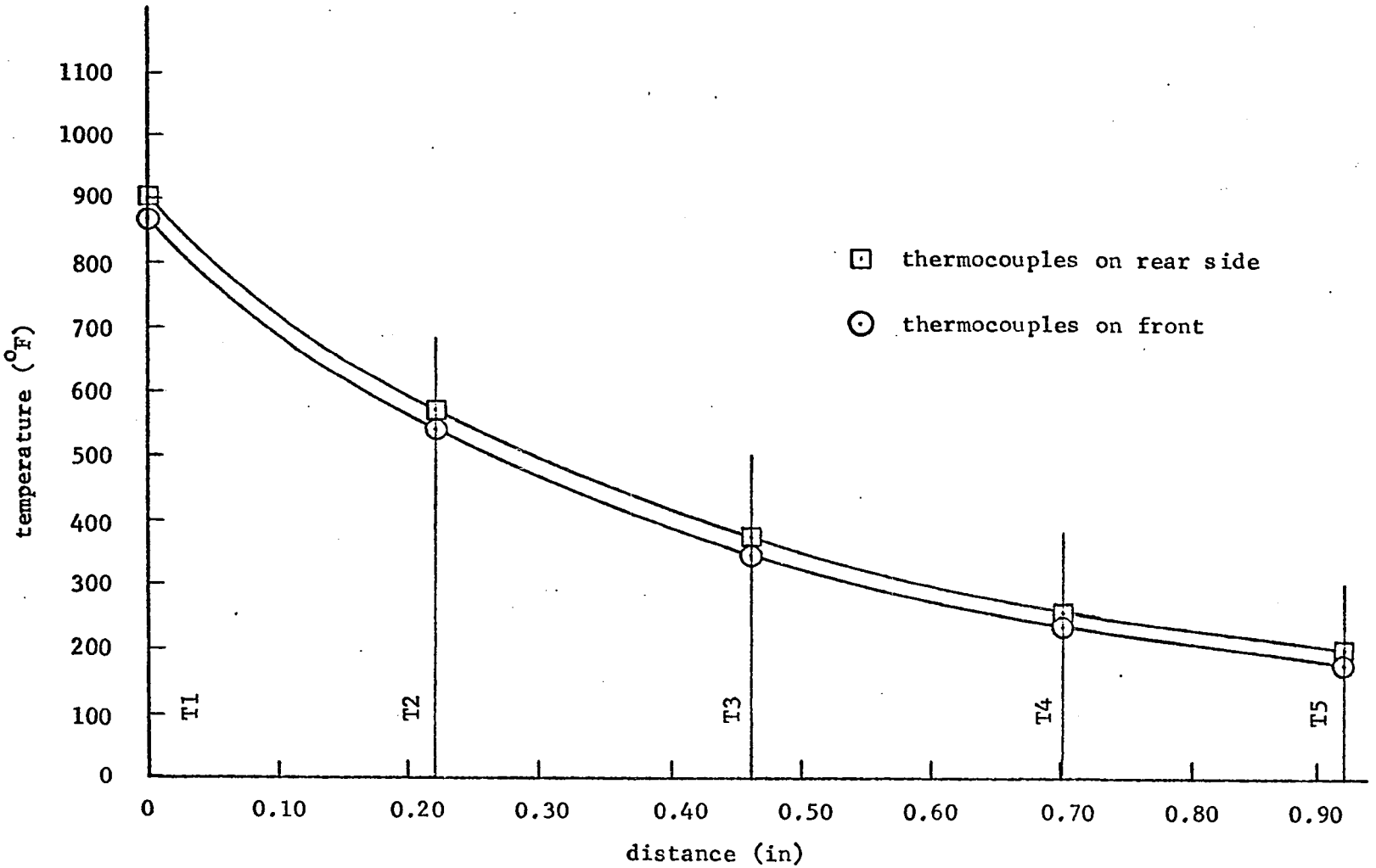

Figure 31. Temperature distribution Chromel-P. Run 10.

Table 9. Effect of orientation of specimens on temperature distribution. Chromel-P. Run 7. (Juxtaposed standard and spot-welded sample. Heat flow parallel to rolling direction. (Figure 6))

Dimensions and isthmus position

dimension	length (in) standard	sample
l	1.00	1.00
w	0.248	0.248
t	0.0050	0.0100
isthmus position		
a		0
b		0.095
c		0.123
d		0.248

Centerline distances, mean temperatures and standard deviations for heater voltages of 140 volts

(Vertical (normal) immediately after infrared photography)

position	distance (in)	temp. (^oF)	T_h (^oR)	diff. (F^o)	Carnot eff.	grad. (F^o/in)	Carnot eff./in
T1	0	851.0±1.0	1311				
T2	0.226	531.5±1.5		319.5±1.5	0.244	1410	1.08
T3	0.484	351.0±1.0		180.5±2.0		700	
T4	0	878.5±2.5	1338.5				
I	0.113						
T5	0.240	521.5±1.5		357.0±2.5	0.267	1490	1.11

Table 9. (Continued)

Effect of placement of specimens on extraneous heat losses and thus centerline temperatures

position	temp. (°F)	temp. diff. (F°)	temp. grad. (F°/in)
(Horizontal, thermocouples on top)			
T1	824.5±1.5		
T2	493.0±0.5	331.5±1.5	1470
T3	323.0±7.5	170.0±7.5	659
T4	897.5±2.0		
T5	571.0±2.0	326.5±3.0	1360
(Vertical, thermocouples on rear)			
T1	787.0±2.5		
T2	435.0±2.0	352.0±3.0	1560
T3	263.0±2.0	172.0±3.0	667
T4	896.5±2.0		
T5	559.5±2.0	337.0±3.5	1400
(Horizontal, thermocouples on bottom)			
T1	843.5±0.0		
T2	528.0±1.0	315.5±1.0	1400
T3	342.5±2.0	185.5±2.0	719
T4	895.0±1.0		
T5	582.0±1.0	313.0±1.5	1300
(Vertical (normal), thermocouples on front, 15 hrs after infrared photography)			
T1	841.0±3.0		
T2	523.5±1.5	317.5±3.0	1400
T3	336.0±1.0	187.5±2.0	727
T4	876.0±2.0		
T5	523.5±1.5	352.5±2.5	1470

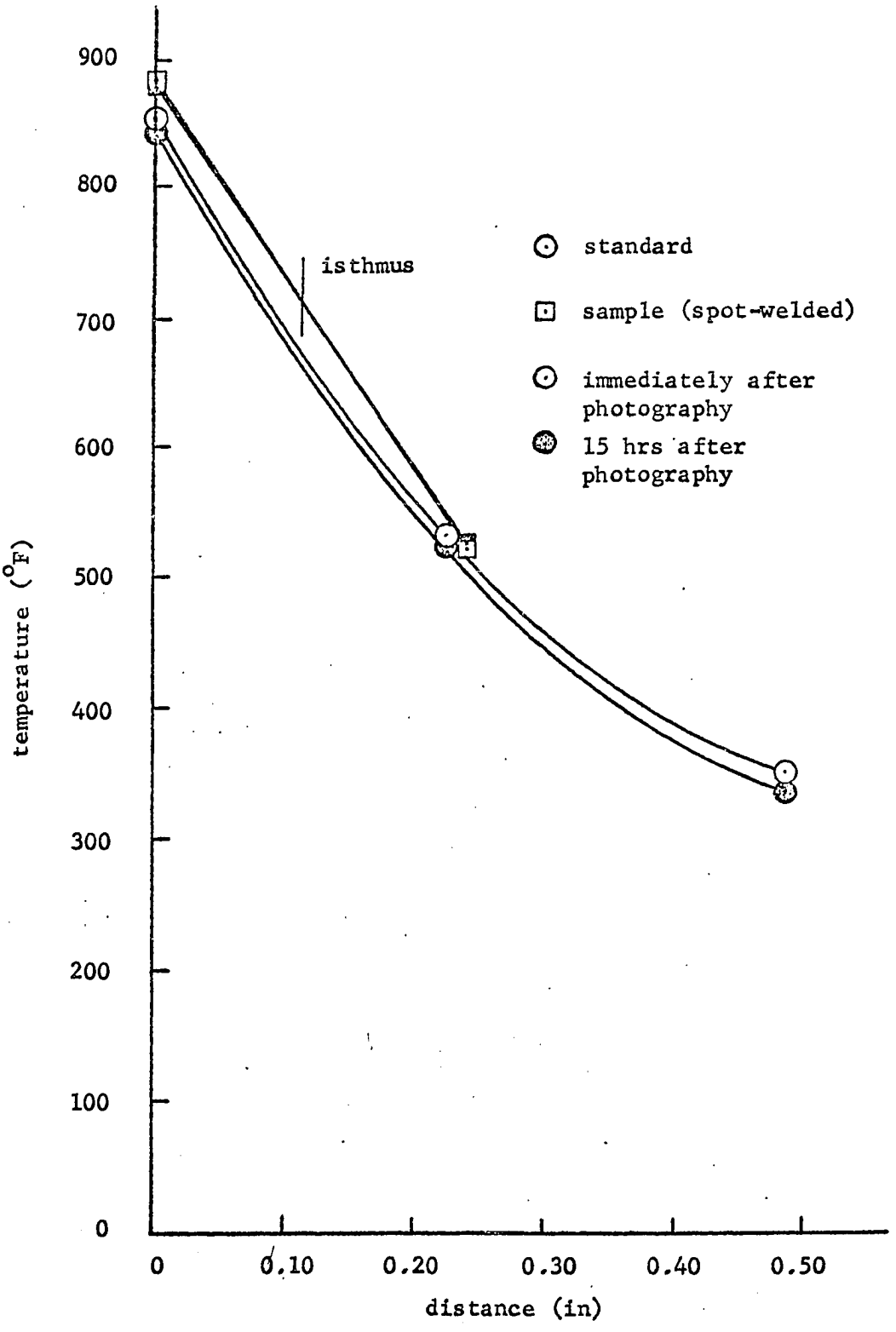

Figure 32. Temperature distribution Chromel-P. Run 7.

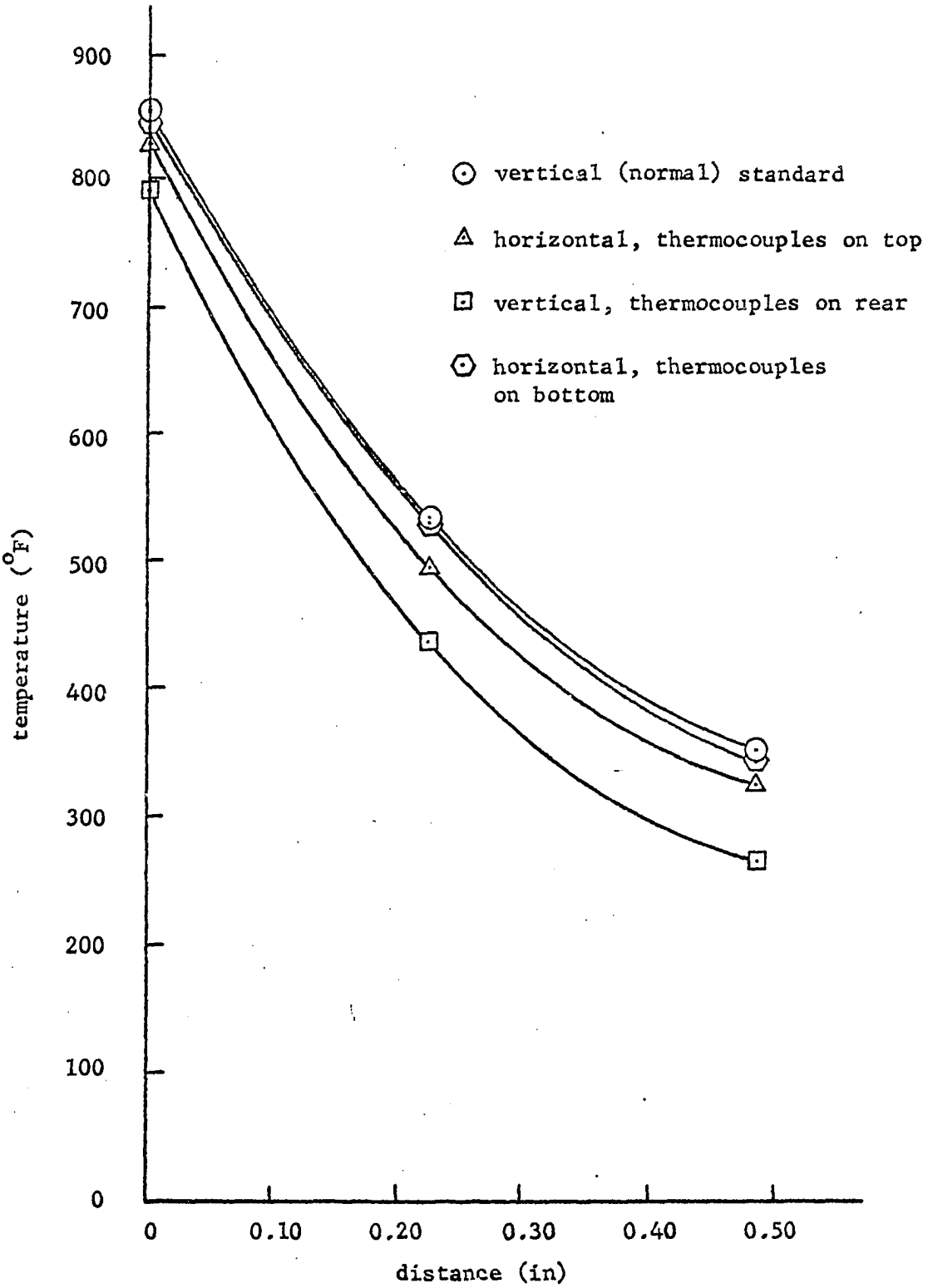

Figure 33. Effect of orientation of specimens on temperature distribution Chromel-P. Run 7.

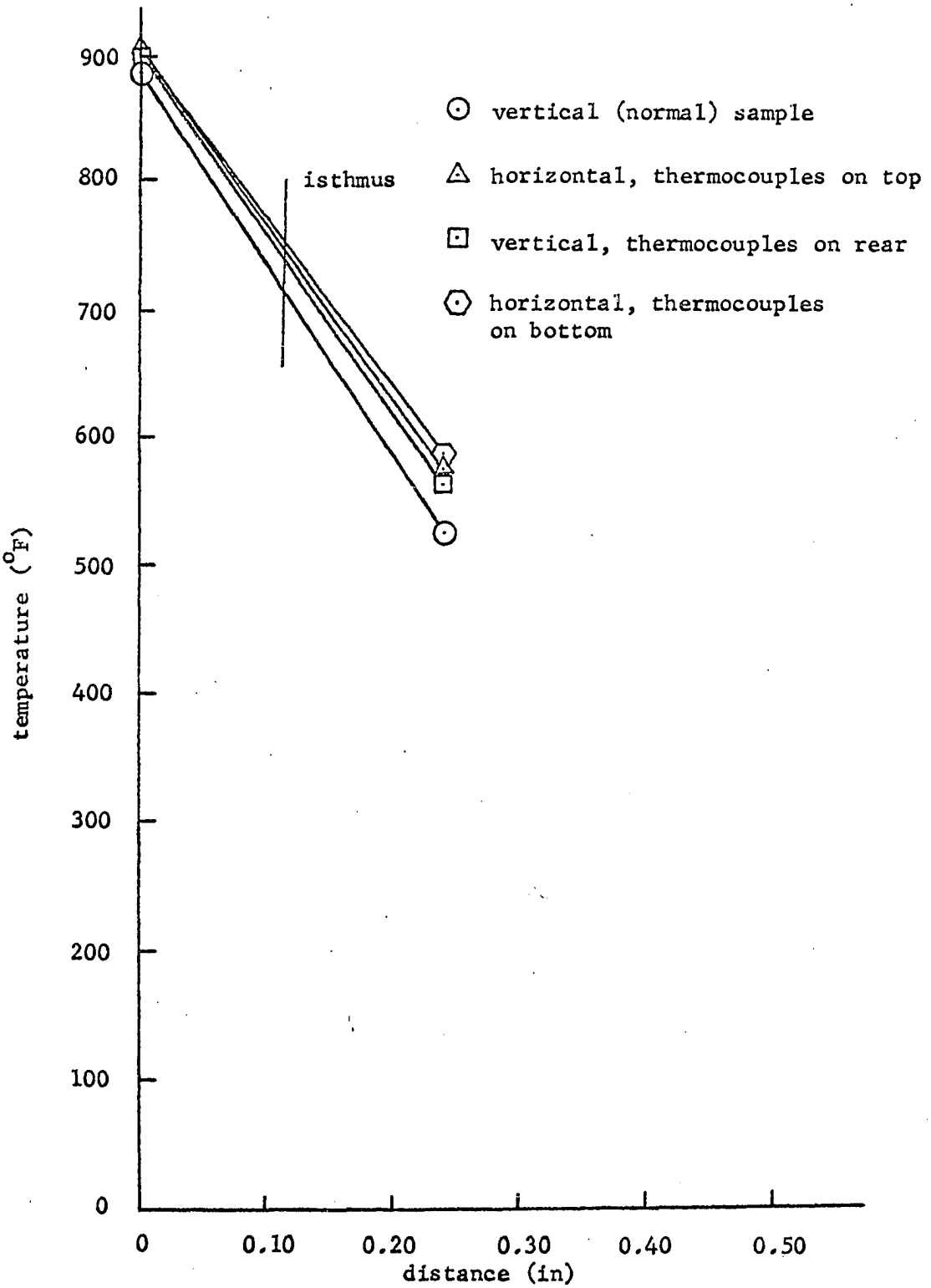

Figure 34. Effect of orientation of specimens on temperature distribution Chromel-P. Run 7.

Table 10. Temperature distribution Chromel-P. Run 5. (Juxtaposed standard and spot-welded sample. Heat flow perpendicular to rolling direction. (Figure 6))

Dimensions and isthmus position

dimension	length (in) standard	sample
l	1.00	1.00
w	0.248	0.249
t	0.0050	0.0100
isthmus position		
a		0
b		0.086
c		0.115
d		0.249

Transient temperatures during heating at a heater voltage of 113 volts

position	temperature (^{o}F)	time (min)
T5	218	5
T2	256.5	7
T2	310.5	9
T5	388	11
T4	650	13
T1	688	15
T1	728	17
T4	771	19
T4	793	21
T5	520.5	23
T2	479.5	25
T2	482	27
T5	536.5	29
T4	832	31
T4	839	35
T4	831	40
T1	816	44
T1	808	49

Table 10. (Continued)

Centerline distances, mean temperatures and standard deviations for (^{o}F) heater voltages of 140 volts

position	distance	temp. (^{o}F)	T_h (^{o}R)	diff. (F^{o})	Carnot eff.	grad. (F^{o}/in)	Carnot eff./in
T1	0	860.0±1.0	1320				
T2	0.245	529.0±1.5		331.0±2.0	0.251	1350	1.02
T3	0.502	364.0±2.0		165.0±2.5		624	
End	0.623						
T4	0	864.0±1.0	1324				
I	0.123						
T5	0.238	556.0±0.0		308.0±1.0	0.233	1290	0.974
End	0.629						

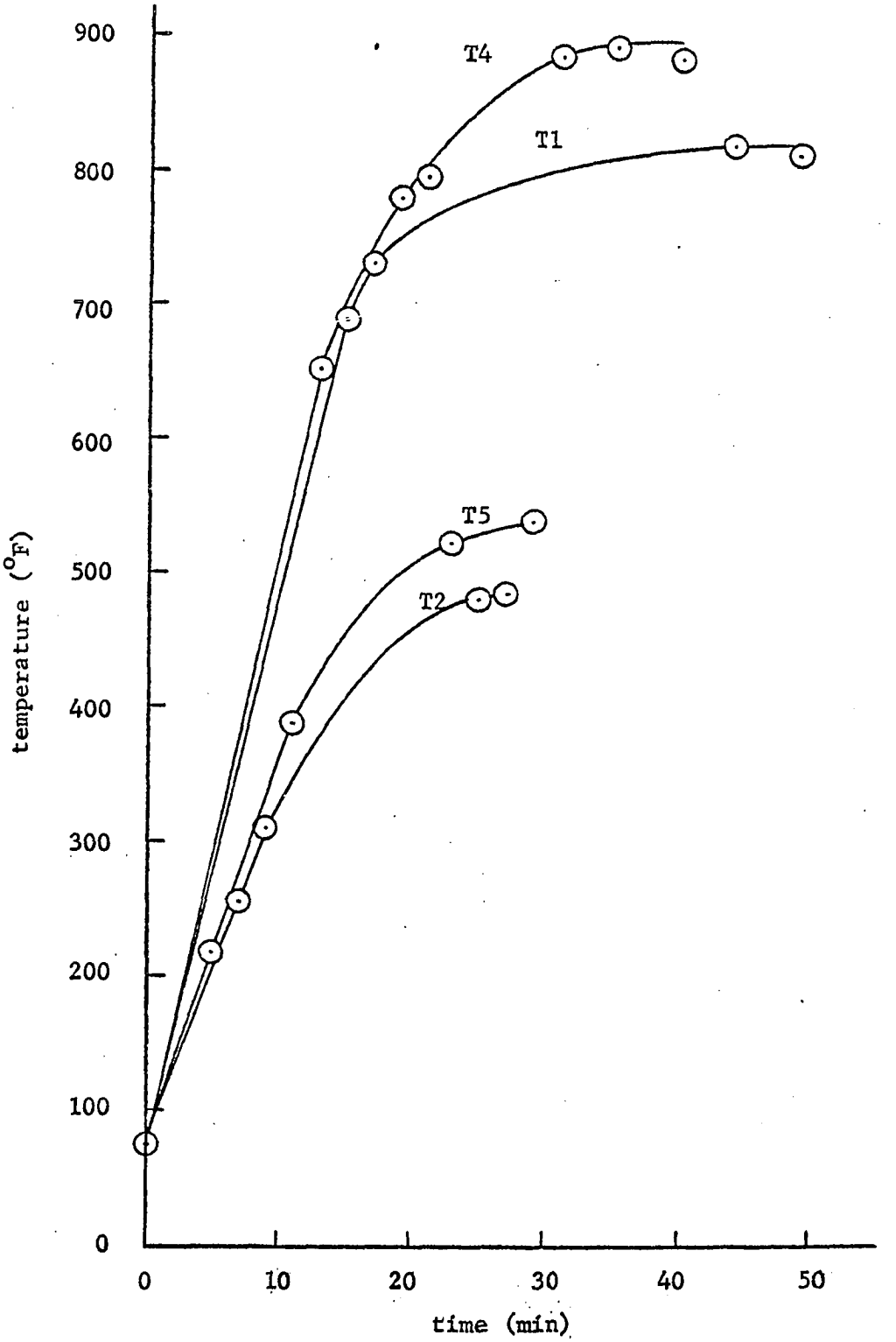

Figure 35. Transient temperatures Chromel-P. Run 5.

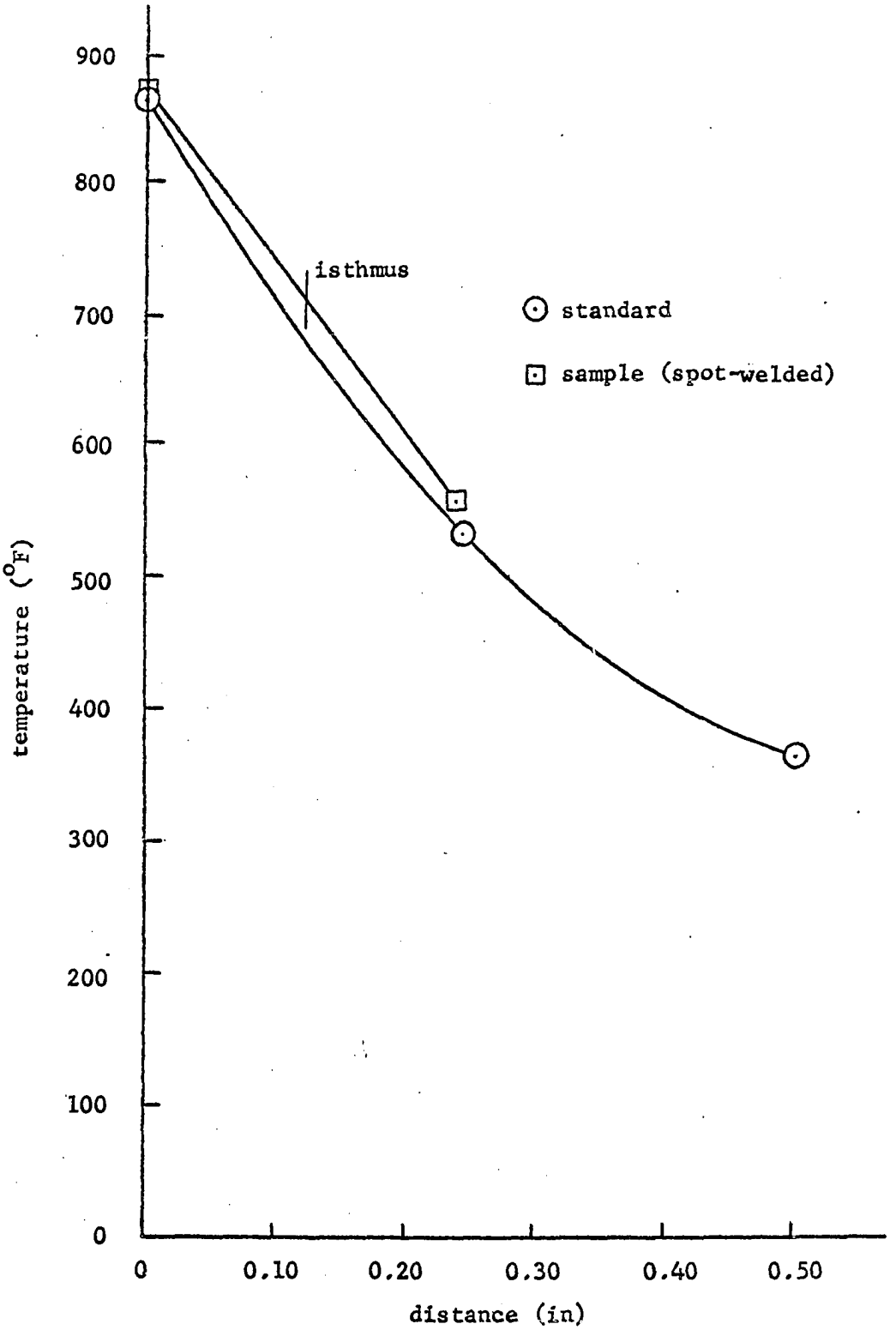

Figure 36. Temperature distribution Chromel-P. Run 5.

Table 11. Temperature distribution Chromel-P. Run 12. (Juxtaposed standard and shears-cut sample. Heat flow parallel to rolling direction. (Figure 6))

Dimensions and isthmus position

dimension	length (in) standard	sample
1	1.00	1.00
w	0.248	0.247
t	0.0050	0.0050
isthmus position		0
a		0
b		0.097
c		0.153
d		0.247

Centerline distances, mean temperatures and standard deviations for heater voltages of 140 volts

position	distance (in)	temp. (^{o}F)	T_h (^{o}R)	diff. (F^{o})	Carnot eff.	grad. (F^{o}/in)	Carnot eff./in
T1	0	801.0±1.5	1261				
T2	0.226	490.0±1.0		311.0±2.0	0.247	1380	1.09
T3	0.484	316.0±1.5		174.0±1.5		674	
T4	0	808.0±2.0	1268				
I	0.113						
T5	0.250	371.0±0.0		437.0±2.0	0.345	1750	1.38
T6	0.519	237.5±0.5		133.5±0.5		496	

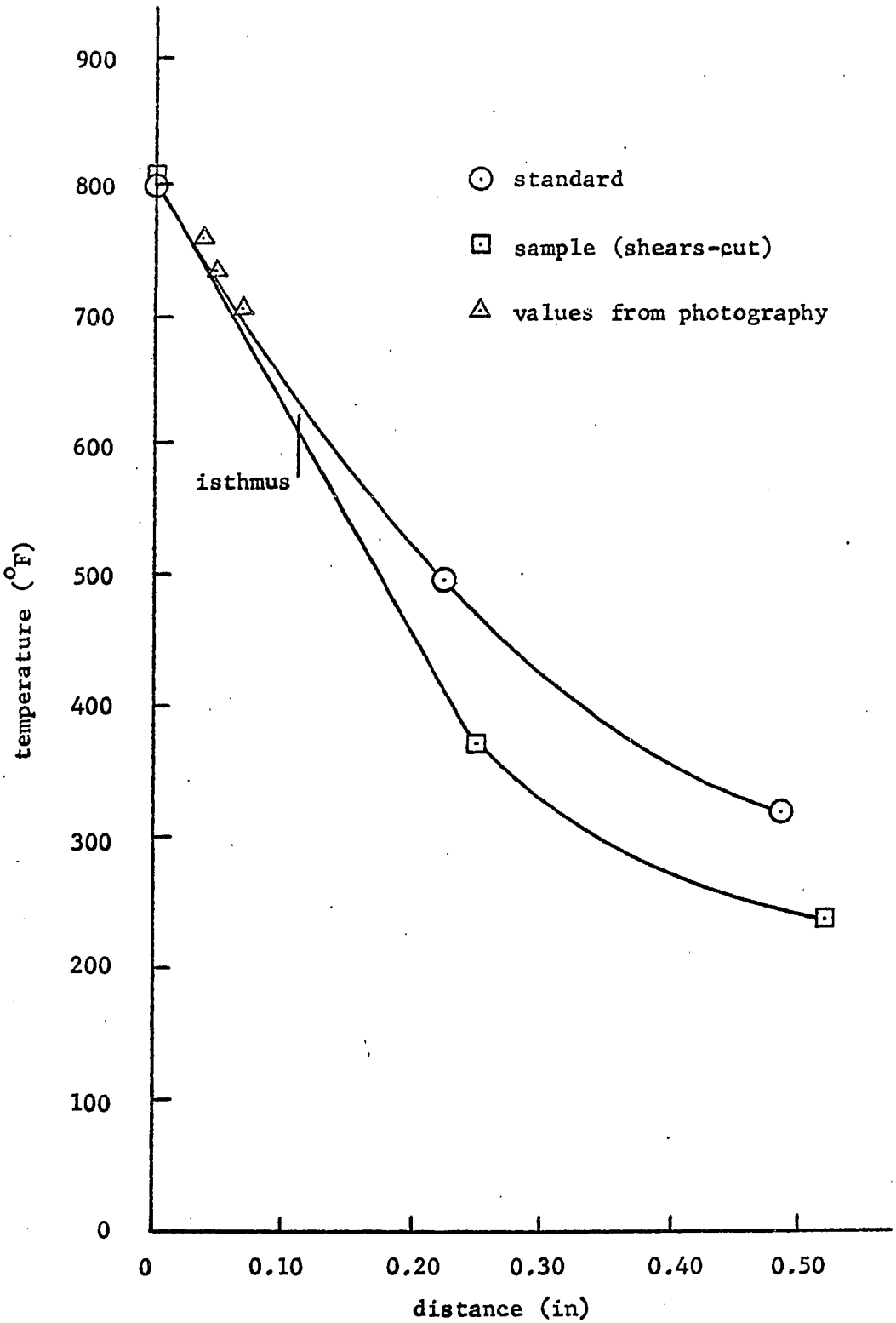

Figure 37. Temperature distribution Chromel-P. Run 12.

Figure 38. Infrared photograph Chromel-P. Run 12. (Exposure: 16 hr 10 min, stop: f/4.0, filter: 87, film: Kodak IR 135-20) (8.9X)

Figure 39. Diagram of film density (temperature) contours Chromel-P. Run 12. (8.9X)

film density	temp. (°F)
2.0	755
2.5	730
2.8	700

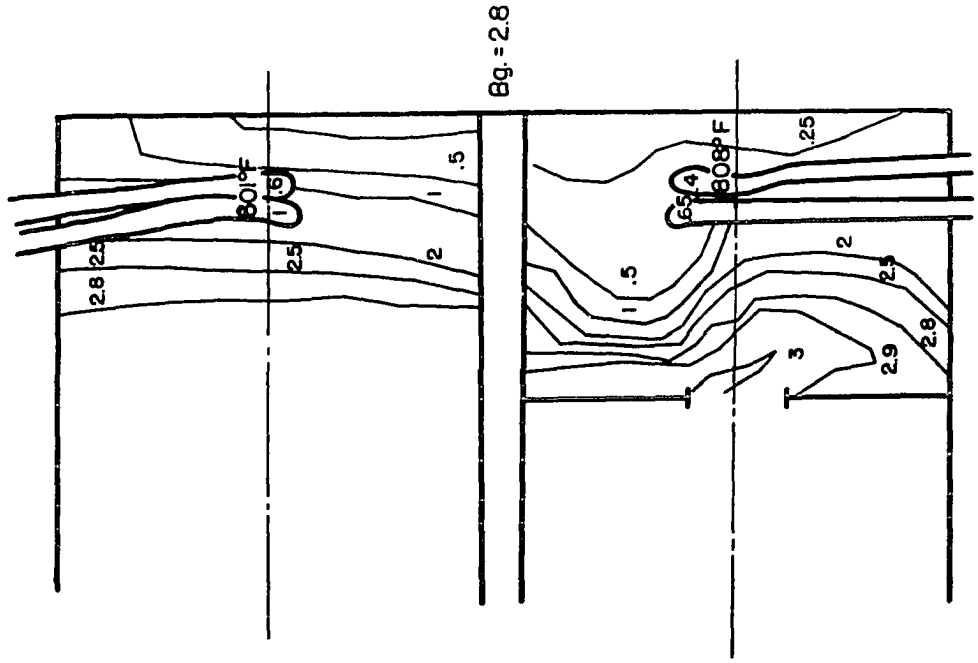
Bg.=2.8
80°F
.5
1
2
2.5
2.8
.25
65.4
80.8°F
.5
1
2
2.5
2.8
2.9
3

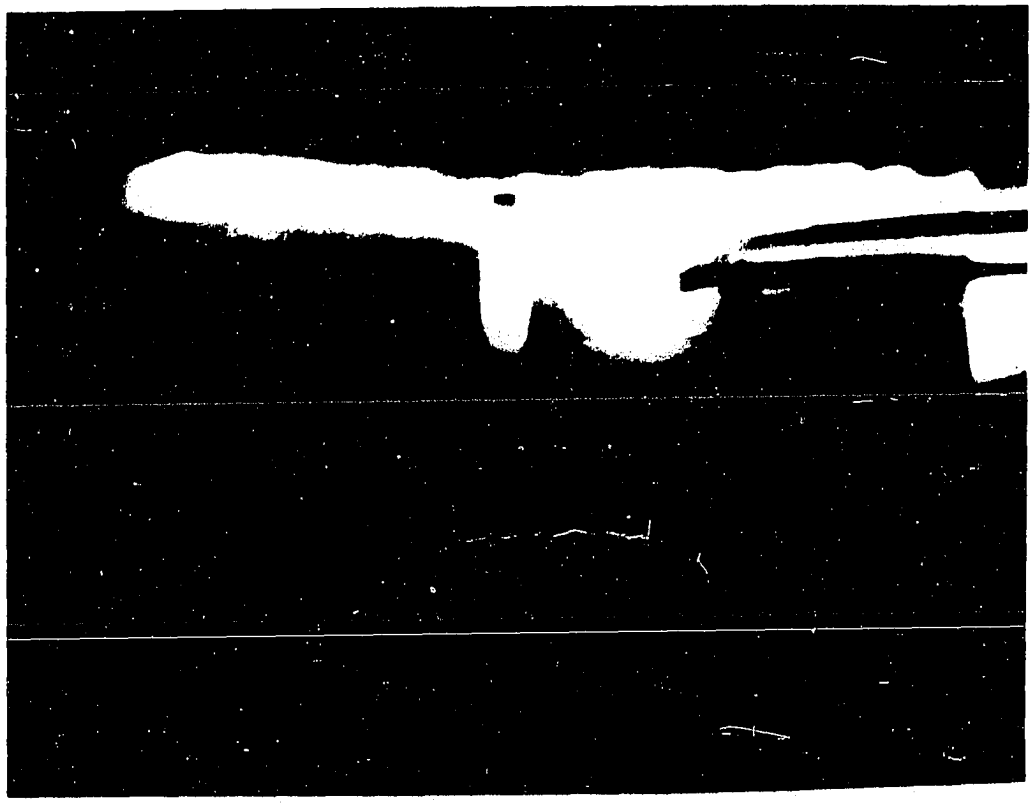

Table 12. Temperature distributions Nichrome V. Run 4. (Juxtaposed standard and spot-welded sample. Heat flow perpendicular to rolling direction. (Figure 6))

Dimensions and isthmus position

dimension	length (in) standard	sample
l	1.00	1.00
w	0.258	0.250
t	0.0050	0.0100
isthmus position		
a		0
b		0.123
c		0.155
d		0.250

Centerline distances, mean temperatures and standard deviations for heater voltage of 140 volts

position	distance (in)	temp. (^{o}F)	Th (^{o}R)	diff. (F^{o})	Carnot eff.	grad. (F^{o}/in)	Carnot eff./in
T1	0	990.5±2.5	1450.5				
T2	0.238	562.0±4.0		428.5±4.5	0.295	1800	1.24
T3	0.491	346.5±4.5		215.5±6.0		852	
T4	0	990.5±2.5	1450.5				
I	0.132						
T5	0.261	546.5±0.5		555.0±2.5	0.306	1700	1.17

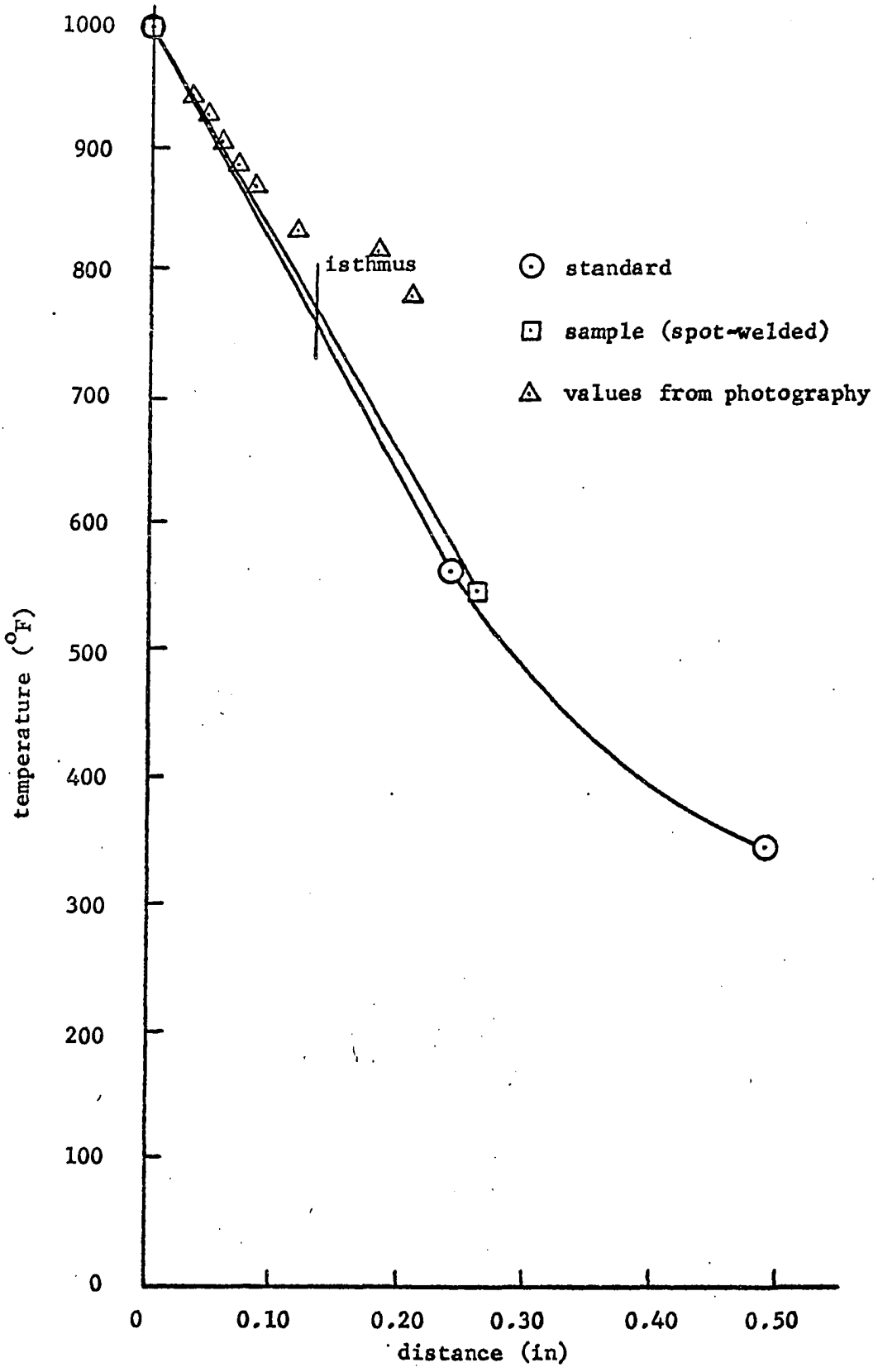

Figure 40. Temperature distribution Nichrome V. Run 4.

Figure 41. Infrared photograph Nichrome V. Run 4. (Exposure: 64 min, stop: f/4.0, filter: 87, film: Kodak IR 135-20) (9.4X)

(Figure 42. Diagram of film density (temperature) contours Nichrome V. Run 4. (9.4X)

film density	temp. (°F)
0.4	935
0.6	920
1.0	897
1.5	880
2.0	863
2.5	830
2.6	810
2.7	775

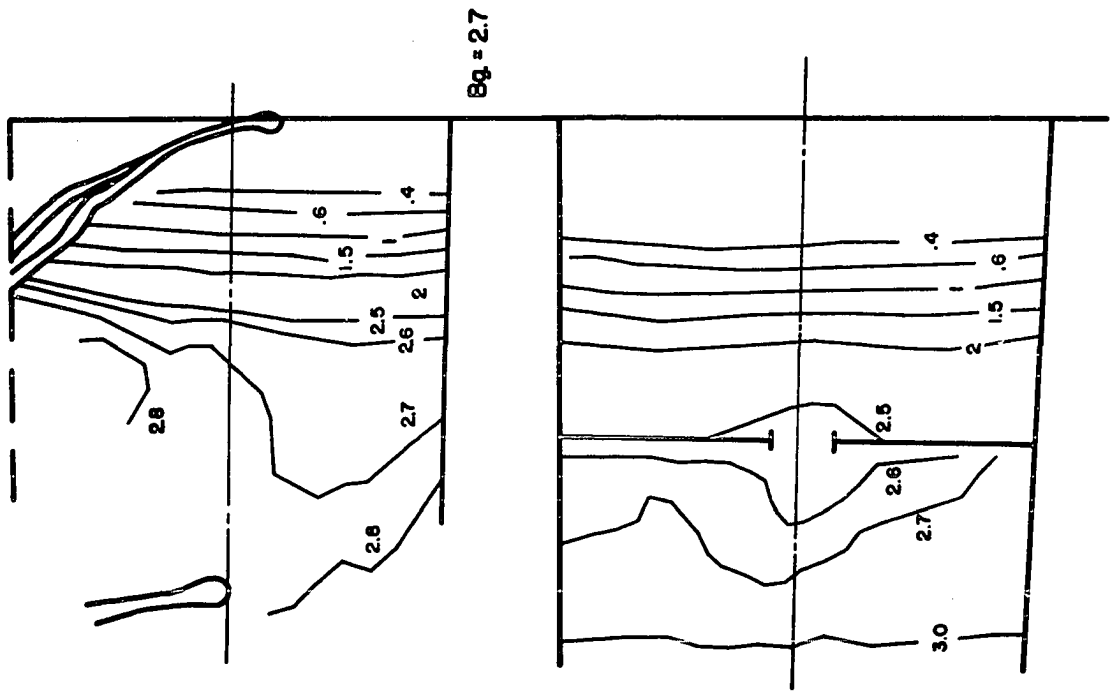
Bg = 2.7
.4
.6
1
1.5
2
2.5
2.6
2.8
2.7
2.8
.4
.6
1.5
2
2.5
2.8
2.7
3.0

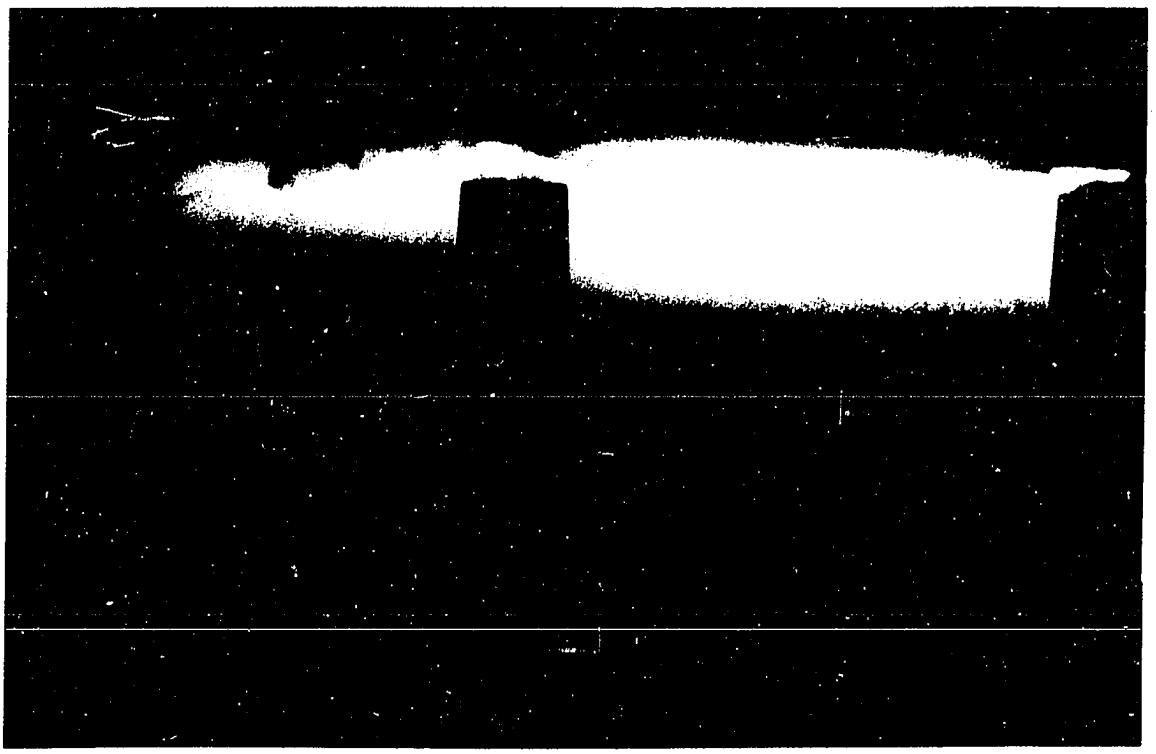

VI. DISCUSSION OF RESULTS

Carnot efficiency and Carnot efficiency divided by the length between the hot and cold thermocouple junctions both have been used as criteria for comparison in these experiments. It has been determined that no pronounced increase in thermoelectric generator efficiency may be obtained by introducing a spot-welded thermal barrier (Figure 1a). The systems in which the thermal barriers were formed by shearing (Figure 1b) did yield a higher efficiency (Tables 6 and 11, and Figures 23 and 37 for Advance and Chromel-P, respectively).

Because of the similarity in composition (Table 13) and the thermal properties (Table 17, Figure 45) of Chromel-P and Nichrome V; only the Chromel-P was studied extensively. Chromel-P has the larger positive thermal emf (Table 16, Figure 44) of the two materials and would be better suited for use in a thermoelectric generator.

The results of this investigation indicate that the standard for Advance had a Carnot efficiency divided by length between thermocouples of 0.943/in while the sample with the sheared isthmus had a value of 1.46/in -- a 55% increase. With the sheared segment twisted 90^{o} the value was 1.60/in -- a 70% increase relative to the standard. This geometry had poor mechanical integrity. The neck was so thin that it broke following the thermocouple measurements. For Chromel-P the value for the standard was 1.09/in and the sheared sample was 1.38/in -- a 27% increase.

The Carnot efficiency calculated for Winckler and Evans' data (1) p. 7 for the standard is 0.117 and for the sample with one isthmus

is 0.386. This would be an increase of 330%. They did not state the material in question, the nature of the isthmus, the dimensions of the specimens, or the distance between points where the temperatures were measured. Winckler and Evans did imply that the distances over which they made their temperature measurements were the same. Thus, their increase of 330% would be the same for a Carnot efficiency divided by length between temperature references.

It has been sufficiently shown that the thermal conductivity is not affected by rolling direction; since the temperature distributions were similar when the heat flow was perpendicular and was parallel to the rolling direction (Runs 6 and 8 for Advance and Runs 5 and 7 for Chromel-P). The alloys were reported to be dead annealed which according to the results they were.

The curves showing the effect of orientation of the samples on the centerline temperature distribution (Figures 33 and 34) indicate that in the normal vertical orientation the standard is slightly heated by convection of the air passing by the sample. The temperature of the standard at position T2 was 20^{o}F above the average of the two horizontal readings, (510^{o}F) while the temperature for the sample at position T4 was 55^{o}F below the average of the two horizontal readings (575^{o}F). When the whole system was rotated 180^{o} and the specimens were again vertical, the temperature of the standard at position T2 was 75^{o}F below the average of the two horizontal readings (510^{o}F), and the temperature for the sample at position T4 was 15^{o}F below the average of the two horizontal readings (575^{o}F). The facts that in one case the thermocouples lead up from the samples and in the other

lead down from the samples, and that the bond between the samples and heater might be altered from one case to the other, might enter into the deviation of the temperatures for the two vertical arrangements.

Perhaps the horizontal arrangement of specimens should have been used but this would have complicated the photographic procedure considerably.

The temperatures on both the standard and the sample with the isthmus approached the steady-state values in similar lengths of time (Figure 35).

The infrared photography portion of this research did prove to be fruitful when the juxtaposed standard and sample with isthmus were used with thermocouples incorporated as references (Figures 21, 24, 38, and 41). Also the infrared photographs of the thermoelectric generator elements alone were valuable (Figures 14, 16, 27, and 29). The photographs that have been included in the results are the ones which most favorably represented the temperature distributions for each configuration and for each thermocouple alloy. A series of stepped exposures was used to establish the proper exposure times. This was done for each run because of the unavoidable differences in the hot junction temperatures, and the possible differences in the films and their development. It was not possible to establish a single exposure time for which the film density would vary properly between the two reference thermocouples. In several cases one exposure was used to photograph the portion of the specimen between the heater and the isthmus and a second exposure was used to photograph the portion beyond the isthmus.

Hot junction temperature has a strong influence on the length of exposure time. This is shown in Figures 27 and 29 which are photographs of the same system, a Chromel-P thermoelectric generator element. The hot thermocouple temperature for Figure 27 was 924.5°F and the exposure time 16 hours, for Figure 29 the temperature was 1036.5°F and the exposure time 3 hours. The second photograph received more exposure than the first.

Standard deviations of the temperature measured with the thermocouples are within the limits of accuracy of the thermocouple wires, according to the discussion in the previous section on thermocouple techniques on p. 41. The accuracy of the distance measurements could not be definitely established because of the uncertainty of the location of the point where the thermocouples indicated the temperature. This point was assumed to be midway between the points where each wire made contact with the surface. The accuracy of the distance measurements has been assumed, therefore, to be within the diameter of a thermocouple wire ($\pm$ 0.013 in for 28 gauge wire). The film densitometer readings were calibrated according to the directions and step wedge (Table 32) provided with the apparatus. Since the comparative method was used wherever temperatures were assigned to the contours, the actual value of the film density was of no concern.

VII. CONCLUSIONS

The experimental research terminating in this dissertation led to the following findings:

1. Infrared photography is satisfactory for measuring surface temperature distributions. A rectangular standard of the same material as that of the surface to be measured must be included in the photograph and the standard should be calibrated with thermocouples (or some other temperature measuring means) along the centerline.

2. Temperature is an important variable in obtaining favorable results with infrared photography. Temperatures of at least $900^{o}F$ are desirable if an infrared filter 87 is used in order to keep the exposure times less than 12 hours.

3. Spot-welded thermocouple alloy strips (Figure 1a) were found not to exhibit any increased temperature drop or increased Carnot efficiency divided by length between thermocouples when compared to a standard of the same material with a similar geometry.

4. Sheared thermocouple alloy strips (Figure 1b) were found to exhibit a 55% increase of Carnot efficiency divided by length in Advance and a 27% increase in Chromel-P when compared to standards of the respective materials.

5. By twisting the second segment of the sheared Advance sample 90^{o}, the Carnot efficiency divided by length was raised to 70% above that for the standard. This geometry had as thin a neck as was possible to fabricate and it broke immediately after the thermocouple readings were taken without being touched or jarred.

6. Experimental evidence indicates that there is an effect of configuration, or "isthmus effect", on the efficiency of thermoelectric generators composed of thermocouple alloys.

Possibilities for further study would include the following:

1. Experimental confirmation of the thermal conductivity data for the thermocouple alloys should be made.

2. Time-lapse infrared photography could be applied to investigate nonsteady-state heat flow in irregular geometries.

3. In order to elaborate upon the technique employed in the investigation leading to this dissertation, higher speed sheet film could be used. Such film is not readily available, must be ordered in large quantitites, and is expensive.

4. A different heater system could be developed which would provide higher temperatures and shorten the required exposure times.

5. The experiment could be run in a vacuum with the thermocouple readings taken and the infrared photography technique omitted. The effects of convective heat loss would be eliminated.

6. An "isthmus effect" might be obtained by evaporating a thin film of metal on a thermoelectric semiconductor. This system might have the electrical conductance and strength of the metallic film but the thermal conductance and Seebeck coefficient of the substrate.

VIII. BIBLIOGRAPHY

1. Winckler, Gunnar A. F. and Richard C. Evans. Isthmus effect -- a new thermoelectric phenomena. Power Sources Conference Proceedings 15:132-134. 1961.

2. Ogburn, George H., Jr. Nuclear energy power sources. Power Sources Conference Proceedings 14:12-18. 1960.

3. Winckler, Gunnar A. F. and Richard C. Evans. Thermoelectric generator unit. U.S. Patent No. 3,048,643. 7 August 1962.

4. Jaumot, Frank E., Jr. Thermoelectric effects. IRE Proceedings 46, No. 3:538-554. March 1958.

5. Sherman, B., Robert R. Heikes, and Roland W. Ure, Jr. Calculation of efficiency of thermoelectric devices. Journal of Applied Physics 31:1-16. January 1960.

6. Gelhoff, A., E. Justi, and M. Kohler. Abhandl. brannschweig. wiss. Ges. 2:149-156. 1950. Original not available; cited in Sherman, B., Robert R. Heikes, and Roland W. Ure, Jr. Calculation of efficiency of thermoelectric devices. Journal of Applied Physics 31:1-16. January 1960.

7. Boerdijk, A. H. Contribution to a general theory of thermocouples. Journal of Applied Physics 30:1080-1083. 1959.

8. Cadoff, Irving B. and Edward Miller, eds. Thermoelectric materials and devices. New York, N. Y., Reinhold Publishers. 1960.

9. Kaye, Joseph and John A. Welsh, eds. Direct conversion of heat to electricity. New York, N. Y., John Wiley and Sons, Inc. 1960.

10. Ioffe, A. F. Semiconductor thermoelements and thermoelectric cooling. (Translated by A. Gelbtuch) London, England., Infosearch Limited. 1957.

11. Chang, Sheldon S. L. Energy conversion. Englewood Cliffs, N. J., Prentice-Hall, Inc. 1963.

12. Boltzmann, L. (Title unknown.) Sitz. Ber. Akad. Wiss. Wien, Math. Naturw. Kl. II, 96:1258. Original not available, cited in Tauc, Jan. Photo and thermoelectric effects in semiconductors. (Translated by Margaret Laner) New York, N. Y., Pergamon Press. 1962.

13. Onsager, Lars. Reciprocal relations in irreversible processes. Physical Review 37:405-426. February 1931.

14. Domenicali, C. A. Irreversible thermodynamics of thermoelectricity. Review of Modern Physics 26:237-275. April 1964.

15. Domenicali, C. A. Thermoelectric power and electron scattering in metal alloys. Physical Review 112:1863-1876. 1958.

16. Domenicali, C. A. and F. A. Otter. Thermoelectric power and electron scattering in metal alloys. Physical Review 95:1134-1144. 1954.

17. Jaumot, Frank E., Jr. Thermoelectricity. Advances in Electronics and Electron Physics 17:207-243. 1962.

18. Redemske, R. F. Materials for thermoelectric conversion. Power Sources Conference Proceedings 14:4-7. 1960.

19. Ginnings, Defoe C. Measurement of thermal conductivity. In Irving B. Cadoff and Edward Miller, eds. Thermoelectric materials and devices. pp. 113-132. New York, N. Y., Reinhold Publishing Corporation. 1960.

20. Ginnings, D. C. Standards of heat capacity and thermal conductivity. In Paul H. Egli, ed. Thermoelectricity. pp. 320-341. New York, N. Y., John Wiley and Sons, Inc. 1960.

21. Bauerle, J. E., P. H. Sutter, and R. W. Ure, Jr. Measurements of properties of thermoelectric materials. In Robert R. Heikes and Roland W. Ure, Jr., eds. Thermoelectricity: science and engineering. pp. 285-338. New York, N. Y., Interscience Publishers. 1961.

22. Campbell, I. High temperature technology. New York, N. Y., John Wiley and Sons, Inc. 1956.

23. Drabble, J. R. and H. J. Goldsmid. Thermal conduction in semiconductors. New York, N. Y., Pergamon Press. 1961.

24. Klemens, P. G. Thermal conductivity and lattice vibrational modes. Solid State Physics 7:1-98. 1958.

25. Keyes, R. W. and J. E. Bauerle. Thermal conduction in thermoelectric materials. In Robert R. Heikes and Roland W. Ure, Jr., eds. Thermoelectricity: science and engineering. pp. 91-119. New York, N. Y., Interscience Publishers. 1961.

26. Williams, Wendell S. Thermal conductivity mechanicms. In Irving B. Cadoff and Edward Miller, eds. Thermoelectric materials and devices. pp. 98-112. New York, N. Y., Reinhold Publishing Corporation. 1960.

27. Krumhansl, J. A. and W. S. Williams. Thermal conductivity in solids. In Paul H. Egli, ed. Thermoelectricity. pp. 77-91. New York, N. Y., John Wiley and Sons, Inc. 1960.

28. Ewing, C. T., B. E. Walker, Jr., J. R. Spann, E. W. Steinkuller, and R. R. Miller. Thermal conductivity of refactory materials. Journal of Chemical and Engineering Data 7, No. 2:251-256. April 1962.

29. Cusack, N. Electrical and magnetic properties of solids. New York, N. Y., Longmans, Green and Co. 1958.

30. Wiedemann, G. and R. Franz. Über die Wärme-Leitungsfähigkeit der Metalle. Annalen der Physik, Ser. 2, 89:497-529. 1853.

31. Mott, N. F. and H. Jones. Theory of the properties of metals and alloys. New York, N. Y., Dover Publications, Inc. 1936.

32. Debye, P. Vorträge über die kinetische Theorie der Materie und Electrizität. Original not available; cited in Wendell Williams. Thermal conductivity mechanisms. In Irving B. Cadoff and Edward Miller, eds. Thermoelectric materials and devices. pp. 98-110. New York, N. Y., Reinhold Publishing Corporation. 1960.

33. Joffe, A. F. Heat transfer in semiconductors. In Summer N. Levine, ed. Selected papers on new techniques for energy conversion. pp. 174-187. New York, N. Y., Dover Publications, Inc. 1961.

34. Peierls, R. Zur kinetischen Theorie der Wärmeleitung in Kristallen. Annalen der Physik, Ser. 5, 3:1055-1099. 1929.

35. Shelton, S. M. and W. H. Swanger. Thermal conductivity of irons and steels and some other metals in the temperature range 0 to 600 degrees centigrade. American Society for Steel Treating Transactions 21-1061-1078. 1933.

36. Silverman, L. Thermal conductivity data presented for various metals and alloys up to 900°C. Journal of Metals 5:631-632. 1953.

37. Driver-Harris Company. Advance, Magnanin and other copper-nickel alloys. Technical catalog CN-58. Harrison, N. J., Author. ca. 1962.

38. Powell, R. W. Thermal conductivities of solid materials at high temperatures. Research, Science and its Application in Industry 7:492-501. December 1954.

39. Rhodes, B. L. and L. S. Cram. Electrical resistance ratio of Chromel-P wire between 4.2° and 600°K. Advances in Cryogenic Engineering 9:437-442. 1962.

40. Atkins, Robert M. Temperature measurement with thermistors. Instruments and Control Systems 33:86-88. 1961.

41. Urbach, F. Thermography. Photographic Journal 90 B:109. 1950.

42. Kehl, George L. Principles of metallographic laboratory practice. 3rd ed. New York, N. Y., McGraw-Hill Book Co., Inc. 1949.

43. Siviter, J. H., Jr. and H. K. Strass. Investigation of photographic technique of measuring high surface temperatures. NASA Tech. Note D-617. November 1960.

44. Green, W. B., ed. Westinghouse thermoelectric handbook. Youngwood, Pa., Westinghouse Electric Company, Semiconductor Division. 1962.

45. Moen, Walter K. Surface temperature measurement. Instruments and Control Systems 33:70-73. 1960.

46. White, F. J. Accuracy of thermocouples in radiant-heat testing. Experimental Mechanics 2:204-210. 1962.

47. Instrument Society of America. Thermocouples and thermocouple extension wires -- limits of error. Recommended Practices 1.3. Pittsburgh, Pa., Author. July 1959.

48. Clark, Walter. Photography by infrared its principles and applications. 2nd ed. New York, N. Y., John Wiley and Sons, Inc. 1946.

49. Jones, L. A. Measurements of radiant energy with photographic materials. In Forsythe, W. E. The measurement of radiant energy. Chapter 8. New York, N. Y., McGraw-Hill Book Co., Inc. 1937. Cited in Walter Clark. Photography by infrared. 2nd ed. New York, N. Y., John Wiley and Sons, Inc. 1946.

50. Eastman Kodak Company. Infrared and ultraviolet photography. No. M-3. Rochester, N. Y., Author. November 1963.

51. Camera maps temperatures. Product Engineering 28:86. December 1957.

52. Photographing heat. Product Engineering 27:214-215. April 1956.

53. American Society for Metals. Metals handbook, 8th ed. Vol. 1. Properties and selection of metals. Novelty, Ohio, Author. 1961.

54. Lohr, James M., Charles H. Hopkins, and C. Leslie Andrews. Thermal electromotive force of various metals and alloys. In American Institute of Physics. Temperature. pp. 1232-1235. New York, N. Y., Reinhold Publishing Corporation. 1941.

55. Sears, Francis Weston and Mark W. Zemansky. University physics. 2nd ed. Reading, Mass., Addison-Wesley Publishing Company, Inc. 1955.

56. Chemical Rubber Publishing Company. Handbook of chemistry and physics. 39th ed. Cleveland, Ohio, Author, 1958.

57. Jakob, Max and George A. Hawkins. Elements of heat transfer. 3rd ed. New York, N. Y., John Wiley and Sons, Inc. 1957.

58. Leeds and Northrup Company. Conversion tables for thermocouples. 077989 Issue 2. Philadelphia, Pa., Author. ca. 1959.

IX. ACKNOWLEDGMENTS

The author wishes to acknowledge the faith and encouragement of his late mother and his father during his attempt at acquiring a higher formal education.

Sincere gratitude is expressed to Dr. Glenn Murphy, Distinguished Professor and Head of the Nuclear Engineering Department, for his kind assistance and encouragement during the course of this study. Dr. Murphy served as major professor.

Thanks are extended to Mr. Louis Facto and the staff of the Photography Laboratory for their technical advice and assistance with the infrared photography.

The materials on which this investigation was performed were provided by Dr. Gunnar A. F. Winckler and Dr. Richard C. Evans of the Johns Hopkins University Applied Physics Laboratory, Silver Spring, Maryland. The assistance, advice and encouragement of these men was appreciated.

Deep appreciation is given to the United States Atomic Energy Commission for its support of this research through the Special Fellowship Program in Nuclear Science and Engineering which is administered by the Oak Ridge Institute of Nuclear Studies.

X. APPENDIX A. PROPERTIES OF THERMOCOUPLE ALLOYS

Table 13. Chemical analyses of various materials, including thermocouple alloys

Material	reference	analysis, weight percent							
		Ni	Cr	Fe	Al	Mn	Si	C	Cu
Advance	Silverman (36)	44.04				1.20	0.003	0.035	54.79
Alumel	Shelton and Swanger (35)	94.94			2.0	2.0	1.0		
Chromel-P	Shelton and Swanger (35)	90.0	10.0						
Chromel-A	Shelton and Swanger (35)	80.0	20.0						
Nichrome V	Silverman (36)	77.94	19.87	0.036		0.06	1.44		
nickel	Shelton and Swanger (35)	99.94		0.03			0.006	0.005	0.006
iron	Silverman[a] (36)			99.89		0.02	0.028	0.026	
copper	Driver-Harris (37)								99.99

[a]Other impurities P 0.021, S 0.011

Table 14. Physical properties of various materials

property (nominal)	alloys Advance	Alumel	Chromel-P	Chromel-A	Nichrome V
k, thermal conductivity (watt/cm-C°) at 100°C	0.212	0.296	0.190	0.136	0.112
ρ, electrical resistivity (ohm/cir-mil-ft)	294	177	425	650	650
(ohm-cm at 20°C)[a]	48.8×10^{-6}	29.4×10^{-6}	70.6×10^{-6}	108×10^{-6}	108×10^{-6}
coefficient of resistance (ohm/ohm-C°)	$\pm0.2\times10^{-4}$	11.3×10^{-4}	3.15×10^{-4}	1.23×10^{-4}	1.1×10^{-4}
(temperature, °C)	20-100	20-760	20-760	20-500	20-500
α, coefficient of thermal expansion (in/in-C°)	14.9×10^{-6}	12.0×10^{-6}	13.1×10^{-6}	13.6×10^{-6}	17.0×10^{-6}
(temperature, °C)	20-100	20-100	20-100	20-100	10-1000
C_v, specific heat (cal/gm-C° at 20°C)	0.094	0.125	0.107	0.107	0.104
d, specific gravity	8.90	8.60	8.73	8.41	8.41
T_m, melting point(°C)	1210	1400	1430	1400	1400
W, average atomic weight	61.4	58.7	58.0	57.3	57.3

[a]Note, divide ρ in mil-ft system by 6.02×10^6 to obtain ohm-cm.

Table 14. (Continued)

property (nominal)	metals nickel[b]	iron	copper
k, thermal conductivity (watt/cm-C°) at 100°C	0.828	0.662	3.88
ρ, electrical resistivity (ohm/cir-mil-ft)	41.2	60.14	10.37
(ohm-cm at 20°C)	6.84×10^{-6}	10.0×10^{-6}	1.72×10^{-6}
coefficient of resistance (ohm/ohm-C°)	69×10^{-4}	50×10^{-4}	39.3×10^{-4}
(temperature, °C)	0-100	at 20	at 20
α, coefficient of thermal expansion (in/in-C°)	13.3×10^{-6}	11.7×10^{-6}	16.6×10^{-6}
(temperature, °C)	0-100	at 20	at 20
C_v, specific heat (cal/gm-C° at 20°C)	0.112	0.1065	0.0921
d, specific gravity	8.90	7.86	8.92
T_m, melting point (°C)	1453	1535	1083
W, atomic weight	58.7	55.8	63.5

[b]Data from Metals handbook (53, p. 1217).

Table 15. Electrical resistivity of various materials (micr ohm-cm)

material	temperature						
	20°C 68°F	100°C 212°F	200°C 392°F	300°C 572°F	400°C 752°F	500°C 932°F	600°C 1112°F
Advance	48.8	48.8	48.8	48.8	49.0	49.8	50.0
Alumel	29.4	36.4	42.1	45.3	48.2	50.9	53.5
Chromel-P	70.6	73.5	76.6	80.2	84.1	86.2	88.4
Chromel-A	108	110	112	114	115	115	115
Nichrome V	108	110	112	114	115	115	115
nickel	6.84	12.3[a]	20.5	27.4	32.8	39.0	42.4
iron	10.0	15.0[b]	23.0	31.0	40.0	54.0	70.0
copper	1.69	2.4[c]	3.1	3.8	4.5	5.3	6.2

[a]Values determined from graph in Metals handbook (53, p. 1218).

[b]Ibid. (53, p. 1209).

[c]Ibid. (53, p. 1204).

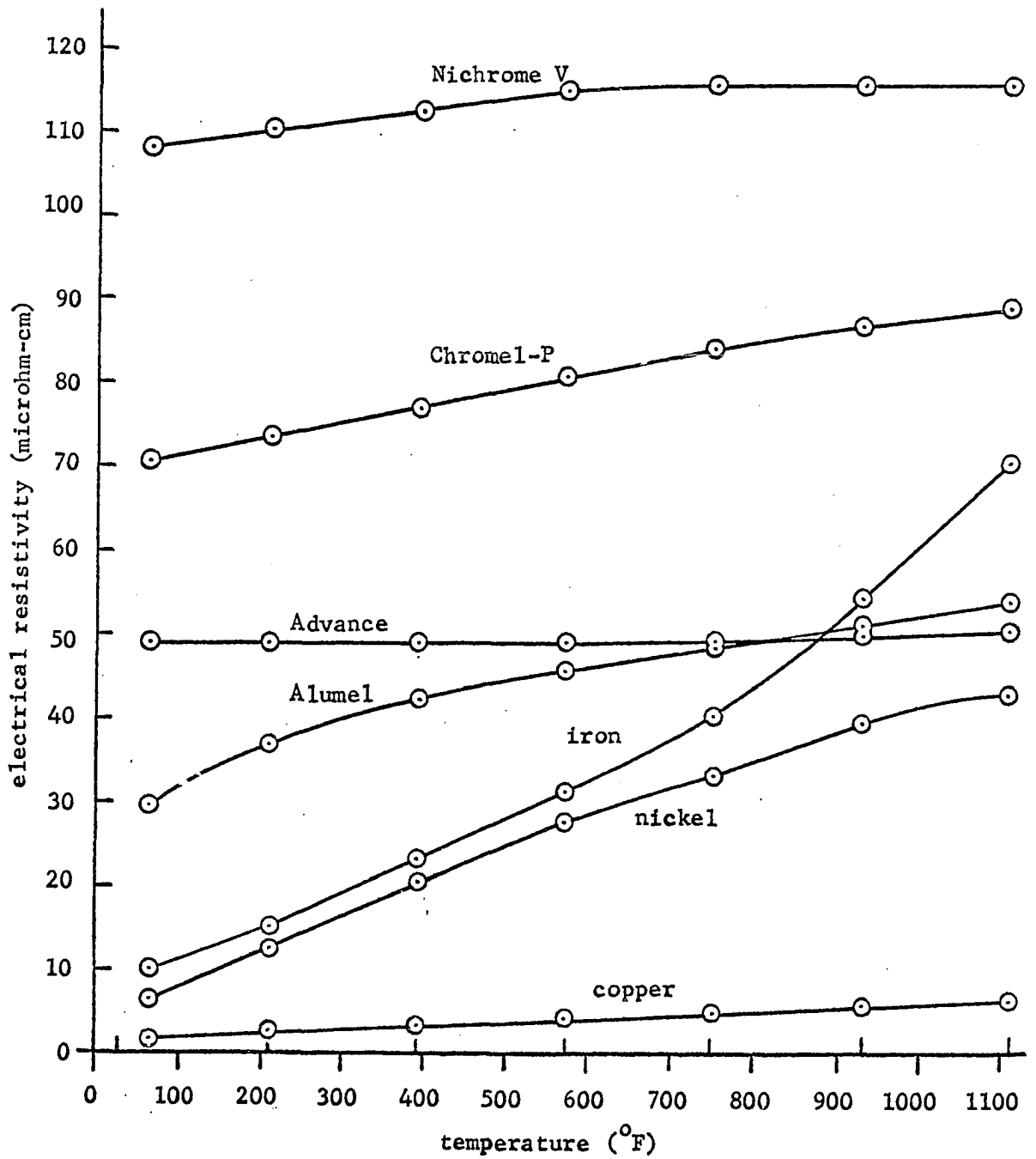

Figure 43. Electrical resistivity versus temperature

Table 16. Thermal emf of various materials, relative to platinum according to Lohr, Hopkins, and Andrews (54, p. 1232) (millivolts)

material	reference junction (°F)	temperature 200°F 93°C	400°F 204°C	600°F 316°C	800°F 426°C	1000°F 538°C	1200°F 649°C
Advance	32	-3.26	-7.64	-12.40	-17.41	-22.55	-27.77
Alumel	32	-1.21	-2.20	-3.00	-3.85	-4.75	-5.72
Chromel-P	32	2.61	6.11	9.85	13.67	17.50	21.26
Nichrome V	68	1.81	3.81	5.95	7.97	10.30	12.76
iron	32	1.77	3.60	5.03	6.12	7.15	8.40

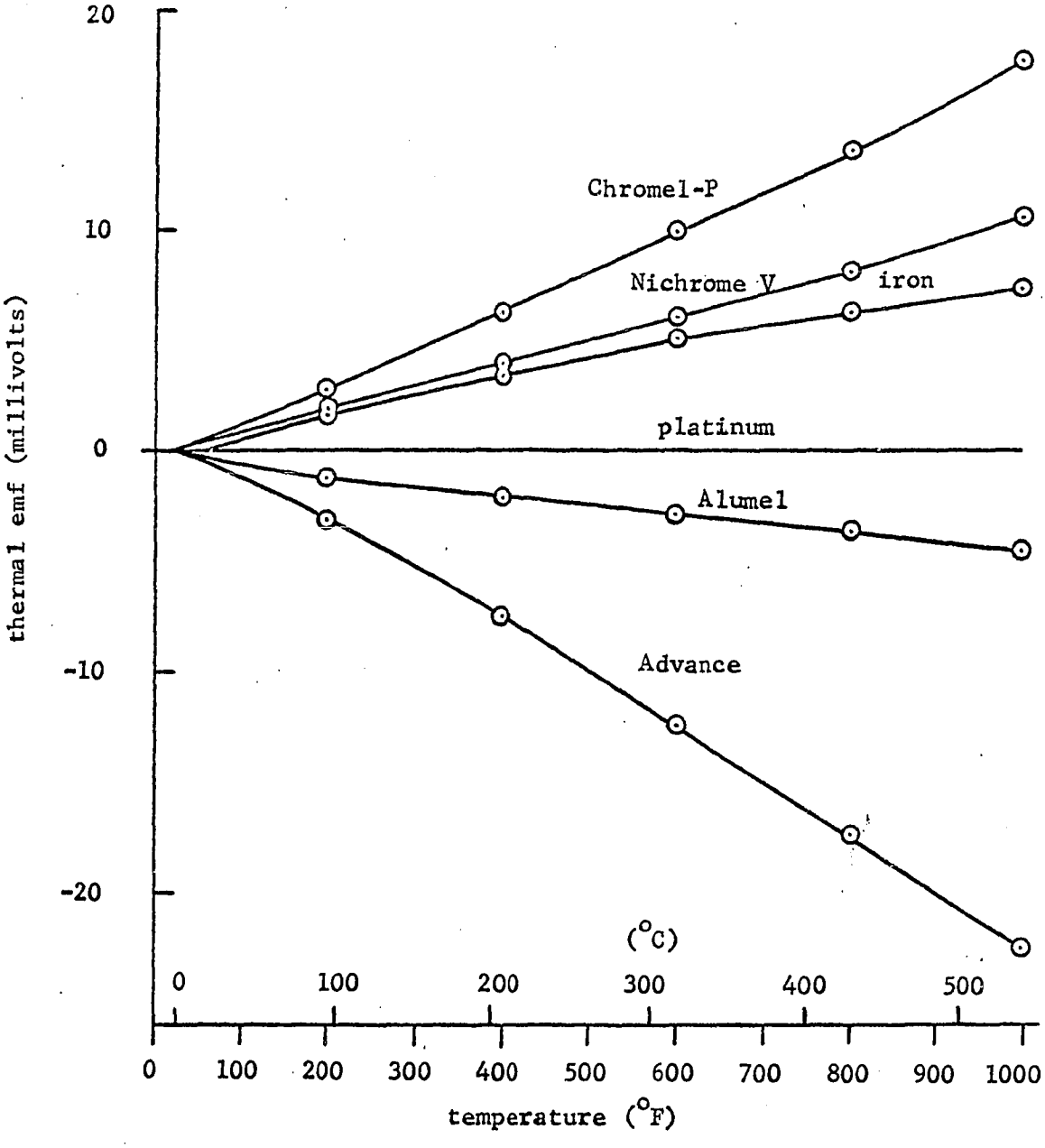

Figure 44. Thermal emf versus temperature

Table 17. Thermal conductivity of various materials (watt/cm-C°)[a]

material	temperature						
	50°C 122°F	100°C 212°F	200°C 392°F	300°C 572°F	400°C 752°F	500°C 932°F	600°C 1112°F
Advance	0.194	0.212	0.251	0.289	0.328	0.367	0.405
Alumel		0.296	0.318	0.350	0.381	0.412	
Chromel-P		0.190	0.209	0.228	0.247	0.266	
Chromel-A		0.136	0.154	0.172	0.189	0.206	
Nichrome V	0.103	0.112	0.130	0.148	0.166	0.183	0.201
nickel		0.828	0.732	0.638	0.593	0.621	
iron	0.690	0.662	0.606	0.552	0.494	0.438	0.384
copper		3.88	3.74[b]	3.52	3.49	3.30	3.11

[a]Multiply k in watt/cm-C° by 0.2389 to obtain cal/sec-cm-C°.
Multiply k in watt/cm-C° by 693.5 to obtain Btu-in/hr-ft^2-F°.

[b]Values determined from graph in Metals handbook (53, p. 1204).

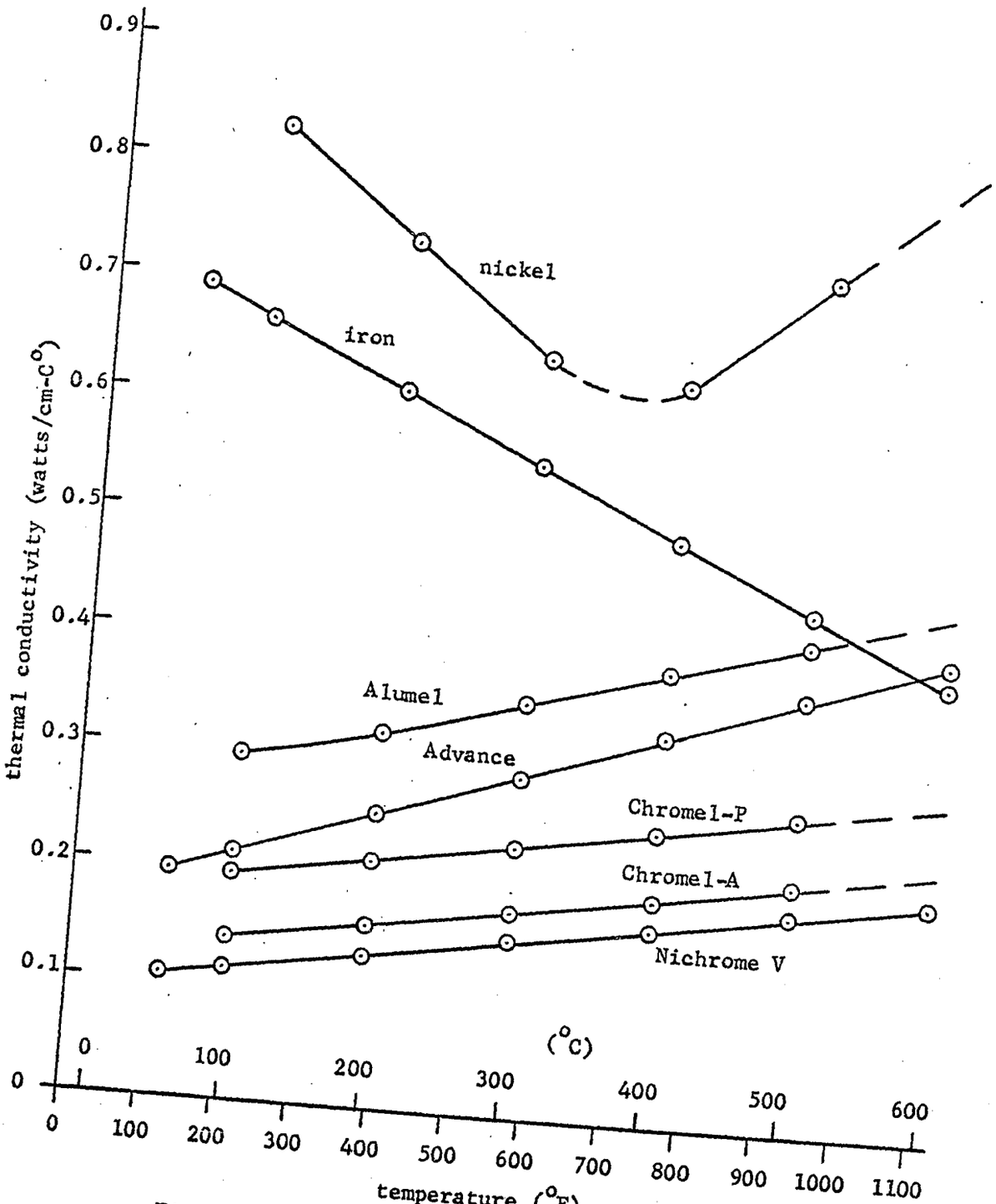

Figure 45. Thermal conductivity versus temperature

XI. APPENDIX B. DETERMINATION OF ELECTRON AND PHONON CONTRIBUTIONS TO THERMAL CONDUCTIVITY

A. Wiedemann-Franz Relation

$$k_e/\sigma = L\,T = \frac{\pi^2}{3}\left(\frac{K}{e}\right)^2 T \tag{20}$$

where

$$L = \frac{\pi^2}{3}\left[\frac{1.38 \times 10^{-16}\ \frac{erg}{K^o} \times 10^{-4}\ \frac{joules}{erg}}{1.602 \times 10^{-19}\ coul}\right]^2$$

$$L = 2.45 \times 10^{-8}\left(\frac{volts}{K^o}\right)^2 \tag{21}$$

Table 18. Calculated values of electron and phonon thermal conductivities at room temperature (80°F (300°K), where $k_e = 735 \times 10^{-8}/\rho$ (watt/cm-K°)) $k_p = k - k_e$

material	k	ρ (ohm)	k_e	k_p	k_p/k
Advance	0.185	48.8×10^{-6}	0.151	0.034	0.184
Alumel	0.284	30.5×10^{-6}	0.241	0.043	0.151
Chromel-P	0.180	71.0×10^{-6}	0.104	0.076	0.422
Nichrome V	0.100	108.5×10^{-6}	0.068	0.032	0.320

Table 19. Calculated values of electron and phonon thermal conductivities at 1000°F (811°K, (where $k_e = 1990 \times 10^{-8}/\rho$ (watt/cm-K°))

material	k	ρ (ohm)	k_e	k_p	k_p/k
Advance	0.382	49.9×10^{-6}	0.398		
Alumel	0.423	52.0×10^{-6}	0.383	0.040	0.095
Chromel-P	0.272	87.0×10^{-6}	0.229	0.043	0.158
Nichrome V	0.192	115×10^{-6}	0.173	0.019	0.099

XII. APPENDIX C: SAMPLE CALCULATIONS OF MATHEMATICAL CONSIDERATIONS

Advance. Run 13. (Juxtaposed standard and shears-cut sample. Heat flow perpendicular to rolling direction. (Figure 6))

1. Approximate electrical resistances

Standard:

$$l_{12} = 0.268 \text{ in}$$

$$t = 0.0050 \text{ in}$$

$$w = 0.257 \text{ in}, \quad A = 0.0013 \text{ in}^2$$

$$\rho = 49.2 \times 10^{-6} \text{ ohm-cm}$$

$$R_{12} = \frac{\rho l_{12}}{A} = \frac{49.2 \times 10^{-6} \text{ ohm-cm } (0.268 \text{ in})}{(0.0013 \text{ in}^2)\ 2.54 \frac{\text{cm}}{\text{in}}}$$

$$R_{12} = 4.0 \times 10^{-3} \text{ ohms.}$$

Sample, with shears-cut isthmus:

$$l_{4I} = 0.117 \text{ in}$$

$$l_I \approx 0.002 \text{ in}$$

$$l_{I5} = 0.122 \text{ in}$$

$$t = 0.0050 \text{ in}$$

$$w = 0.255 \text{ in}, \quad A = 0.0013 \text{ in}^2$$

$$w_I = 0.039 \text{ in}, \quad A_I = 0.00020 \text{ in}^2$$

$$\rho = 49.2 \times 10^{-6} \text{ ohm-cm}$$

$$R_{45} = \rho \left[\frac{l_{4I}}{A_{4I}} + \frac{l_I}{A_I} + \frac{l_{I5}}{A_{I5}} \right]$$

$$R_{45} = \frac{49.2 \times 10^{-6}}{2.54 \frac{\text{cm}}{\text{in}}} \text{ ohm-cm} \left[\frac{0.117 \text{ in}}{0.0013 \text{ in}^2} + \frac{0.002 \text{ in}}{0.00020 \text{ in}^2} + \frac{0.122 \text{ in}}{0.0013 \text{ in}^2} \right]$$

$$R_{45} = 3.76 \times 10^{-3} \text{ ohm}$$

2. Heat transfer assuming all temperature drop due to conduction alone

Standard:

$$T1 - T2 = 335.5F^{o}$$

$$k = 0.374 \text{ watt/cm}C^{o}$$

$$q_{T_{12}} = kA \frac{(T1 - T2)}{L_{12}}$$

$$= 0.374 \frac{\text{watt}}{\text{cm}C^{o}} \frac{(0.0013 \text{ in}^2)}{0.268 \text{ in}} 2.54 \frac{\text{cm}}{\text{in}} (335.5F^{o}) \frac{5C^{o}}{9F^{o}}$$

$$q_{T_{12}} = 0.858 \text{ watt}$$

Sample, with shears-cut isthmus:

$$T4 - T5 = 464F^{o}$$

$$K = 0.362 \text{ watt/cm}C^{o}$$

$$q_{T_{45}} = \frac{k (T4 - T5)}{\left[\frac{L_{4I}}{A_{4I}} + \frac{L_{I}}{A_{I}} + \frac{L_{I5}}{A_{I5}}\right]}$$

$$= \frac{0.362 \text{ watt/cm}C^{o} (464F^{o}) \frac{5C^{o}}{9F^{o}} 2.54 \frac{\text{cm}}{\text{in}}}{\left[\frac{0.117 \text{ in}}{0.0013 \text{ in}^2} + \frac{0.002 \text{ in}}{0.00020 \text{ in}^2} + \frac{0.122 \text{ in}}{0.0013 \text{ in}^2}\right]}$$

$$q_{T_{45}} = 1.22 \text{ watt}$$

3. Rough calculation of convection loss H, coefficient of natural convection in air h for a vertical plate, according to Sears and Zemansky (55, p. 291) is

$$h = 0.424 \times 10^{-4} (\bar{T}-T_R)^{\frac{1}{4}} \frac{\text{cal}}{\text{Sec} \cdot \text{cm}^2 \cdot C^{o}}$$

Standard:

$$H = h A' (\bar{T}-T_R)$$

$$\bar{T} = 697^{o}F = 370^{o}C = 1157^{o}R$$

$$T_R = 20^{o}C = 68^{o}F = 528^{o}R$$

$$A' = l_{12}\, w = 2\ (0.0689\ in^2)$$

$$H = 0.424 \times 10^{-4} \frac{cal}{sec\text{-}cm^2\text{-}C^o}\ 2\ (0.0689\ in^2)\ (2.54)^2 \frac{cm^2}{in^2}\ (350C^o)^{5/4}$$

$$= 56.7 \times 10^{-3} \frac{cal}{sec} \times 4.18 \frac{joule}{cal}$$

$$= 0.230 \text{ watt}$$

4. Rough calculation of radiation loss

$$\phi = \epsilon\, \sigma\, A' (T_{out}^4 - T_{in}^4)$$

$\epsilon = 0.7$ (56, p. 2751)

$\sigma = 0.174 \times 10^{-8}$ Btu/hr-ft^2-F^{o4} (57, p. 218)

$$\phi = 0.7\ (0.174 \times 10^{-8} Btu/hr\text{-}ft^2\text{-}F^{o4}) \frac{1\ ft^2}{144\ in^2}\ 2\ (0.0689\ in^2)(1157^oR^4 - 528^4)$$

$$= 2.03 \frac{Btu}{hr} \times \frac{1000 \text{ watt}}{3413 \frac{Btu}{hr}}$$

$$= 0.594 \text{ watt}$$

XIII. APPENDIX D. TRAVELING MICROMETER DISTANCE MEASUREMENTS AND THERMOCOUPLE THERMAL EMF MEASUREMENTS

Equipment: Traveling micrometer, Gaertner Scientific Corporation, Ser. No. 2970-P, No. 3; Potentiometer, Minneapolis-Honeywell Company. Rubicon, model 2745, ISU No. 151098; Multimeter, Precision Apparatus Co., Inc. Model 120, ISU No. 133698.

All thermocouple cold junctions were held in ice-water baths ($32^{\circ}F$). Potentiometer readings (mv) were converted to temperatures ($^{\circ}F$) by using Leeds and Northrup Company tables (58).

Table 20. Chromel-P. Runs 1 and 3. (Spot-welded sample. Heat flow parallel to rolling direction. 24g. Iron-Constantan thermocouples.) Effect of environment on temperature distribution.

Run 1. (Sample and heater surrounded by two inches of diatomaceous earth within 4" x 4" x 12" insulated box.)

heater (v)	Run	T	emf (mv)	temp. (^{o}F)
16.8	1	1	4.59	189
		2	3.42	150
		2	3.46	153
		1	4.62	190
22.0	1	1	6.31	246
		2	4.53	187
		2	4.60	190
		1	6.39	249
27.1	1	1	8.43	316
		2	5.95	235
		2	6.00	236
		1	8.47	317
32.0	1	1	10.36	378
		2	7.17	275
		2	7.20	276
		1	10.39	379
37.4	1	1	12.43	445
		2	8.54	319
		2	8.59	321
		1	12.49	447
46.7	1	1	17.84	621
		2	12.28	440
		2	12.32	442
		1	17.87	622

Table 20. (Continued)

Run 3. (Sample exposed to air and heater enclosed within 4" x 4" x 12" insulated box.)

heater (v)	Run	T	emf (mv)	temp. (°F)
16.8	3	1	2.99	136
		2	1.92	99
		2	1.85	97
		1	2.98	135
22.0	3	1	3.88	166
		2	2.28	112
		2	2.19	109
		1	3.85	165
27.1	3	1	4.75	195
		2	2.50	119
		2	2.53	120
		1	4.75	195
32.0	3	1	5.66	225
		2	2.84	131
		2	2.82	130
		1	5.70	226
46.7	3	1	9.19	340
		2	3.93	167
56.2	3	2	4.68	192
		1	11.70	422
		1	11.70	422
		2	4.77	195

Table 21. Advance, Run A. (Wedge shaped generator element. Heat flow parallel to rolling direction. 24g. Iron-constantan thermocouples.)

position	distances (in) Run 1	Run 2
heater	1.5814	1.5817
N1	1.5632	1.5631
T1	1.4433	1.4435
N2	1.3296	1.3298
T2	1.2202	1.2205
N3	1.0949	1.0949
T3	0.9838	0.9838
N4	0.8655	0.8660
T4	0.7354	0.7353
N5	0.6335	0.6340
T5	0.5168	0.5170

heater (v)	Run	T	emf (mv)	temp. (^{o}F)
85	1	1	16.96	593
		2	10.89	396
		3	6.86	265
		4	4.48	186
		5	3.55	155
	2	1	17.00	594
		2	10.88	395
		3	7.00	269
		4	4.42	184
		5	3.47	152
	3	1	17.11	598
		2	11.17	405
		3	7.07	271
		4	4.59	189
		5	3.62	157
104	1	1	22.43	771
		2	14.61	516
		3	9.06	336
		4	5.78	229
		5	4.36	182

Table 21. (Continued)

heater (v)	Run	T	emf (mv)	temp. (°F)
	2	1	22.34	768
		2	14.68	518
		3	9.05	336
		4	5.73	227
		5	4.53	187
122	1	1	26.98	919
		2	17.82	621
		3	11.00	399
		4	6.86	265
		5	5.14	208
	2	1	26.83	914
		2	17.69	616
		3	10.87	395
		4	6.82	263
		5	5.18	209
140	1	1	32.33	1088
		2	21.60	744
		3	13.50	480
		4	8.82	328
		5	6.65	258
	2	1	32.22	1084
		2	21.03	725
		3	12.95	462
		4	8.24	310
		5	6.11	240
	3	1	31.62	1066
		2	20.51	708
		3	13.16	469
		4	8.38	314
		5	6.36	248
	4	1	31.99	1077
		2	20.93	722
		3	13.91	493
	5	1	31.79	1071
		2	21.19	730
		3	13.21	471
		4	8.16	307
		5	6.18	242

Table 22. Advance, Run 11. (Wedge shaped standard. Heat flow parallel to rolling direction. 28g. Chromel-Alumel thermocouples.)

position	distances (in) Run 1	Run 2
End	1.9492	1.9506
T1	1.5923	1.5937
T2	1.3682	1.3698
T3	1.1447	1.1461
T4	0.8805	0.8817
T5	0.6690	0.6703
End	0.3723	0.3737

heater (v)	Run	T	emf (mv)	temp. (^{o}F)
140	before	1	19.22	872
		1	19.23	872
		2	11.92	559
		2	11.87	557
		3	7.14	347.5
		3	7.14	347.5
		4	4.64	235.5
		4	4.57	232.5
		5	3.45	184
		5	3.43	183
		1	18.97	861
		2	11.82	555
		1	19.00	862.5
140	after	1	18.50	841.5
		1	18.50	841.5
		2	11.64	547
		2	11.59	545
		4	4.53	231
		4	4.54	231
		3	7.02	342
		3	6.98	340
		5	3.44	183.5
		5	3.43	183

Table 22. (Continued)

heater (v)	Run	T	emf (mv)	temp. (^{o}F)
		1	18.62	846.5
		1	18.59	845.5
		2	11.61	546
		3	7.01	341
		4	4.54	231
		5	3.45	184

Table 23. Advance, Run 8. (Juxtaposed standard and spot-welded sample. Heat flow parallel to rolling direction. 28g. Chromel-Alumel thermocouples.)

position	Run 1	Run 2	Run 3
T1	0.5637	0.5625	0.5637
T2	0.8034	0.8026	0.8041
T3	1.0529	1.0519	1.0532
End	1.1792	1.1786	1.1798
T4	1.2713	1.2728	1.2714
I	1.1610	1.1624	1.1611
T5	1.0249	1.0261	1.0249
End	0.6550	0.6564	0.6549

heater (v)	Run	T	emf (mv)	temp. (^{o}F)
140	after	1	20.19	913
		1	20.21	913.5
		2	13.30	619
		2	13.10	610.5
		3	9.50	453
		3	9.70	462
		4	20.59	929.5
		4	20.64	932
		4	20.62	921
		5	13.36	622
		5	13.28	618

Table 24. Advance. Run 6. (Juxtaposed standard and spot-welded sample. Heat flow perpendicular to rolling direction. 28g. Chromel-Alumel thermocouples.)

position	distances (in) Run 1	Run 2	Run 3
T1	1.0987	1.0971	1.0984
T2	1.3546	1.3516	1.3536
T3	1.5916	1.5902	1.5919
T4	1.3891	1.3909	1.3898
I	1.2564	1.2581	1.2569
T5	1.1232	1.1243	1.1231

heater (v)	Run	T	emf (mv)	temp. (^{o}F)
140	before	1	20.47	924.5
		1	20.49	925.5
		2	13.37	622
		2	13.32	620
		3	9.54	455
		3	9.51	453.5
		4	20.77	937
		4	20.80	938.5
		5	13.17	613.5
		5	13.21	615
		1	20.64	932
		1	20.62	931
		2	13.49	627.5
		2	13.49	627.5
		3	9.62	458.5
		3	9.60	457.5
		3	9.43	450
		4	20.79	938
		4	20.75	936.5
		5	13.13	612
		5	13.14	612
140	after	1	20.60	930
		1	20.60	930
		2	13.34	621
		2	13.31	619.5

Table 24. (Continued)

heater (v)	Run	T	emf (mv)	temp. (^{o}F)
		3	9.53	454.5
		3	9.56	456
		4	20.71	935
		4	20.70	934
		5	13.07	609
		5	13.01	606.5
		5	12.99	606
		3	9.54	455

Table 25. Advance, Run 13. (Juxtaposed standard and shears-cut sample. Heat flow perpendicular to rolling direction. 28g. Chromel-Alumel thermocouples.)

position	distances (in) Run 1	Run 2	Run 3
T1	1.2776	1.2757	1.2770
T2	1.5459	1.5443	1.5454
T3	1.7862	1.7854	1.7856
End	1.9141	1.9130	1.9142
T4	1.6447	1.6458	1.6446
I	1.5286	1.5276	1.5278
T5	1.4054	1.4072	1.4054
T6	1.1524	1.1537	1.1522
End	1.0386	1.0400	1.0384

heater (v)	Run	T	emf (mv)	temp. (^{o}F)
140	after	4	19.13	868
		4	19.14	868
		5	8.42	405
		5	8.39	403.5
		6	5.84	289
		6	5.86	289.5
		1	19.07	865.5
		1	19.03	864
		2	11.22	529
		2	11.25	530
		3	7.75	375
		3	7.76	375
2nd segment twisted 90^{o}				
		4	19.33	876.5
		4	19.33	876.5
		5	7.52	364.5
		5	7.50	363.5
		6	5.30	264.5
		6	5.38	268
		6	5.39	268.5
2nd segment broken off				
		4	20.12	910
		4	20.13	910
		4	20.13	910

Table 26. Chromel-P, Run 9. (Rectangular generator element. Heat flow parallel to rolling direction. 30 g. Iron-Constantan thermocouples.)

position	distances (in) Run 1	Run 2	Run 3	Run 4
N1	1.7629	1.7641	1.7628	1.7643
T1	1.6546	1.6558	1.6546	1.6560
N2	1.5354	1.5361	1.5351	1.5365
T2	1.4314	1.4328	1.4315	1.4332
N3	1.3077	1.3088	1.3073	1.3089
T3	1.2049	1.2061	1.2045	1.2062
N4	1.0807	1.0818	1.0805	1.0816
T4	0.9699	0.9704	0.9694	0.9707
N5	0.8508	0.8514	0.8505	0.8512
T5	0.7256	0.7270	0.7257	0.7269

heater (v)	Run	T	emf (mv)	temp. (°F)
140	after	1	27.14	924
		1	27.16	925
		2	17.60	614
		2	17.62	614
		3	11.56	417
		3	11.61	419
		4	7.96	301
		4	7.96	301
		5	5.93	234
		5	5.87	232
158	1	1	30.67	1036
		1	30.70	1037
		2	19.70	682
		2	19.66	681
		3	12.82	458
		3	12.89	460.5
		4	8.88	330
		4	8.97	333
		5	6.27	245
		5	6.32	247
		1	30.69	1037
		2	19.65	680

Table 27. Chromel-P. Run 10. (Rectangular standard. Heat flow parallel to rolling direction. 28g. Chromel-Alumel thermocouples.)

position	distances (in) Run 1	Run 2	Run 3	Run 4
End			2.0105	2.0092
H	1.8249	1.8264	1.7650	1.7645
T1	1.7083	1.7100	1.6501	1.6487
T2	1.4853	1.4869	1.4268	1.4252
T3	1.2443	1.2455	1.1852	1.1889
T4	1.0064	1.0053	0.9465	0.9453
T5	0.7913	0.7930	0.7326	0.7314
End	0.5279	0.5291	0.4687	0.4683

heater (v)	Run	T	emf (mv)	temp. (^{o}F)
140	after (rear)	1	19.82	897
		1	19.83	897.5
		2	12.10	567
		2	12.12	568
		3	7.64	370
		3	7.66	371
		4	5.04	253
		4	5.10	256
		5	3.82	200
		5	3.78	198
		1	19.75	894
		1	19.70	892
		2	12.07	566
		2	12.06	565.5
140	after (front)	1	18.94	860
		1	18.95	860.5
		2	11.42	537.5
		2	11.41	537
		3	7.02	342
		3	6.96	339
		4	4.64	235.5
		4	4.64	235.5
		5	3.34	179
		5	3.27	176

Table 27. (Continued)

heater (v)	Run	T	emf (mv)	temp. (^{o}F)
		1	18.89	858
		2	11.34	534
		2	11.32	533
		1	18.93	860
		1	18.97	860
		2	11.37	535

Table 28. Chromel-P. Run 7. (Juxtaposed standard and spot-welded sample. Heat flow parallel to rolling direction. 28g. Chromel-Alumel thermocouples.) Effect of orientation of specimens on temperature.

position	distances (in) Run 1	Run 2	Run 3
T1	0.9712	0.9700	0.9715
T2	1.1977	1.1965	1.1978
T3	1.4562	1.4549	1.4563
T4	1.5013	1.5029	1.5014
I	1.3882	1.3895	1.3882
T5	1.2615	1.2629	1.2614

heater (v)	Run	T	emf (mv)	temp. (^{o}F)
140	after	1	18.74	851.5
		1	18.71	850
		2	11.24	529.5
		2	11.26	530.5
		3	7.19	349.5
		3	7.21	350.5
		4	19.42	880
		4	19.44	881
		5	11.08	522.5
		5	11.00	519
		1	18.75	852
		1	18.72	850.5
		2	11.31	533
		2	11.32	533
		3	7.23	351.5
		3	7.24	352
		4	19.37	878
		4	19.30	875
		5	11.06	522
		5	11.06	522
horizontal, thermocouples on top				
		4	19.86	899
		4	19.86	899
		5	12.17	570
		5	12.15	569

Table 28. (Continued)

heater (v)	Run	T	emf (mv)	temp. (°F)
		3	6.71	328
		3	6.82	333
		2	10.38	492
		2	10.43	494
		1	18.09	824
		1	18.07	823
		1	18.25	826.5
		2	10.41	493
		3	6.43	315
		3	6.47	317
		5	19.77	895
		5	12.26	574
vertical, thermocouples on rear				
		4	19.82	897
		4	19.84	898
		5	12.01	563
		5	11.95	560.5
		1	17.20	786
		1	17.17	785
		2	9.05	433
		2	9.16	438
		3	5.33	266
		3	5.27	263
		3	5.20	260
		4	19.73	893
		4	19.83	897.5
		5	11.82	555
		5	11.93	560
		1	17.31	791
		1	17.21	786.5
		2	9.12	436
		2	9.04	433.5
		3	5.25	262.5
horizontal, thermocouples on bottom				
		1	18.55	843.5
		1	18.55	843.5
		2	11.18	527
		2	11.23	529
		3	7.04	343
		3	6.98	340
		3	7.08	344.5

Table 28. (Continued)

heater (v)	Run	T	emf (mv)	temp. (^{o}F)
		5	12.48	583.5
		5	12.44	582
		5	12.42	581
		4	19.80	896
		4	19.76	894.5
vertical (normal), thermocouples on front				
		1	18.44	839
		1	18.53	843
		2	11.07	522
		2	11.13	525
		3	6.91	337
		3	6.88	335.5
		4	19.36	878
		4	19.28	874.5
		5	11.14	525
		5	11.06	522

Table 29. Chromel-P, Run 5. (Juxtaposed standard and spot-welded sample. Heat flow perpendicular to rolling direction. 28g. Chromel-Alumel thermocouples.)

position	distances (in) Run 1	Run 2	Run 3
T1	0.5072	0.5062	0.5063
T2	0.7524	0.7512	0.7523
T3	1.0093	1.0083	1.0095
End	1.1290	1.1295	1.1302
T4	1.1293	1.1308	1.1291
T	1.0052	1.0082	1.0069
T5	0.8920	0.8935	0.8918
End	0.5013	0.5027	0.5012

heater (v)	Run	T	emf (mv)	temp. (^{o}F)
140	after	1	18.99	862
		1	18.95	860.5
		2	11.28	531.5
		2	11.21	528
		3	7.48	363
		3	7.46	362
		4	19.02	863.5
		4	19.05	865
		5	11.84	556
		5	11.84	556
		5	11.84	556
		4	19.01	863
		4	19.04	864
		3	7.55	366
		3	11.22	529
		2	11.21	528
		1	18.91	859
		1	18.91	859

transient temperatures during heating at a heater voltage of 113v

time (min)	T	emf (mv)	temp. (^{o}F)
5	5	4.24	218
7	2	5.12	256.5
9	2	6.32	310.5

Table 29. (Continued)

time (min)	T	emf (mv)	temp. (^{o}F)
11	5	8.05	388
13	4	14.02	650
15	1	14.90	688
17	1	15.82	728
19	4	16.85	771
21	4	17.36	793
23	5	11.03	520.5
25	2	10.10	479.5
27	2	10.15	482
29	5	11.40	536.5
31	4	18.28	832
35	4	18.44	839
40	4	18.26	831
44	1	17.90	816
49	1	17.71	808

Table 30. Chromel-P, Run 12. (Juxtaposed standard and shears-cut sample. Heat flow parallel to rolling direction. 28g. Chromel-Alumel thermocouples.)

position	distances (in) Run 1	Run 2	Run 3
T1	0.9712	0.9700	0.9715
T2	1.1977	1.1965	1.1978
T3	1.4562	1.4549	1.4563
T4	1.1426	1.1436	
I	1.0291	1.0304	
T5	0.8919	0.8929	
T6	0.6224	0.6239	

heater (v)	Run	T	emf (mv)	temp. (^{o}F)
140	after	1	17.52	800
		1	17.51	899
		2	10.36	491
		2	10.32	489
		3	6.43	315
		3	6.48	317.5
		4	17.66	806
		4	17.66	806
		5	7.67	371
		5	7.66	371
		6	4.68	237
		6	4.69	238
		4	17.75	809.5
		4	17.76	810
		5	7.67	371
		5	7.65	370.5
		1	17.61	803.5
		1	17.56	801.5

Table 31. Nichrome V, Run 4. (Juxtaposed standard and spot-welded sample. Heat flow perpendicular to rolling direction. 28g. Chromel-Alumel thermocouples.)

position	distances (in) Run 1	Run 2
T1	0.8430	0.8409
T2	1.0805	1.0794
T3	1.3338	1.3324
T4	1.0221	1.0225
I	0.8892	0.8900
T5	0.7598	0.7610

heater (v)	Run	T	emf (mv)	temp. (^{o}F)
140	after	1	21.98	988.5
		2	12.02	563.5
		3	7.13	347
		5	11.61	546
		4	21.98	988.5
		5	11.63	547
		1	22.10	993.5
		2	12.00	563
		3	7.22	351
		3	7.19	349.5
		2	12.07	566
		1	22.06	992
		5	11.61	546
		5	11.63	547
		1	21.96	987.5
		2	11.84	556
		3	6.96	339
		4	22.10	993.5
		4	21.96	987.5

Table 32. Calibration of step wedge (Type No. 3826, I. D. No. 1585)

Densichron

W. M. Welch Scientific Co.

Chicago 10, Illinois

Photo. Lab. (Louis Facto)

step	ASA diffuse density[a]
2	0.18
3	0.245
4	0.33
5	0.43
6	0.56
7	0.68
8	0.82
9	0.96
10	1.13
11	1.30
12	1.44
13	1.63
14	1.78
15	1.94
16	2.12
17	2.30
18	2.47
19	2.63
20	2.80
21	2.96

[a]Diffuse density, $D = 2 - \log_{10} T$ (%) where T - transmission.

XIV. APPENDIX E. LIST OF SYMBOLS

symbol	meaning (typical units)
a_o	lattice spacing ($\mathring{A}$)
A	cross-sectional area of thermoelement leg (cm^2, or in^2)
α	coefficient of thermal expansion (cm/cm-C^o, or in/in-F^o)
α_{AB}	Seebeck coefficient, or thermoelectric power, for a circuit of materials A and B (millivolts/C^o)
d	density (gm/cc), or specific gravity (unitless)
d	differential operator
D	diffuse density
δ	partial differential operator
C	heat capacity per unit volume (cal/C^o - cm^3, or Btu/F^o - Ft^3)
C_v	specific heat (cal/gm - C^o, or Btu/lb - F^o)
e	charge on an electron (1.602×10^{-19} coul)
e	base of natural, or Naperian, logarithms (2.718)
e_{AB}	Seebeck enf generated in a circuit of materials A and B (millivolts)
ϵ	emissivity
ξ_m	materials efficiency (unitless)
γ	Grüneisen parameter (dimensionless)
h	Planck's constant (6.625×10^{-27} erg-sec)
h	coefficient of natural convection in air (cal/sec-cm^2-C^o)
$\hbar$	Planck's constant divided by 2π (1.054×10^{-27} erg-sec)
H	convection heat loss (watts)
η	overall efficiency of a thermoelectric generator

θ_D	Debye temperature (^oK, or ^oR)
i	electrical current (amps)
k	thermal conductivity (watt/cm-C^o)
k_{calc}	thermal conductivity calculated (watt/cm-C^o)
k_e	electron contribution to thermal conductivity (watt/cm-C^o)
k_m	"molecular" contribution to thermal conductivity
k_{obs}	thermal conductivity observed (watt/cm-C^o)
k_p	phonon contribution to thermal conductivity (watt/cm-C^o)
K	Boltzmann's constant (1.380×10^{-16} erg/C^o)
l	length of thermoelement leg (cm, or in)
L	Lorentz number (2.45×10^{-8} volts^2/C^{o2})
λ_e	mean free path of the electrons (cm)
λ_p	mean free path of the phonons (cm)
m	effective mass of the charge carrier (gms)
N	subscript for semiconductors with negative charge carriers
ν_p	frequency of the phonon (cps)
P	subscript for semiconductors with positive charge carriers
π	ratio of circumference to diameter of a circle (3.142)
π_{AB}	Peltier coefficient for a circuit of materials A and B (millivolts, or joules/coul)
ϕ	radiation heat loss (watts)
q	Peltier heat (joules)
q_T	heat flux (cal/cm^2 - sec, or Btu/in^2 - hr)
$\bar{q}$	wave vector

$\bar{Q}$	reciprocal lattice vector
R	load resistance (ohms)
ρ	electrical resistivity (ohm-cm)
σ	electrical conductivity (ohm^{-1} - cm^{-1})
σ	Stefan-Boltzmann constant (0.174×10^{-8} Btu/in - Ft^2 - F^{o4})
t	thickness of thermocouple alloy strip (in)
T	temperature (^oC, ^oF, ^oK, or ^oR)
t	transmission through film
T_h	absolute temperature at the hot junction (^oK, or ^oR)
T_c	absolute temperature at the cold junction (^oK, or ^oR)
T_m	melting point (^oC or ^oF)
$\bar{T}$	mean temperature between T_h and T_c (^oK, or ^oR)
τ_A	Thomson coefficient for a single material A (watts/amp-C^o)
v	velocity of sound, or phonons, in a given material (cm/sec)
w	width of thermocouple alloy strip (in)
W	mean atomic weight
ω	angular frequency (sec^{-1})
Z	figure of merit ($1/K^o$, or $1/R^o$)
ζ	Fermi energy (ergs)